Gene flow and environmental differentiation between viviparous and ovoviviparous populations of *Salamandra algira tingitana*

Marco André Ferreira Dinis
Mestrado em Biodiversidade, Genética e Evolução
Departamento de Biologia
2016
Orientador
Guillermo Velo-Antón, Investigador, CIBIO
Coorientador
Fernando Martínez-Freiría, Post-Doc, CIBIO

U.PORTO

FACULDADE DE CIÊNCIAS
UNIVERSIDADE DO PORTO

Todas as correções determinadas pelo júri, e só essas, foram efetuadas.
O Presidente do Júri,

Porto, _____/_____/_____

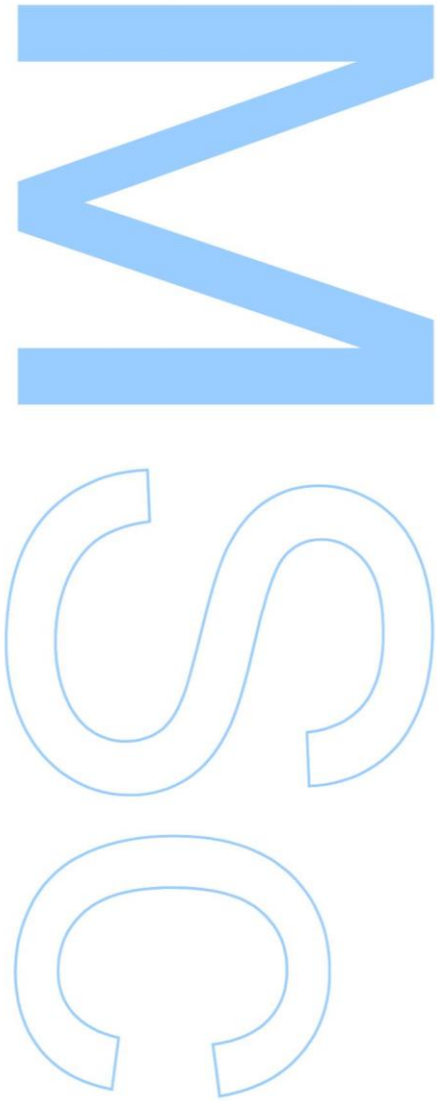

Agradecimentos

Aos meus orientadores por esta oportunidade fantástica, pela disponibilidade e apoio demonstrados em todos os momentos, e pelo seu contagiante exemplo daquilo que um investigador deve almejar ser.

Ao grande João Campos, o navegador exímio que descobriu a rota que me trouxe aqui, e que foi em diferentes momentos o meu batedor, mentor, anfitrião, *consiglieri* e amigo. Esta tese não existiria sem ti. *Grazie mille, capo!*

Ao Doutor José Carlos Brito e a todos os elementos do Biodeserts pelo excelente acolhimento e pelo constante encorajamento à expansão de horizontes científicos.

Ao André Lourenço, um agradecimento especial pelo inestimável apoio durante o trabalho de laboratório. E por não me deixar esquecer o Alentejo que me repousa na alma.

Aos meus estimados companheiros de Mestrado, pelos quilómetros de estrada que palmilhámos juntos. Que venham muitos mais.

À minha famíla, que mesmo à distância foi e será sempre o meu lar, epicentro e porto seguro.

Este trabalho foi parcialmente financiado pelo projecto EVOVIV – Evolution of viviparity: an integrative framework for the study of an evolutionary novelty in *Salamandra salamandra*" (PTDC/BIA-EVF/3036/2012).

Index

Table Index

Figure Index

List of Abreviations

MSC: Messinian Salinity Crisis

GCM: Global Circulation Model

LGM: Last Glacial Maximum

LGMcc: LGM prediction from the CCSM4 GCM

LGMme: LGM prediction from the MPI-ESM GCM

LGMmi: LGMprediction from the MIROC-ESM GCM

LIG: Last Inter-Glacial

MidHol: Mid-Holocene

a.s.l: above sea level

RH: Relative Humidity

PCR: Polymerase Chain Reaction

cyt-b: Cytochrome B

β-fibint7: β-fibrinogen intron 7

ng: nanograms

µl: microliters

bp: base pairs

DNA: Deoxyribonucleic acid

mtDNA: mitochondrial DNA

nDNA: nuclear DNA

c. circa

K: number of populations assumed by STRUCTURE software

pp: posterior probability

ENM: Ecological Niche Model

AUC: Area Under the Curve

ROC: Reciever Operator Characteristic

NDVI: Normalized Difference Vegetation Index

NDWI: Normalized Difference Water Index

Abstract

The Mediterranean Basin is a Global Hotspot of Biodiversity, exhibiting high levels of endemism and is considered an important centre of diversification, which is attributable to its complex biogeographic history, shaped by periods of connectivity between the European and African continents and by the interplay between the climatic oscillations of the Quaternary, and the high topographic complexity of the region.

The North African fire salamander *Salamandra algira* is the sole African representative of the Palearctic genus *Salamandra*, believed to have colonized North Africa across the Strait of Gibraltar. Past climatic oscillations likely played a key role in the evolutionary history of this species, resulting in four allopatric subspecies presently restricted to Moroccan and Algerian mountain ranges. Like in other North African species of Palearctic origin, *S. algira* populations tend to be associated with relatively mild climates and vegetation cover, which likely contributes to its fragmented distribution.

In the Moroccan Rif, four sublineages, belonging to the subspecies *S. a. tingitana* and *S. a. splendens*, occur in a relatively small area of complex topography, separated by narrow contact zones. The Rif populations of *S. algira* are an interesting research model due to the occurrence of pueriparous reproduction in a sublineage of *S. a. tingitana*, while larviparity is the predominant reproductive strategy for most of the species.

This work seeks to assess the impact of Pleistocene climatic oscillations and detect potential climatic refugia for *S. algira*, to assess the geographic structure of genetic diversity and the effect of topo-climatic and habitat variability on the ecological niche segregation in the Rif sublineages, and to elucidate the evolutionary and ecological context of pueriparity. To accomplish these goals, an integrated approach combining microsatellite and mtDNA information with ecological niche models and niche overlap tests was used. Furthermore, the extent and severity of habitat degradation due to vegetation loss from 2006 to 2014 was assessed for North Africa, with particular focus on the threat to Palearctic relicts, using *S. algira* as model.

Results reveal new insights on the context of pueriparity in the Rif, with the identification of a new pueriparous population on a sublineage previously believed to

be strictly larviparous, and evidence for an association between pueriparity and relatively water-independent habitats.

Population structure and gene flow at secondary contact zones between Rif sublineages and subspecies were identified. Lineages showed distinct responses to climate and habitat factors, though partial overlap between models suggests distributions in the Rif may not be fully allopatric and niches not fully divergent. Independent areas of climatic stability were identified for each subspecies.

Habitat degradation by vegetation loss was identified in areas of intense human activity in the Rif, Middle Atlas and eastern Algeria. Populations of *S. algira* subject to recent vegetation loss were identified in the contact zone between Rif subspecies, within the Talassemtane National Park.

Overall, these results suggest a pattern of allopatric divergence within Paleoclimatic refugia at both the subspecies and sublineage levels, followed, in the case of the Rif populations, by secondary contact facilitated by non-fully divergent ecological niches. Despite the still undisclosed evolutionary history of pueriparity in *S. algira*, this work supports the “dry climate hypothesis” for the evolution of pueriparity in *Salamandra*. The identification of areas of severe habitat degradation provides a valuable resource for prioritizing future conservation efforts for relict Palearctic species in North Africa, and for *S. algira* in particular.

Keywords: biogeography, contact zones, habitat degradation North Africa, Palearctic relicts, Paleoclimatic refugia, pueriparity, *Salamandra algira*, vegetation loss,

Resumo

A Bacia do Mediterrâneo é um *hotspot* global de biodiversidade, exibindo elevados níveis de endemismo atribuíveis à sua complexa história biogeográfica, caracterizada por períodos de conectividade entre Europa e África e pela interação entre as oscilações climáticas do Quaternário e a elevada complexidade topográfica da região. Consequentemente, a região desempenhou no passado um papel importante enquanto centro de diversificação, promovendo estruturas populacionais complexas e elevados níveis de endemismo.

A salamandra norte-africana *Salamandra algira* é a única representante africana do género Paleártico *Salamandra*, acreditando-se que terá colonizado o norte de África através do Estreito de Gibraltar. Oscilações climáticas no passado terão tido um papel central na história evolutiva da espécie, resultando em quatro subespécies alopátricas, atualmente restritas a cadeias montanhosas em Marrocos e Argélia. Tal como noutras espécies norte-africanas de origem Paleártica, as populações de *S. algira* tendem a encontrar-se associadas a climas amenos e cobertura vegetal, o que provavelmente contribui também para a sua distribuição fragmentada.

No Rif marroquino ocorrem quatro sublinhagens pertencentes às subespécies *S. a. tingitana* e *S. a. splendens*, separadas por estreitas zonas de contato situadas numa área relativamente reduzida e de alta complexidade topográfica. As populações de *S. algira* do Rif são um modelo interessante devido à ocorrência de reprodução pueríparа numa sublinhagem de *S. a. tingitana*, quando, em contraste, a estratégia reprodutiva predominante na espécie é o larviparismo.

O objetivo deste trabalho é caracterizar o impacto de antigas oscilações climáticas em *S. algira* e detetar potenciais refúgios climáticos para a espécie, de modo a compreender a sua estruturação geográfica de diversidade genética e o efeito da variabilidade topoclimática e de *habitat* na segregação ecológica das sublinhagens do Rif, bem como esclarecer o contexto evolutivo e ecológico do pueriparismo. Para cumprir estes objetivos foi utilizada uma abordagem integrativa, incorporando informação mitocondrial, de microssatélites, modelação ecológica e testes de sobreposição de nicho. Adicionalmente, foi caracterizada a extensão e severidade de degradação de *habitat* devido a perda de vegetação para o norte de África no período

de 2006-2014, com particular enfase nos riscos para populações relictas de origem Paleártica, e em particular para *S. algira*.

Os resultados revelaram novas perspetivas sobre o contexto do pueriparismo no Rif, com a identificação de uma nova população puerípara dentro de uma sublinhagem até agora aceite como inteiramente larvípara, e com a descoberta de evidência de uma associação entre pueriparismo e *habitats* relativamente independentes da disponibilidade de água.

Foram identificados estrutura populacional e fluxo genético em zonas de contato secundário entre sublinhagens e subsespécies do Rif. Diferentes linhagens exibem respostas distintas a fatores climáticos e de *habitat*. Porém, a sobreposição parcial entre modelos sugere que as distribuições de sublinhagens no Rif poderão não ser completamente alopátricas, e que os nichos destas não são verdadeiramente divergentes. Foram identificadas áreas de estabilidade climática independentes para cada subespécie.

Foi identificada degradação de *habitat* devida a perda de vegetação em regiões de intensa atividade humana no Rif, Médio Atlas e no este da Argélia. Foram identificadas populações de *S. algira* expostas a perda de vegetação recente na zona de contacto entre subespécies do Rif, dentro do Parque Nacional de Talassemtane.

Os resultados sugerem um padrão de divergência alopátrica em refúgios paleoclimáticos, tanto ao nível da divergência entre subespécies como entre sublinhagens. No caso das sublinhagens do Rif, ter-se-á seguido contato secundário, facilitado por conservação de nicho. Apesar de restarem dúvidas quanto ao contexto da evolução de pueriparismo em *S. algira*, este trabalho reforça a “hipótese do clima seco” para a evolução de pueriparismo em anfíbios. A identificação de áreas de degradação severa de *habitat* representa um recurso valioso para a seleção de ações prioritárias para futuros esforços de conservação de populações Paleárticas relictas no norte de África, particularmente para *S. algira*.

Palavras-chave: biogeografia, degradação de *habitat,* Norte de África, perda de vegetação, populações Paleárticas relictas, pueriparismo, refúgios paleoclimáticos, *Salamandra algira*, zonas de contato.

Chapter 1: General introduction

1.1 North Africa: an important biogeographic component of the Mediterranean Basin hotspot.

The Mediterranean Basin, which extends across southern Europe, the northern Maghreb, as well as part of the Near East, is a Global Hotspot of Biodiversity, exhibiting high levels of endemism that are attributable to its complex biogeographic history (Myers et al., 2000). Most of this complexity is due to the biogeographic relationship between Southern Europe and North Africa (Schmitt, 2007; Gómez et al., 2008; Husseman et al., 2013). While the Mediterranean Sea is an important biogeographic barrier restricting dispersal between continents, particularly for salt intolerant taxa like amphibians (Stebbins & Cohen, 1995; Gómez et al., 2008), two regions have at times acted as corridors facilitating trans-Mediterranean colonization: The strait of Sicily, between Italy and Tunisia (e. g. Stöck et al., 2008a), and the strait of Gibraltar, between Spain and Morocco (e. g. Martínez-Solano et al., 2004; Velo-Antón et al., 2015a). The latter one has been particularly important for trans-Mediterranean dispersal of terrestrial vertebrates, particularly during the Messinian Salinity Crisis (MSC), when the strait closed, isolating the Mediterranean from the Atlantic for c. 260,000 years (Hsü et al., 1973; Duggen et al., 2003). This event led to a decrease of the sea level in the Mediterranean, creating areas of inhospitable salt desert but also establishing an important land bridge connecting Gibraltar to the Tingitana peninsula in Morocco. This corridor, associated with the availability of ecologically similar habitats on both sides of the Mediterranean at specific points in history, namely during the Last Glacial Maximum (LGM) and at the onset of the post-glacial stages (Jolly et al., 1998; Jedoui et al., 2002; reviewed in Husemann et al., 2014), was particularly important for trans-Mediterranean dispersal of reptiles and amphibians, as evidenced by the close phylogenetic relationships between lineages found in Iberia and North Africa (e.g. Martínez-Solano et al., 2004; Stöck et al., 2008b; Velo-Antón et al., 2015a; Veríssimo et al., 2016). The reopening of the Strait at the end of the Miocene reestablished the isolation between continents (Dobson and Wright, 2000), enforcing wide-scale vicariance between populations on opposite sides of the Mediterranean (e. g. Steinfartz et al., 2000; Carranza et al., 2006; Velo-Antón et al., 2012).

The Quaternary climatic fluctuations, particularly since 2.4 million years ago, have led to a well described pattern of species seeking refuge in the southern European

peninsulas of Iberia, Italy and the Balkans, particularly in the case of climate-susceptible thermophilic organisms (Hewitt, 1999, 2000; Schmitt, 2007). At a finer scale, the complex topography found in these regions led to a pattern of refugia-within-refugia (Reinig, 1950), as species sought refuge by performing altitudinal range shifts along the mountainous ranges found in the region. This resulted in a complex history of population fragmentation and posterior secondary contact, making these southern refugia into veritable centers of diversification which promoted the emergence of endemisms and complex population structures (Gómez & Lunt, 2007; Weiss & Ferrand, 2007). While traditionally neglected, there has been a recent focus on the impact of climatic oscillations and topographically complexity in North Africa.

North Africa is a climatically and floristically complex region, characterized by Mediterranean climate and biodiversity along the northwest coast, surrounded by several thousand kilometers of arid Saharan landscape south and east (Dobson and Wright, 2000). As a consequence, aridity has been a historical driver of population fragmentation and subsequent divergence (Cosson et al., 2005), particularly during the mid-Pliocene to Pleistocene, when the region regularly experienced alternating humid and hyper-arid phases (Street & Gasse, 1981; Quezel & Barbero, 1993). The region is as complex topographically as it is climatically, with two major mountain systems: the Atlas complex and the Rif (Figure 1.1). The orographic barrier effects caused by these mountain ranges have promoted the development of strong phylogeographic structures in the region that were mostly shaped by Pleistocene glacial cycles promoting altitudinal range shifts as species sought refugia along the slopes of these main mountain ranges (Barata et al., 2008, 2012; Beukema et al., 2010; Velo-Antón et al., 2012a; Ben Hassine, 2016; Nicolas et al., 2015; Veríssimo et al., 2016). Biogeographic patterns of the Rif region have not yet, to the best of our knowledge, been elucidated in detail, but it is apparent that this dual role of mountain systems as barriers to dispersal and as climatic refugia has promoted diversification and strong population structure in distinct vertebrate groups.

1.2 The *Salamandra* genus

The true salamanders of the *Salamandra* genus are a group of amphibians with a predominantly Western Palearctic distribution. Six species are currently recognized (Thiesmeier, 2004; Frost, 2013, Vences 2014): *S. salamandra, S. algira*, *S. corsica* and

S. infraimmaculata group into the fire salamanders (so called due to their black and bright yellow coloration), while *S. atra* and *S. lanzai* are predominantly melanistic high-altitude species. The distribution of this genus is predominantly European, with the only exceptions being *S. algira* in North Africa and *S. infraimmaculata* in the Near East. Within Europe, the most prevalent species is *S. salamandra,* extending through most of South and Central Europe, while *S. corsica* is restricted to the island of Corsica and both *S. atra* and *S. lanzai* are endemic to the Alps. Despite some remaining uncertainty regarding phylogenetic relationships within the genus, a sister species relationship between the species *S. salamandra* and *S. algira* has been consistently recovered (Steinfartz, 2000; Escoriza, 2006; Beukema, 2010; Vences, 2014; Merabet, 2016; Ben Hassine et al., 2016).

1.2.1 The North African Fire Salamander (*Salamandra algira* Bedriaga 1883)

Some uncertainty remains regarding the time and context of the colonization of North Africa by the genus *Salamandra* and divergence between the sister species *S. salamandra* and *S. algira*. So far, two competing hypotheses have been proposed: either colonization took place during the MSC across the land bridge of Gibraltar, and the reopening of the Strait at the end of the MSC led to the isolation and subsequent divergence between the sister species, approximately 4.6 million years ago (Escoriza, 2006; Beukema, 2010; Vences, 2014); or, alternatively, divergence between these species occurred approximately 8-12 million years ago, well before the MSC, possibly caused by the expansion of the northern Betic Sea (Steinfartz et al., 2000; Ben Hassine et al., 2016). The current distribution of *S. algira* extends from the Tingitana peninsula in Morocco to eastern Algeria, with historical occurrence records in Tunisia reported but as of yet unconfirmed (Figure 1.1; Bogaerts et al., 2013). Its distribution is thought to be fragmented and mostly confined to mountain ranges at an altitude of 0-2455 m above sea level (a.s.l), with four subspecies recognized (Donaire-Barroso & Bogaerts, 2003; Escoriza & Comas, 2007; Beukema et al., 2013): *S. a. tingitana* occupies the northwestern Rif, ranging from Ceuta to Chefchouen; *S. a. splendens* extends into the south-central Rif, from Chefchouen southwards, including also a possibly isolated population in the Middle Atlas; *S. a. spelaea* is restricted to a small range in the Beni Snassen massif, near the Morocco-Algeria border; and the nominal

S. a. algira is restricted to Algeria, in the coastal mountainous regions of Annaba, Kabylia, Blida Atlas and Oranie (Figure 1.1). While the known distribution of the nominal subspecies is highly fragmented, recent phylogeographic insights into the species show weak structure among Algerian populations (Merabet et al., 2016; Ben Hassine et al., 2016), suggesting that fragmentation of their range is either recent or non-existent, and the gaps in the known distribution are likely a sampling bias associated with logistical difficulties of field work in Algeria. Phylogenetic work on this species has confirmed the validity of the four subspecies, while identifying two main clades estimated to have diverged either 3.6 million years ago, at the start of a cyclic period of climatic and vegetation fluctuations (Beukema et al., 2010) or 7.4 million years ago, during the Miocene (Ben Hassine et al.; 2016): a western clade including subspecies *S. a. tingitana* and *S. a. splendens*; and an eastern clade including *S. a. spelaea* and *S. a. algira* (Steinfartz et al., 2000; Merabet et al., 2016; Ben Hassine et al., 2016). The main biogeographic barrier promoting isolation between these clades seems to be the arid lower Moulouya river basin, which has been implicated in similar patterns of east-west divergence in other vertebrates (Alvarez et al., 2000; Barata et al., 2008; Velo-Antón et al., 2012a; Stuckas et al., 2014). This seems in line with what is expected of an amphibian species of northern Palearctic origin, for which aridity should be an important limiting factor (Franchimont & Saadaoui, 2001; Escoriza et al., 2006). Divergence between western subspecies *S. a. tingitana* and *S. a. splendens* took place in the Pliocene, 1.6-3.8 million years ago (Beukema et al., 2010; Ben Hassine et al., 2016), while the eastern subspecies *S. a. algira* and *S. a. spelaea* diverged during the Plio-Pleistocene, 2.5 Million years ago (Ben Hassine et al., 2016). Divergence within each major lineage may have been associated with periods of climatic fluctuations in North Africa, with phases of persisting aridity imposing vicariance in mountain refugia (Beukema et al., 2010; Ben Hassine et al., 2016).

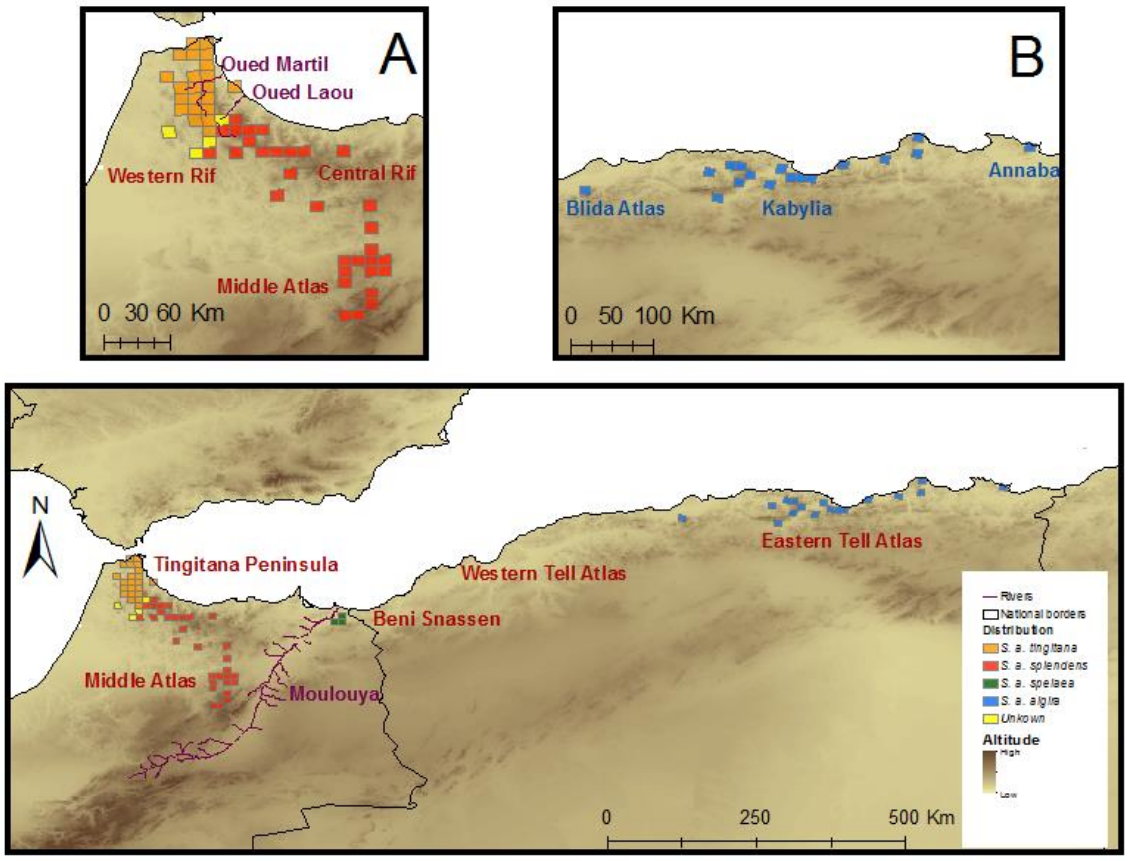

Figure 1.1 Bottom figure: Distribution of *S. algira.* Populations near the contact zone between *S.a. tingitana* and *S. a. splendens* for which genetic information is not available are identified in yellow. Inset A: overview of the Rif and Middle Atlas; Inset B: overview of western Algeria. Geographic features (red), rivers (purple) and localities (blue) are identified

1.2.2 Pueriparity in the *Salamandra* genus

Salamandra presents two reproductive modes: an ancestral mode, larviparity (i.e. ovoviviparity), in which females deliver aquatic larvae, and a derived mode, pueriparity (i.e. viviparity), where fully developed young are delivered, thus providing greater independence from water bodies.

Pueriparity in *Salamandra* has evolved in at least four independent events. While predominantly larviparous, pueriparity occurs in the Alpine species *S. atra* and *S. lanzai* (Buckley et al., 2007), as well as among restricted populations of *S. salamandra* in Iberia (García-Paris et al., 2003; Velo-Antón et al., 2007, 2012b). Only two species, *S. salamandra* and *S. algira*, show intraspecific variation in reproductive modes (Buckley 2012; Beukema et al.; 2010; Velo-Antón et al., 2014). The occurrence of multiple independent events of emergence of pueriparity within the genus suggests some

phenotypic plasticity may be associated with the trait. Pueriparity in *S. salamandra* seems to be connected with changes in the timing of embryonic development associated with intrauterine cannibalistic behavior among the larvae, which promotes a rapid development leading to metamorphosis occurring prior to oviposition (Buckley et al., 2007). This pattern is distinct from that described in *S. atra*, where only one egg per oviduct is fertilized, and the embryos feed on both unfertilized eggs and a nutritious material secreted in the uterus (Wake, 1993; Greven and Guex, 1994; Greven, 1998). It is not known what the physiological context of pueriparity in *S. algira* is.

Most of the *S. algira* populations are larviparous, however, pueriparous behavior has been described in populations belonging to the *S. a. tingitana* lineage located north of Oued Martil, and this has been connected with a distinct ecological niche from the larviparous populations of this subspecies (Beukema et al., 2010; Escoriza & Ben Hassine, 2014).

The drivers for the occurrence of pueriparity among salamanders are poorly understood. Viviparity among reptiles has been associated with adaptation to harsh climatic conditions, in what is known as the “cold climate hypothesis” (e.g. Hodges, 2004). Likewise, a “dry climate hypothesis” has been postulated as explanation for viviparity among salamanders, suggesting that arid conditions related with low precipitation or porous karstic substrates lead to a shortage of available surface water for ovoposition and larvae survivability, promoting selection for a reproductive strategy that bypasses the aquatic stage (García-París et al., 2003; Velo-Antón et al., 2007; Beukema et al., 2010).

1.2.3 Habitat and ecology of *Salamandra algira*

Salamandra algira occurs on temperate-to-cold winter and sub-humid to humid climates, with the exception of *S. a. spelaea*, which is restricted to semi-arid zones. It occupies thermic, mesothermic (0-1400 m a.s.l.) or supra-Mediterranean (1400-1800 m a.s.l.) forests, though it also occurs in more open habitats, namely in alpine meadows in the Middle Atlas and in bare karstic formations in the Tingitana Peninsula (Ben Hassine & Escoriza, 2014).

Salamandra a. tingitana presents distinct habitats through its distribution, which have been suggested to be associated with distinct reproductive strategies. Pueriparous populations were originally described on *Pinus* and *Quercus* forests and in barely vegetated limestone formations up to 390 m a.s.l., in the Mediterranean-influenced northeast Tingitana peninsula, while a distinct habitat has been described for the southernmost larviparous populations of this subspecies, consisting of mountainous or hilly terrain up to at least 1,274 m a.s.l. near water sources and in half-open forests, agricultural terraces and limestone outcrops (Donaire-Barroso & Bogaerts, 2003a, 2003b; Beukema et al., 2013). Ecological niche-based models have identified a weaker association with vegetation abundance and increased reliance on karstic substrates among the pueriparous populations (Beukema et al., 2010)

Salamandra a. splendens occurs at altitudes of up to 2,000 m a.s.l., on open limestone formations, forests composed of *Abies marrocana, Cedrus atlantica, Pinus* sp. and *Quercus* sp., or at low altitudinal *Pistacia* sp. shrublands, usually near water sources (Donaire-Barroso & Bogaerts, 2003b; Martínez-Medina, 2007; Beukema et al., 2013).

Salamandra a. spelaea is restricted to the Beni Snassen massif, at altitudes of 600-1,300 m a.s.l.. Its habitat consists of mixed forests of *Quercus, Pinus* and *Olea* trees with availability of water bodies for reproduction, which, due to the karstic lithology of Beni Snassen, are predominantly man-made (Escoriza et al., 2006; Escoriza & Comas, 2007).

Little is currently known about the ecology of the nominal *S. a. algira* other than its association with humid and sub-humid forest on mountainous regions near the Mediterranean coast of Algeria (Merabet et al., 2016).

Microclimatic characterization of the habitat of all Moroccan subspecies of *S. algira* has shown that the species occurs within a mean annual temperature range of 13.6-18.6 ºC, at a mean annual relative humidity (RH) exceeding 64%. The latter appears to be the most important variable of the two. Pueriparous populations of *S. a. tingitana* occupy the areas with highest RH, while the Rif populations of *S. a. splendens* occupy those with the lowest. Microclimatic stability is greatest in the region north of Oued Laou, and lowest in the areas of the Rif and Middle Atlas where *S. a. splendens* is distributed. The niche of pueriparous populations of *S. a. tingitana* seems, therefore, to be markedly different from the other populations. Its coastal distribution may provide

more stable climatic conditions, which reduce the dependency on vegetation's climatic buffer effect found on other populations of the species. The discovery of great microclimatic stability in the sites of occurrence of *S. a. spelaea*, together with the habitat discontinuity in the Beni Snassen massif, suggests that a greater importance of microclimate in this subspecies may account for its highly localized distribution (Escoriza and Ben Hassine, 2014).

Conditions suitable for surface activity occur through the entire Moroccan distribution from November to April, extending from October to May at the highest altitudes. Larval size heterogeneity peaks in January (suggesting co-occurrence of several larval cohorts), and decreases in March, signaling the end of larval recruitment, onset of metamorphosis, and increased cannibalistic pressure. Larval abundance is not correlated with pond size or microclimatic conditions (Escoriza and Ben Hassine, 2014). *S. algira* larvae have been found in distinct water body types, from temporary ponds to stream pools, but most commonly in springs with clear water and low-density aquatic vegetation. Morphological analyses of larvae suggest the species is of the spring-type larval variety (Ben Hassine & Escoriza, 2014)**.**

1.2.4 *S. algira* diversity in the Rif

The western lineage's two subspecies (*S. a. tingitana* and *S. a. splendens*) are distributed on both sides of a contact zone in the Oued Laou (Figure 1.1). Likewise, strong geographic structure is also evident within subspecies. *Salamandra a. tingitana* is divided into three sublineages: a basal clade restricted to Jebel Sugna, Beni Maharone and Dar Chaoui, which diverged 800.000 years ago, as well as a clade that further subdivided into two sublineages 600.000 years ago, distributed on opposite sides of Oued Martil (Beukema et al., 2010; Velo-Antón et al., 2014). The northernmost of these two sublineages is notorious for the occurrence of viviparous reproductive behavior (Donaire-Barroso & Bogaerts, 2003; Escoriza, 2006; Beukema et al., 2010).

Salamandra a. splendens also shows geographic structuring, with one sublineage occurring in the Western and Central Rif, while another is restricted to the Middle Atlas (Figure 1.1). Divergence between the sublineages that inhabit the Rif may be related to range shifts driven by the climatic oscillations of the Quaternary, resulting in vicariance and, subsequently, in differentiation (Beukema et al., 2010).

While previous work has described important climatic differences between the region of the Tingitana peninsula north of Oued Martil and the range of the remaining *S. a. tingitana* (Beukema et al., 2010), and its likely the arid Middle Atlas is climatically distinct from the Rif, there is no reason to suspect climatic differentiation between the regions immediately North and South of Oued Laou, where the contact zone between subspecies is located. It is not clear whether the current distribution of *S. algira* populations in the Rif is shaped by biotic or abiotic constraints, or if there are important barriers limiting dispersal.

1.3 Thesis structure and objectives:

The remarkable genetic and reproductive diversity of *S. algira*, as well as its notorious affinity with environmental factors, reinforce the species role as a multi-purpose study model to infer: a) the evolutionary and ecological context of the emergence of novel traits (namely pueriparity); b) biogeographical patterns of Palearctic relicts in North Africa; and c) consequences of contemporary habitat degradation for North African Palearctic relicts. To address these questions, this work was structured in three main sections:

1.3.1 Spatial patterns of genetic diversity in Rifean populations of *S. algira* (Manuscript I)

Due to the elusiveness of *S. algira*, there are currently gaps in the known distribution of this species. Particularly in the Rif, the occurrence of pueriparous populations presents a remarkable opportunity to address questions regarding the evolutionary context of differential survival strategies in an apparently continuous distribution. Yet, such lines of inquiry are hindered by a lack of detailed knowledge on the distribution of reproductive strategies and spatial patterns of genetic diversity in the region. The major goals of this chapter are to a) improve the knowledge on *S. algira* distribution in the Rif, with special emphasis on the distribution of the distinct reproductive modes; b) further delineate the spatial distribution of presently known mitochondrial lineages; c) assess the existence of population structure and gene flow between lineages; and d) quantify the degree of genetic differentiation between populations.

1.3.2 Historical and contemporary ecological niche of *S. algira* (Manuscript II)

Presently, very little is known about the ecology of *S. algira.* As an amphibian of northern Palearctic origin, it is expected to be heavily reliant on availability of temperate to Mediterranean, relatively humid climate, suitable microclimatic refugia provided by dense vegetation or rock crevices, and surface water for reproduction. However, the aridity of North Africa likely makes rare commodities of most of these requirements, which may explain the heavily fragmented and mostly mountainous distribution of this species. Under the assumption of this relatively restrictive ecological tolerance, it is expected for past climatic oscillations to have played a significant role on the evolutionary history of this species, shaping its distribution and patterns of genetic diversity. The objectives of this chapter are to a) reconstruct the biogeographic history of *S. algira* in North Africa and in the Rif; b) characterize the potential distribution and assess the relative importance of distinct niche components for the Rif lineages; and c) estimate the degree of ecological niche divergence and its role on the evolutionary differentiation among subspecies and within the Rif.

1.3.3 Impact of landscape-change on habitat availability in a Palearctic relict in northern Maghreb (Manuscript III)

Northern Palearctic-origin taxa in North Africa are mostly restricted to relatively moderate conditions of temperature and humidity, and as such tend to be associated to, and dependent on, dense vegetation cover, which due to the prevailing aridity of the region results in predominantly fragmented habitats. Yet, the ongoing increase in human population density in the region is gradually leading to a shift from traditional methods of land-management to more intensive land uses which decrease the availability of natural vegetation habitats, with potentially dangerous consequences for more vulnerable species. While little factual data is currently available on the degree of damage to habitats and consequences for wildlife so far, the availability of Remote Sensing data makes it possible to obtain accurate information on the temporal and spatial patterns of change in land use across the region. This chapter aims to a) characterize temporal trends of variation in vegetation cover in North Africa in recent

years; b) identify the natural areas most affected by vegetation loss; and c) identify at-risk populations of *S. algira*.

Chapter 2: Spatial patterns of genetic diversity in Rifean populations of *S. algira* (Manuscript I)

2.1 Introduction

The high levels of endemism in North Africa (Husseman et al., 2013; Martínez-Freiría et al., 2013) make the region a major contributor to the recognition of the Mediterranean Basin as a global hotspot of biodiversity (Myers et al., 2000). This is partially due to the complexity of the evolutionary histories of North African taxa, marked by periods of connectivity with southern Europe which allowed colonization across the Mediterranean in both directions (Hsü et al., 1973; Krijgsman et al., 1999; Duggen et al., 2003; Velo-Antón et al., 2015a). Another contributing factor to diversification in the region was the complex succession of climatic oscillations during the Quaternary (Street & Gasse, 1981; Quezel & Barbero, 1993), forcing species to adapt, pursue suitable climate through successive range shifts, or persist in climatically stable refugia for long term periods (Cosson et al., 2005).

The complex topography of the region likely produced similar patterns to those found in Europe (Schmitt et al., 2009; Mouret et al., 2011), with populations tracking climate fluctuations and finding refugia by performing altitudinal shifts along mountain slopes (e.g. Beukema et al., 2010; Nicolas et al., 2015; Veríssimo et al., 2016). These shifts promoted periods of vicariance which acted as drivers for diversification, either by genetic drift or differential adaptation to local conditions.

The Rif Mountains, located in the Tingitana peninsula, probably exemplify these processes. They were once a major pathway for colonization across the Mediterranean, as the peninsula was connected to Iberia across the Strait of Gibraltar during the Messinian Salinity Crisis (Hsü et al., 1973; Duggen et al., 2003). This complex mountain range, reaching altitudes of 2.455 m, likely promoted diversification of taxa forced to survive in the region during periods of climatic instability, particularly in the case of species with low dispersal ability, for which large scale range shifts were not a viable strategy. This may explain the high amphibian and reptile species richness that is found in the western and central Rif (Mediani et al., 2016).

Salamandra algira is the sole African representative of the northern Palearctic *Salamandra* genus, and is currently distributed from western Morocco to Eastern Algeria. Yet, its distribution is highly fragmented and restricted to mountain ranges. The subspecies *S. a. tingitana* and *S. a. splendens* are endemic to northwest Morocco and

distributed on both sides of a narrow contact zone in Oued Laou, with the former occurring in the northern part of the Rif and the latter occupying the area from Chefchaouen to the central Rif, as well as an apparently isolated area of the Middle Atlas (Figure 2.1). The occurrence of two possibly parapatric subspecies in a relatively small area, and the fact that further genetic substructure has been described within subspecies, with three major sublineages of *S. a. tingitana* and two of *S. a. splendens* (Beukema et al., 2010), suggests the Rif and Middle Atlas may have served as an important centre of diversification in the past. Furthermore, the observation of a pueriparous reproductive strategy among populations of the northernmost sublineage of *S. a. tingitana* (Donaire-Barroso & Bogaerts, 2003; Beukema et al., 2010) reveals a diversification of reproductive strategies has occurred alongside the genetic differentiation in the region. However, the full evolutionary context of pueriparity has not yet been clarified, and would require a more detailed understanding of the distribution of genetic diversity and reproductive modes in the region, which so far has been hindered by the elusiveness of the species and by sampling difficulties associated with human activities in the region, which have caused a rapid decline in habitats available for salamanders and other biogeographically similar species (e.g. Brito et al., 2011).

The present work aims to bridge this knowledge gap by improving our understanding of the distribution of *S. algira* diversity and characterizing present-day population structure. The main objectives of this chapter are to a) improve the knowledge on *S. algira* distribution in the Rif, with special emphasis on the distribution of the distinct reproductive modes; b) further delineate the distribution of presently known mitochondrial lineages; c) assess the existence of population structure and contact zones between lineages; and d) quantify the degree of genetic differentiation between populations.

2.2 Methods

2.2.1 Study area and sampling strategy

With the aim of obtaining a representative geographic coverage of the distribution of *S. a. tingitana* and *S. a. splendens,* sampling was performed on the Western-Central Rif and Middle Atlas mountain systems, in Morocco (Figure 2.1). Two expeditions were performed during the spring in search of larvae (May 2015) and during the highest

peak of activity of adult salamanders (December 2015). Sampling effort was focused in areas with forest cover and surface water availability, with particular emphasis on the predicted contact zones between lineages, near Oued Laou and Oued Martil. Sampling of larvae was performed by screening ponds and water reservoirs with dipping nets, and by visual inspection of streams. Sampling of adults and metamorphosed juveniles was performed by searching under rocks and inside dead wood, and by nocturnal transects on humid and/or rainy nights to capture active adults. Road kills were also collected whenever found. Pregnant females were kept in captivity up to five days until they gave birth. Tissue samples (tail and finger tips) were collected and preserved in tubes with 100 % ethanol to ensure DNA integrity. GPS coordinates were recorded on all points of occurrence. All available samples provided by colleagues were also considered for subsequent analyses.

2.2.2 DNA extraction and amplification

Tissue samples were placed overnight in PBS buffer to neutralize skin toxins which may act as inhibitors of subsequent reactions. Genomic DNA was extracted from 105 tissue samples using Genomic DNA Tissue Kit (EasySpin) following the manufacturer's protocol. DNA concentration and integrity were verified by electrophoresis in 0.8% agarose gel died with GelRed™ (Biotium). Results were visualized by UV on a Bio-Rad Universal Hood II molecular imager (Bio-Rad)**.** DNA concentration was roughly estimated from gel visualization and samples were diluted with ultra-pure water as needed, to guarantee a concentration of 50 ng/µl. Extracted DNA was kept at -20 ºC until further use.

A section of c. 1,400 base pairs (bp) of one mitochondrial fragment, cytochrome b and adjacent tRNAs (*cyt-b*; ca. 1400 bp), and ca. 700 bp of the intron of the nuclear gene β-fibrinogen (*β-fibint7*), were amplified and sequenced for each sample. The *cyt-b* fragment was amplified using primers Glu14100L (forward, 5' GAA AAA CCA AYG TTG TAT TCA ACT ATA A 3') and Pro15500H (reverse, 5' AGA ATT YTG GCT TTG GGT GCC A 3') (Zhang et al., 2008), while the *β-fibint7* gene was amplified using BFIB_F (forward, 5' TGG GAC TGG CAG TTG TTT AG 3') and BFIB_R (reverse, 5' TGA TTC ACG AGT TTG TTG CTC 3') (Pereira et al., 2016).

Each polymerase chain reaction (PCR) had a total volume of 10–11 µl: 5 µl of MyTaq™ HS Mix 2X (Bioline), 3 µl of distilled H2O, 0.5 µl of each primer from a primer solution of 10 µM and 1–2 µl of DNA extract (~50 ng/µl). A negative control was employed to identify possible contaminations. For the *cyt-b* gene, cycling conditions were as follows: initial denaturation at 94°C for 5 min, followed by 40 cycles of 40 s at 94°C, 40 s of annealing at 51°C and 72°C for 2 min 30 s, finishing with a final extension cycle of 5 min at 72°C. PCR conditions for *B-fibint7* gene were as follows: initial denaturation at 94°C for 5 min, followed by 40 cycles of 30 s at 94°C, 30 s of primer annealing at 59°C and elongation at 72°C for 45 s, finishing with a final extension cycle of 5 min at 72°C. PCR product quality and quantity was assessed by visual inspection in a 2% agarose gel. Sequencing of PCR products was outsourced to Beckman Coulter Genomics (Essex, UK). The same primers used in PCRs were employed for sequencing. All the obtained chromatograms were verified, aligned and corrected by eye using GENEIOUS PRO version 4.8.5 (http://www.geneious.com/).

A total of 13 microsatellite markers developed for *S. salamandra* and previously tested in *S. algira* (Steinfartz et al., 2004; Hendrix et al., 2010; Table 7.1, Supplementary materials) were amplified in four different PCR multiplexes. Each multiplex mix consisted of distilled H_2O, fluorescently labelled forward (6-FAM, VIC, NED or PET) and reverse primers modified with a ‘‘PIG-tail’’ (GTTT) at the 5’ end. Each PCR reaction contained a total volume of 10–11 µl: 5 µl of Multiplex PCR Kit Master Mix (QIAGEN, Valencia, CA, USA), 3 µl of distilled H2O, 1 µl of primer multiplex mix and 1–2 µl of DNA extract (~50 ng/µl). A negative control was always used to identify possible contaminations. PCR touchdown cycling conditions were similar for three of the four multiplex reactions (panelS1, panelS4 and panelS5): the reaction started with an initial step at 95°C for 15 min, 19 cycles at 95°C for 30 s, 90 s of annealing at 65°C (decreasing 0.5°C each cycle), 72°C for 40 s, followed by 25 cycles of 95°C for 30 s, 56°C for 60 s, 72°C for 40 s, and ended with a final extension of 30 min at 60°C. For panelS2, a similar protocol was performed but with 27 cycles instead of 19 and with the annealing temperature during the last 25 cycles set to 52°C instead of 56ºC. PCR amplification quality was assessed by visual inspection in 2 % agarose gels. PCR products were run on an ABI3130XL capillary sequencer (Applied Biosystems), and allele scoring was performed using GeneMapper version 4.0 (Applied Biosystems).

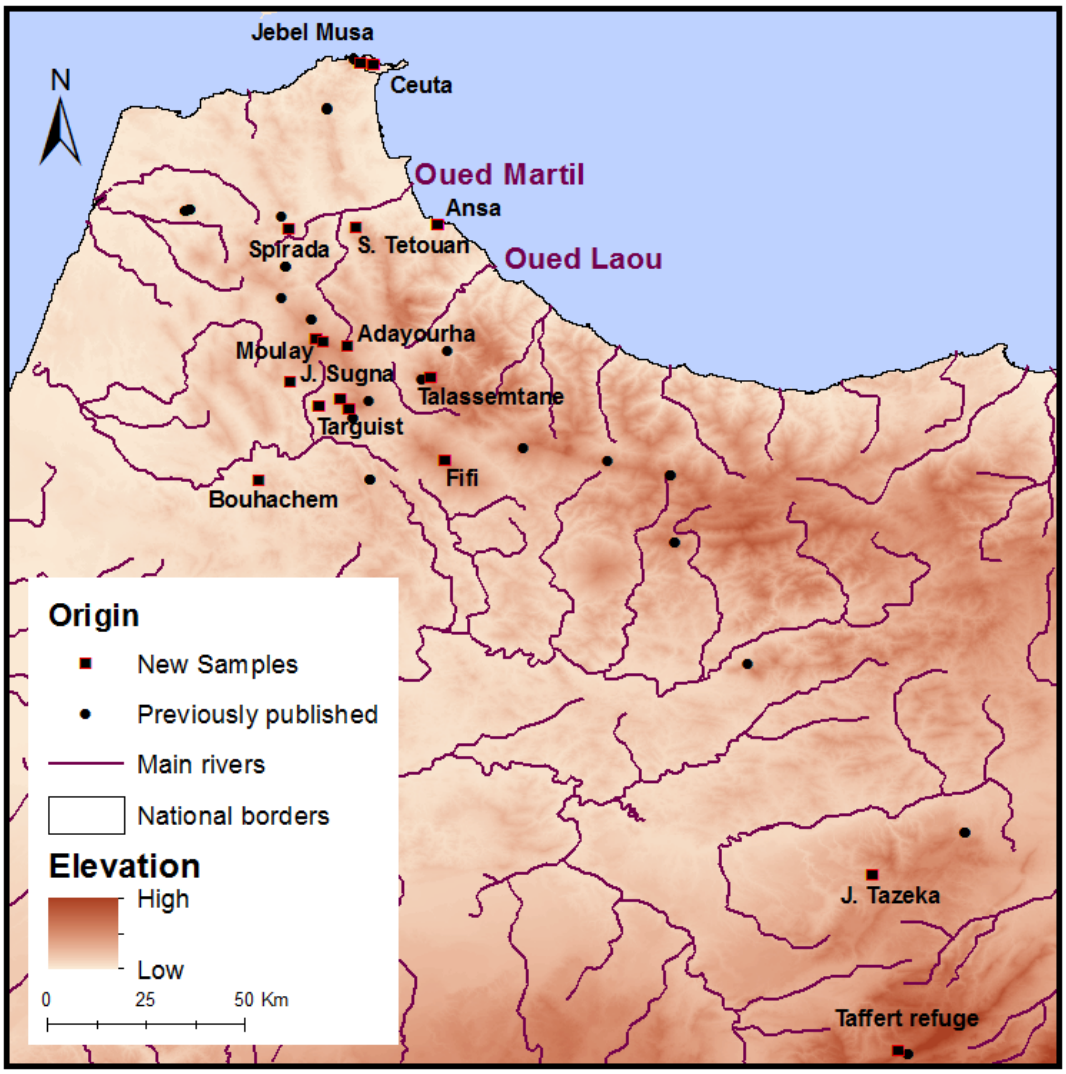

Figure 2.1. Distribution of previously published (circles) and new (squares) data on genetic diversity of *S. algira* in the Rif. Names of the new localities and rivers Oued Martil and Oued Laou, where the contact zones between distinct lineages are located, are displayed

2.2.3 Molecular analyses

Because the *B-fibint7* gene exhibited very low levels of polymorphism among our samples and no genetic differentiation among subspecies, it was not considered for subsequent analyses (See Results for details). Thus, phylogenetic relationships were inferred based on the *cyt-b* gene only. A region of ca. 300 bp was trimmed in all *cyt-b* sequences after the *cyt-b* stop codon, which contained tRNA Thr, part of tRNA Pro, and a large non-coding region. This region could not be unambiguously aligned and was excluded from the analyses, resulting in a final alignment of ca. 1100 bp for the *cyt-b*. All available *cyt-b* sequences for S. algira were downloaded and used in subsequent

analyses, including those corresponding to smaller (351 bp) fragments (Donaire-Barroso & Bogaerts, 2003; Escoriza & Comas, 2007; Beukema et al., 2010; Velo-Antón et al., 2014; Vences et al., 2014; Ben Hassine et al., 2016; Merabet et al., 2016). Sequences from *S. salamandra longirostris* were included as outgroup. Bayesian analyses were conducted in BEAST v1.7.5 (Drummond et al., 2012). JMODELTEST v.2.1.4 (Darriba et al., 2012) was used to test for the best fitting model of nucleotide substitution for the *cyt-b* (HKY+I), under the Bayesian Information Criteria. A lognormal relaxed clock and a coalescence constant size model were used as tree priors. Markov Chain Monte Carlo (MCMC) analyses were run in three independent runs of 100 million generations, with a sampling frequency of 10,000 generations and discarding 10% of the trees as burn-in.

Parameter convergence was verified by examining the effective sample sizes (ESSs) using TRACER v1.7. After discarding 10% trees as burn-in, the remaining trees were used to obtain the subsequent maximum clade credibility summary tree with posterior probabilities for each node using TREEANNOTATOR. The resulting consensus tree was visualized on FigTree (http://tree.bio.ed.ac.uk/software/figtree).

Uncorrected genetic distances between the main lineages were calculated in MEGA7 (Kumar et al., 2016), applying a p-distance substitution model and considering only the samples for which the 1,100 bp sequence was available. A median joining haplotype network was created in PopART version 1.7 (Leigh & Bryant, 2015), with the same data used for calculating genetic distances.

MICROCHECKER 2.2.3 (Van Oosterhout et al., 2004) was used to test microsatellite data for null alleles and allele dropout. Each microsatellite locus was tested for Hardy–Weinberg Equilibrium (HWE) and Linkage Disequilibrium (LD) using a Markov Chain method with 10,000 dememorization steps and 1,000 batches of 10,000 iterations per batch as implemented on GENEPOP 4.2 (Raymond & Rousset, 1995; Rousset, 2008). The Bonferroni correction (Rice, 1989) was applied to account for multiple comparisons.

A Bayesian assignment test was used to infer the number of genetic demes present in our sample, as implemented in STRUCTURE 2.3.1 (Pritchard et al., 2000). 1 million iterations were performed, with a burn-in period of 100,000, and applying an admixture model with correlated allele frequencies and no prior information on sample population

membership. The program was run with a number of clusters (K) ranging from 1 to the number of included localities plus one (10), with 10 iteration per K. The most likely value for K was estimated by the highest value of log probability of data L(K) (Falush et al., 2003), and D(K), a measure based on the second order rate of change in L(K) (Evanno et al., 2005). Both estimates were calculated on STRUCTURE HARVESTER (Earl & vonHoldt, 2012). Additionally, to account for potential errors caused by uneven sampling, four alternative estimators of the most likely K (MedMeaK, MaxMeaK, MedMedK and MaxMedK) were calculated (Puechmaille, 2016). The program CLUMPP 1.1.2 (Jakobsson and Rosenberg, 2007) was used to align cluster membership coefficients from the 10 replicate cluster analyses from each value of K. For populations where admixture was detected by STRUCTURE, the posterior probability of each sample belonging to one of six parental or hybrid classes (P1, P2, F1, F2, B1, B2) was estimated using a Bayesian MCMC-based approach, as implemented in NEWHYBRIDS (Anderson & Thompson, 2002). Three independent runs were performed to ensure consistency of results, using uniform priors and 1 million iterations, with 100,000 steps of burn-in. Genetic differentiation between populations and between mitochondrial lineages was calculated using pairwise F_{ST} values (Nei, 1977) in GenAlEx version 6.502 (Peakall & Smouse, 2006, 2012).

2.3 Results

2.3.1 Field work and laboratory analyses

Pregnant females were only observed in a population in Amsa, near Tetouan. This population was located in a west-oriented slope, 85 m a.s.l., on a coastal patch of well-preserved coniferous forest, surrounded by landscape fragmented by human land use. No surface water was observed, though the rugged topography suggests temporary ponds may form sporadically. Females from this population exhibited pueriparous reproduction by giving birth to fully metamorphosed juveniles in captivity. No larvae were detected north of Oued Martil.

A total of 182 new *S. algira* samples were collected from 17 unique localities (Figure 2.1; Supplementary Materials Table 7.2). DNA extraction was performed for 95 of these samples, of which 82 (86 %) produced quality DNA extracts which were used in

subsequent analyses. All the thirteen samples which did not produce suitable DNA extracts were provided by colleagues, and DNA degradation caused by long-term storage in unsuitable preservation conditions was the likely reason for the failed extractions. 72 samples were sequenced for phylogenetic analyses, in order to clarify the mtDNA distribution across the entirety of the *S. a. tingitana* and *S. a. splendens* distribution (Supplementary Materials Table 7.2). 91 samples were amplified with all microsatellite panels, to obtain a geographic representation of genetic structure and allow the assessment of gene flow in the Rif (Supplementary Materials Table 7.2).

2.3.2 Phylogenetic analyses

For the *cyt-b* gene, 40 of 72 samples were successfully sequenced, and 23 unique haplotypes were obtained. For the *B-fibint7* gene, nine samples from all Rif subspecies and sublineages were successfully amplified. The final fragment was 627 bp long, with six unique haplotypes that differ at least 3 bp from *S. s. longirostris*, yet no differentiation was found between subspecies, and thus *B-fibint7* was not considered for subsequent analyses.

A total of 138 sequences (including all previously published *S. algira cyt-b* sequences, as well as three *S. salamandra longirostris* samples as outgroup) were used for creating the *cyt-b* tree (Table 7.2, Supplementary Materials Table 7.2). The resulting gene tree identified two main clades: the western clade, consisting of three sublineages belonging to *S. a. tingitana* and two sublineages of *S. a. splendens*, and an eastern clade which further subdivides into the subspecies *S. a. spelaea* and *S. a. algira* (Figure 2.2). All subspecies, as well as the sublineages observed within each lineage, are monophyletic and well supported (Bayesian posterior probability > 0.8; Figure 2.2). The pueriparous sublineage 1 of *S. a. tingitana* is a sister group to sublineage 2, in accordance with previous work on these populations (Beukema et al., 2010; Figure 2.2). All of the main nodes are highly supported (posterior probability (pp) > 0.95) except for the divergence between *S. a. tingitana* lineages 1 and 2 (pp = 0.1; Figure 2.2). This phylogenetic inference agrees with the mtDNA phylogenetic structure previously described for this species (Steinfartz et al., 2000; Beukema et al., 2010; Merabet et al., 2016; Ben Hassine et al., 2016).

Regarding the spatial distribution of mitochondrial lineages in the Rif (Figure 2.3), all populations north of Oued Martil belong to *S. a. tingitana* sublineage 1, except for the populations in Dar Chaoui (as reported in Velo-Antón et al., 2014) and Spirada, where a population from sublineage 2 was found, c. 3.5 km away from a population belonging to sublineage 1. New populations of *S. a. tingitana* 1 were found in the Spanish municipality of Ceuta and in Jebel Musa, in the commune of Taghramt. The pueriparous population of Amsa (near Tetouan), as well as populations in Moulay and the aforementioned Spirada, were identified as members of *S. a. tingitana* 2. Populations of *S. a. tingitana* sublineage 3 were identified in Moulay, Adayourha, Jebel Sugna and Dar Chaoui. New populations of *S. a. splendens* sublineage 1 were found immediately south of Oued Laou, in the provinces of Talassemtane and Fifi, and a new population of *S. a. splendens* sublineage 2 was identified in Bou Iblane, near Taffert (Middle Atlas).

Genetic distances were moderate (all below 0.05) when comparing lineages of the same main clade (east or west) and higher (all above 0.05) when comparing lineages of distinct clades, with the exception of the distances between *S. a. algira* and lineages 1 and 2 of *S. a. tingitana* (0.042 and 0.041, respectively; Table 2.1). Distance between the two subspecies of the eastern clade was 0.029, while within the western clade distances were almost all higher (0.027-0.043; average=0.0357), with the only exception between *S. a. tingitana* sublineage 3 and *S. a. splendens* sublineage 1 (0.027; Table 2.1).

Distances between sublineages of the same subspecies were higher for *S. a. splendens* (0.025) than for *S. a. tingitana* (0.001-0.011; Table 2.1). The monophyletic *S. a. tingitana* sublineages 1 and 2 showed the lowest genetic distance among all groups analysed (0.001; Table 2.1).

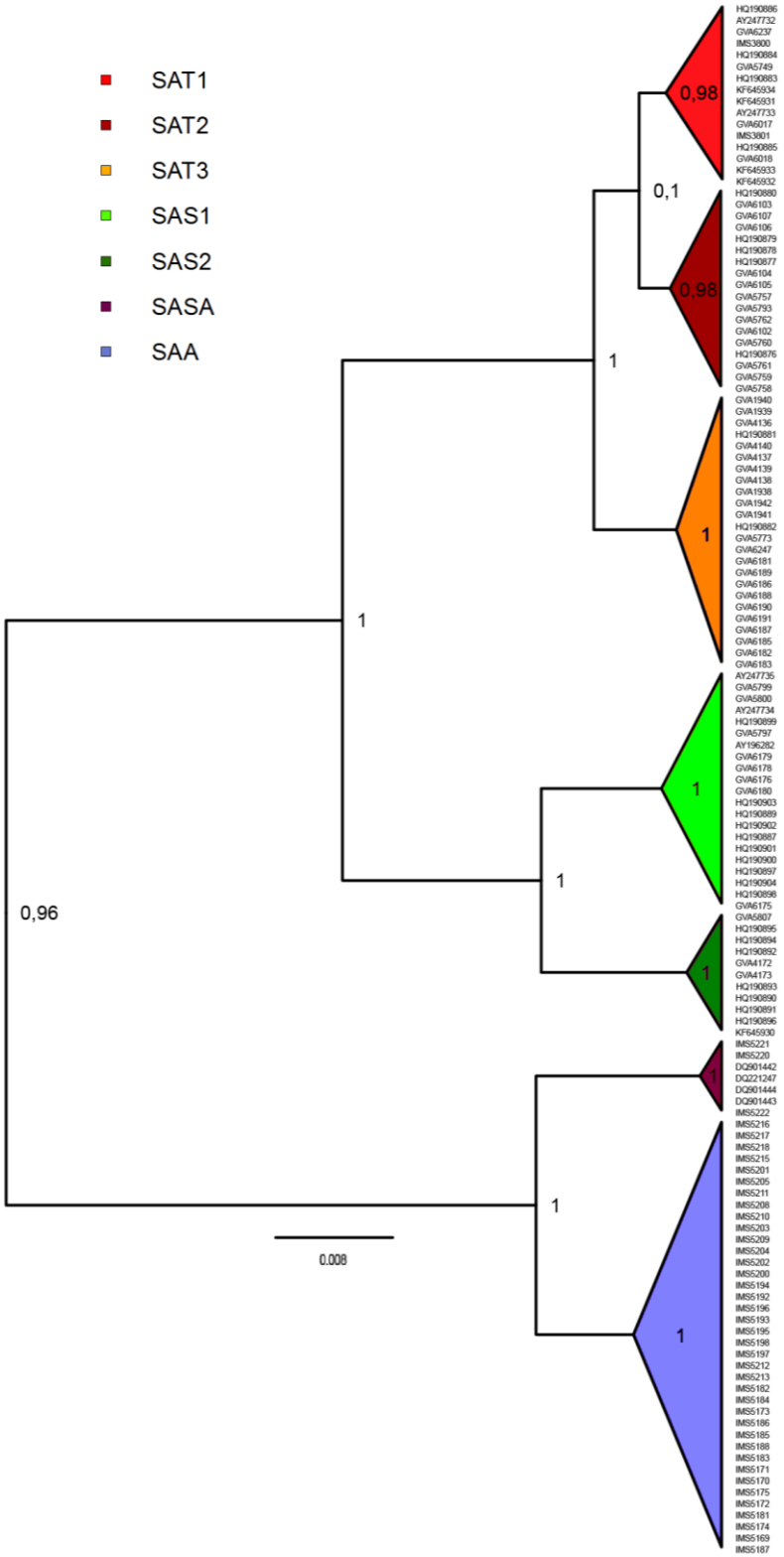

Figure 2.2 Bayesian cyt-b gene tree for *S. algira*. Numbers on nodes represent posterior probabilities. Sample codes starting with GVA correspond to our newly collected samples, for which genbank numbers are not yet available. SAT1: *S. a. tingitana* 1; SAT2 *S. a.t ingitana* 2; SAT3: *S. a. tingitana* 3; SAS1: *S. a. splendens* 1; SAS2 : *S. a. splendens* 2; SASA: *S. a. spelaea*; SAA: *S. a. algira*

Table 2.1 Genetic distances between mitochondrial lineages of *S. algira.* Highly differentiated values (>0.05) are outlined in bold. Sample size used for genetic distance estimation and haplotype network (N) and number of haplotypes per lineage (Hap) are also presented. SAT1: *S. a. tingitana* 1*;* SAT2: *S. a. tingitana* 2; SAT3: *S. a. tingitana* 3; SAS1: *S. a. splendens* 1; SAS2: *S. a. splend*ens 2; SASA: *S.a. spelaea*; SAA: *S. a. algira*

	genetic distances						N	Hap
	SAT1	SAT2	SAT3	SAS1	SAS2	SASA		
SAT1							6	3
SAT2	0.001						13	3
SAT3	0.011	0.01					22	9
SAS1	0.032	0.032	0.027				8	5
SAS2	0.043	0.042	0.038	0.025			3	2
SASA	**0.061**	**0.061**	**0.071**	**0.078**	**0.079**		3	2
SAA	0.042	0.041	**0.051**	**0.07**	**0.081**	0.029	38	12
						Total	93	36

A Median Joining haplotype network (Figure 2.4) identified 36 distinct mitochondrial haplotypes among lineages of *S. algira*. Number of haplotypes was highest in *S. a. algira* (12) and *S. a. tingitana* 3 (9), and lowest in *S. a. spelaea* and *S. a. splendens* 2 (2 for each). *S. a. splendens* 1 has five haplotypes and *S. a. tingitana* 1 and 2 have three each. It should be noted that sample sizes are not identical (Table 2.1), and it is thus entirely possible that the number of haplotypes may be severely underrepresented, particularly in the lineages that presented the lowest numbers of haplotypes. There is overall agreement with the gene tree regarding the structure of mitochondrial diversity, with the eastern and western clades well-separated by 57 substitutions, and the *S. a. tingitana* sublineages 1 and 2 forming an independent branch. *S. a. splendens* comprises a deeply divergent branch (34 substitutions), with further deep divergence between sublineages 1 and 2 (20 substitutions).

2.3.3 Genetic structure and contact zones

A total of 98 samples were genotyped for all four microsatellite panels, including seven samples from Dar Chaoui which had been previously collected (Velo-Antón et al., 2014) but for which no microsatellite data had yet been analysed. Marker Sal23 failed to amplify on all samples, and was excluded from subsequent analyses. Samples for which more than five markers failed to amplify were also excluded. The final dataset consisted of 83 samples genotyped for 12 microsatellites, with 1.3 % missing data. From the microsatellites selected for analyses, SalE7 was the one with the highest

percentage of missing data (6.1 %), and the amplification success rate across all markers was 98.6 %. No evidence of null alelles or allele dropout was found using a 99 % confidence interval. No significant deviations from Hardy Weinberg equilibrium or evidence of Linkage Disequilibrium were found, so all remaining samples and markers were kept for subsequent analyses.

Estimates of the best K for the STRUCTURE analysis were divided between K=6 (L(K) and D(K)) and K=7 (MedMeaK, MaxMeaK, MedMedK and MaxMedK). Plots for both values of K agreed in the overall structure, with the only difference being in the improved ability of K=7 to distinguish between the two populations of *S. a. splendens* included in the analysis (Figure 2.3). The 7 clusters identified mostly correspond to discrete geographic locations. Cluster 1 is restricted to Dar Chaoui; cluster 2 includes the neighbouring pueriparous populations of Ceuta and Taghramt; cluster 3 corresponds to the pueriparous population of Ceuta; cluster 4 includes the populations of Spirada and Moulay, separated by c. 28.5 km; clusters 5 and 6 correspond to the *S. a. splendens* populations of Fifi and Talassemtane, respectively, and cluster 7 includes the populations of Adayourha and Jebel Sugna. Clusters 5, 6 and 7 all present patterns of admixture between each other, and admixture between clusters 4 and 7 was found in individuals of Spirada and Jebel Sugna.

While lack of better geographic coverage and population sample sizes may preclude in-depth analysis of hybridization and gene flow between populations, NEWHYBRIDS runs considering clusters 4-7, 5-7 or 4 and 7 consistently identify two parental populations which correspond roughly to clusters 4/7 *(S. a. tingitana*) and 5/6 *(S. a. splendens*), and also identify several of the admixed individuals as potential hybrids, though different sets of data result in different assignments of the admixed individuals to the distinct hybrid classes.

Pairwise F_{ST} values are overall higher when compared between clusters than between mitochondrial lineages (Table 2.2). The highest differentiation between clusters (0.213) is found between 1 and 3, which are geographically separated by c. 51 km, while the lowest (0.079) occurs between 4 and 7, which have a contact zone near Moulay where cluster 4 is shared between *S. a. tingitana* sublineages 2 and 3. Differentiation is highest between *S. a. tingitana* 1 and *S. a. splendens* 1, and lowest between *S. a.*

tingitana 2 and 3.

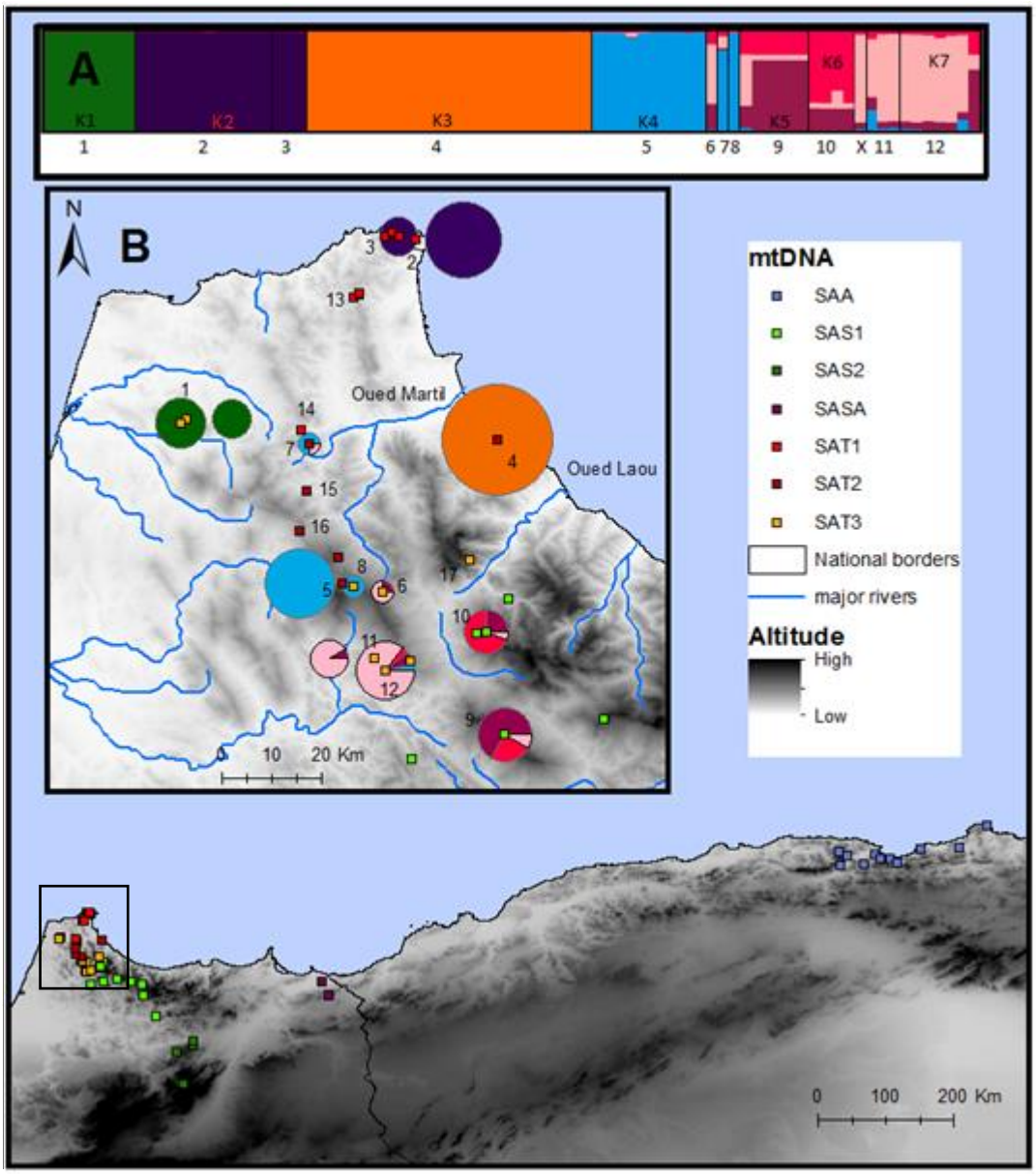

Figure 2.3 Bottom: Distribution of mitochondrial lineages in North Africa; inset A: STRUCTURE plot for K=7. Inset B: Detail of the distribution of mitochondrial lineages (squares) and genetic demes (circles) in the Rif, as well as main river systems. Size of circles representing genetic demes reflects sample size. Abbreviations: SAA: *S. a. algira*, SAS1: *S. a. splendens* 1, SAS2: *S. a. splendens* 2, SASA: *S. a. spelaea*, SAT1: *S. a. tingitana* 1, SAT2: *S. a. tingitana* 2, SAT3: *S. a. tingitana* 3; Numbers in insets A and B represent sampling localities: 1: Dar Chaoui, 2: Ceuta, 3: Jebel Musa, 4: Ansa, Tetouan, 5: Moulay 1, 6: Adayourha, 7: Spirada, 8: Moulay 2, 9: Fifi, 10: Talassemtane, 11: Jebel Sugna 1, 12: Jebel Sugna 2, 13: Taghramt, 14: Ain Lahsen, 15: Jbel Hamziouat,16: Tazia, 17: Beni Maharone. The 'X' in inset A identifies a population sampled in Jebel Sugna for which the precise geographic location is not known

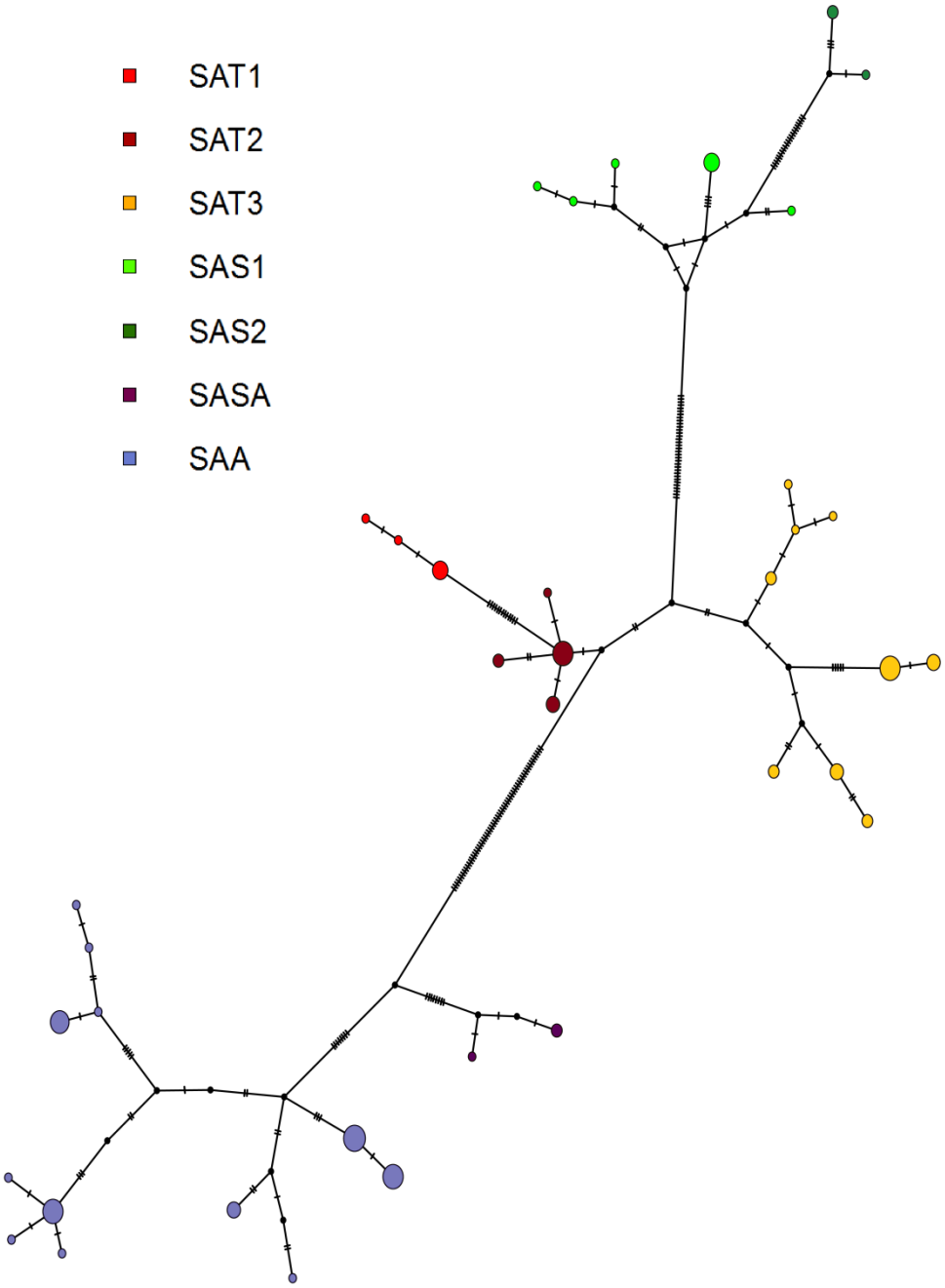

Figure 2.4 Median Joining *cyt-b* haplotype network. SAT1: *S. a. tingitana* 1; SAT2: *S. a. tingitana* 2; SAT3: *S. a. tingitana* 3; SAS1: *S. a. splendens* 1; SAS2: *S. a. splendens* 2; SASA: *S. a. spelaea*; SAA: *S. a. algira.*

Table 2.2 Pairwise F_{ST} values between clusters as assigned by STRUCTURE (Top half) and between mitochondrial lineages (bottom left). F_{ST} values are displayed below the diagonal, and probability based on 999 permutations above the diagonal. Descriptive statistics comparing the values by cluster and by lineage are also displayed (bottom right). K1-7: Cluster 1-7; tin1-3: *S. a. tingitana* lineages 1-3; spl1: *S. a. splendens* lineage 1; Avg: average; SD: Standard deviation; Max: maximum; Min: minimum

Pairwise Fst Values by Structure clusters

	K1	K2	K3	K4	K5	K6	K7
K1		0.001	0.001	0.001	0.002	0.004	0.001
K2	0.182		0.001	0.001	0.001	0.001	0.001
K3	0.213	0.131		0.001	0.001	0.001	0.001
K4	0.138	0.124	0.122		0.001	0.002	0.001
K5	0.191	0.152	0.170	0.121		0.004	0.002
K6	0.190	0.139	0.145	0.130	0.094		0.001
K7	0.158	0.125	0.096	0.079	0.101	0.113	

	Pairwise Fst Values by mtDNA lineage					**K**	**mtDNA**
	tin1	tin2	tin3	Spl1			
tin1		0.002	0.003	0.003	Avg	0.139	0.100
tin2	0.121		0.001	0.001	SD	0.035	0.028
tin3	0.121	0.056		0.001	Max	0.213	0.135
spl1	0.135	0.094	0.074		Min	0.079	0.056

2.4 Discussion

2.4.1 Phylogenetic relationships within *Salamandra algira*

The phylogenetic approach performed in this work had the primary objective of clarifying the distribution of mitochondrial diversity in the Rif, and its applicability for a full assessment of the evolutionary history of *S. algira* is limited by the use of a single evolutionary unit (mtDNA). Nonetheless, the structure of the phylogenetic tree created in this work agrees with previously proposed scenarios for the diversification of *S. algira*. An early east-west split 3.6-7.4 MYA (Beukema et al., 2010; Ben Hassine et al., 2016) was followed by divergence between the eastern subspecies *S. a. algira* and *S. a. spelaea* 2.5 MYA (Ben Hassine, 2016), and between the western subspecies *S. a. tingitana* and *S. a. splendens* 1.6-3.8 MYA (Beukema et al., 2010; Ben Hassine et al., 2016).

Subsequent diversification within *S. a. tingitana* consisted of a basal split of sublineage 3, 0.8 MYA, followed by the split between sublineages 1 and 2, 0.6 MYA (Beukema et al., 2010). The two *S. a. splendens* sublineages have been proposed to have diverged approximately at the same time than *S. a. tingitana*, 0.7 MYA (Beukema et al., 2010). However, the high genetic distance and number of substitutions separating *S. a. splendens* from other lineages of *S. algira* suggest this lineage may have undergone a deep divergence, and the same is true for the divergence between its sublineages, which would reflect prolonged vicariance between them.

The low genetic distance between subspecies *S. a. spelaea* and *S. a. algira* (0.02) has raised the question of whether *S. a. spelaea* truly represents a distinct subspecies or simply a highly divergent branch of *S. a. algira* (Ben Hassine et al., 2016). The genetic distance between these subspecies uncovered in the present work is similar, and further reinforces the doubts regarding the taxonomical classification of *S. a. spelaea*.

The lack of insight using nuclear marker *B-fibint7* hinders a more detailed assessment of the evolutionary history of *S. algira*. Previous attempts to draw phylogenetic inferences on *Salamandra* species using other nuclear markers have also been unsuccessful, due to low genetic variation and ample haplotype sharing (Ben Hassine et al., 2016; Vences et al., 2014), which may reflect widespread incomplete lineage sorting caused by the relatively young age of clades within this genus (Vences et al., 2014).

2.4.2 Patterns of genetic diversity in the Rif

An important contribution was made to our understanding of the distribution of *S. algira*, with the addition of 12 new localities where salamander presence had never been described before, filling important gaps in the Rif and Middle Atlas. Knowledge on the distribution of Rif mitochondrial sublineages was greatly improved, providing a particularly important clarification of the distribution of *S. a. tingitana* sublineages. Previous work on the distribution of *S. algira* in the Rif hypothesized Oued Martil to represent a contact zone between *S. a. tingitana* sublineages 1 and 2, with sublineage 3 being restricted to two isolated populations in Jebel Sugna and Beni Maharone, just north of the contact zone with *S. a. splendens* sublineage 1, in Oued Laou (Beukema et al., 2010). A later work identified an isolated population of *S. a. tingitana* sublineage

3 in Dar Chaoui, marking the first known occurrence of a sublineage other than *S. a. tingitana* sublineage 1 north of Oued Martil (Velo-Antón et al., 2014). In this work, a population of *S. a. tingitana* sublineage 2 is reported for the first time north of Oued Martil, in the locality of Spirada. Together with the new populations uncovered in Ansa and Moulay, this sets new northern, eastern and southern limits to the distribution of this sublineage. The known distribution of *S. a. tingitana* sublineage 3 was also expanded with the discovery of populations north of Jebel Sugna, in the localities of Adayourha and Moulay.

Results obtained from microsatellite data allowed a more accurate identification of secondary contact between *S. algira* sublineages in the Rif. Ample admixture was found between the populations of Adayourha/Jebel Sugna and Fifi/Talassemtane, located northwest and southeast of Oued Laou respectively and belonging to subspecies *S. a. tingitana* and *S. a. splendens*. The two populations of *S. a. splendens* represented are predominantly assigned to distinct genetic demes (K5 and K6), which suggests some degree of distinctiveness between them, yet both show admixture with each other and with the southernmost *S. a. tingitana* populations. At this point it is not clear what are the drivers of population structure and predominant direction of gene flow in this area, and increased representation of nearby populations on both sides of Oued Laou will be necessary to allow a clarification of the interaction between subspecies on this contact zone.

Regarding evidence of gene flow between *S. a. tingitana* sublineages 1 and 2 in their suggested contact zone along Oued Martil, our results are not conclusive due to limited sampling data north of Oued Martil. The sparsely vegetated character of this region, when compared to the rest of the Rif, reduces salamander habitat and hinders sampling. However, the proximity of the Spirada population of *S. a. tingitana* sublineage 2 to a population of sublineage 1 (c. 3.5 km) might indicate ongoing gene glow between these two sublineages.

We found clear evidences of population structure along the Rif. The populations of Dar Chaoui (sublineage 3), Ceuta/Jebel Musa (sublineage 1) and Ansa (sublineage 2) were assigned to distinct and unique genetic demes (K1, K2 and K3, respectively), which may reflect some manner of population structure isolating them from each other, as well as from other populations of their respective lineages, or simply be a signature of

isolation by distance, compounded by insufficient sampling in the areas between them. On the other hand, shared membership to the same genetic deme (K7) between the populations of Jebel Sugna and Adayourha provides evidence of gene flow and a potentially continuous distribution connecting these populations of *S. a. tingitana* sublineage 3. In the nearby locality of Moulay, the occurrence of a genetic deme (K4) shared by nearby populations of sublineages 2 and 3 suggests gene flow between mitochondrial lineages, suggesting that mitochondrial and nuclear contact zones occur in the Adayourha-Moulay region, yet are non-overlapping. The presence of admixture between K4 and K7 in the Spirada population, located c. 30 km north of Moulay, also suggests these contact zones are likely more complex than a simple north/south barrier, and their full delineation would require a further understanding of population structure in the region, particularly in the area between Moulay and Spirada.

The detection of putative hybrids between mitochondrial sublineages, observed pattern of admixture between both sublineages and genetic demes, and overall greater values of pairwise F_{ST} between isolated populations than between sublineages, all represent strong evidence of a lack of reproductive barriers within the western clade of *S. algira*. While male-biased dispersal has not, to the best of our knowledge, been confirmed for the *Salamandra* genus, it has been hypothesized as an explanation for patterns of introgression in *S. salamandra* (García-París et al., 2003), and could also account for the distribution of genetic diversity of *S. algira* in the Rif.

2.4.3 Evolutionary context of pueriparity

The discovery of pueriparous reproductive behaviour in a population of *S. a. tingitana* sublineage 2 near Tetouan marks the first observation of this strategy outside of sublineage 1 of the same subspecies. Pueriparity in the sister species *S. salamandra*, the only other case of intraspecific variation in reproductive modes among salamanders, is believed to have evolved independently at least two or three times: one in the Cantabrian mountains and in shared or independent events in the two insular populations of Galicia (García-París et al., 2003; Velo-Antón et al., 2007, 2012). For the former, pueriparity likely spread east across the Cantabrian mountains under a model of mtDNA capture where nuclear DNA crossed contact zones faster than mitochondrial DNA, possibly due to a combination of male-biased dispersal and

selection for traits coded in the nuclear genome, which may include pueriparity itself (García-París et al., 2003).

Given the widespread and mutually independent occurrence of pueriparity in four *Salamandra* species, and the fact that pueriparity in salamanders is related to an association between heterochronic processes during embryonic development and intrauterine cannibalism (Buckley et al., 2007), the transition to pueriparity appears to be relatively easy. Therefore, the occurrence of independent episodes of pueriparity evolution in distinct mitochondrial sublineages of *S. algira tingitana* is likely. However, the restricted geographic extent of the distribution of *S. a. tingitana* and the close proximity between the distributions of the sublineages where pueriparity is observed suggest that an adoption of pueriparity across contact zones by means of mtDNA capture should be considered as an alternative scenario to explain pueriparity occurring in two *S. a. tingitana* sublineages. The present results do not allow a choice of one explanatory hypothesis over the other and more information is necessary on the location of contact zones between the two sublineages exhibiting pueriparity and on how widespread this reproductive strategy is south of Oued Martil. Also fundamental is the consideration of phylogenetic information capable of reflecting evolutionary patterns of the nuclear genome, which is at this point non-existent.

Aknowledgements

We thank Javier Medina, Saul Yubero, Francisco Giménez and Luis García-Cardenete for sharing tissue samples.

Chapter 3: Historical and contemporary ecological niche of *S. algira* (Manuscript II)

3.1 Introduction

The remarkable degree of endemism found in North Africa (Myers et al., 2000; Husseman et al., 2013; Martínez-Freiría et al., 2013) is mostly due to its location at a crossroad of distinct biogeographic regions, reflected in a species composition originated in distinct northern Palearctic, Afrotropical and arid Palearctic sources (Dobson & Wright, 2000). Delimited north and south by the Mediterranean Sea and the Sahara Desert, respectively, its relatively low permeability to long-range colonization, and particularly to jump dispersal from Southern Europe (Dobson & Wright, 2000), has allowed periods of isolation which promoted diversification and, consequently, the emergence of unique taxa. Moreover, as a result of the proximity to the Sahara, aridity has historically acted as a limiting factor to the distribution of taxa, particularly those of northern Palearctic affinities, promoting strong phylogeographic structure among local taxa (Cosson et al., 2005).

Two predominant biogeographic patterns can be retrieved within northern Palearctic species. The first is a dual role of mountain systems as both geographical barriers and climatic refugia, with the Rif and the Atlas systems being particularly important in this regard (e.g. Barata et al., 2008, 2012; Beukema et al., 2010; Nicolas et al., 2015; Veríssimo et al., 2016). The second is a tendency for divergence within lineages to occur along a west-east axis (e.g. Beukema et al., 2010; Velo-Antón et al., 2012a; Stuckas et al., 2014), which has been proposed to be associated with historical sea transgression of river valleys (Veith et al., 2004; Paulo et al., 2008) or with periods of climatic fluctuations ranging from humid to hyper-arid conditions (Cosson et al., 2005), and particularly with periods of aridity in the Moulouya river basin (Alvarez et al., 2000; Barata et al., 2008). These patterns, which are known to have sometimes acted together in shaping the evolutionary history of a species (as suggested for *Salamandra algira,* Beukema et al., 2010), point towards a predominantly allopatric model of diversification, with ecological niche conservatism promoting vicariance as past climatic oscillations created barriers of unsuitable environmental conditions between populations.

However, smaller-scale patterns of divergence have not been assessed with sufficient detail. The previous chapter of the present work revealed that despite the existence of well-defined mitochondrial lineages of *S. algira* in the Moroccan Rif, there is evidence

of gene flow, which suggests a pattern of at least partial overlap in their present distribution. A model of allopatric divergence on distinct mountainous refugia followed by secondary contact facilitated by niche conservatism fits well with these results (Futuyma, 1998; Coyne & Orr, 2004), yet this has not been demonstrated conclusively. Considering that the sublineages that occur in the Rif belong to two distinct subspecies showing evidence of hybridization in a narrow contact zone, it is pertinent to verify how adequately niche conservatism in allopatry can explain the diversification of subspecies and respective sublineages in *S. algira*. Furthermore, the occurrence of pueriparity among some Rifean populations of *S. algira* (Donaire-Barroso & Bogaerts, 2003; Beukema et al., 2010; previous chapter of this thesis) raises the question of whether differential adaptation to local environments has occurred among distinct populations, and if so, did niche divergence promote a sympatric mode of diversification or was allopatric divergence followed by stochastic niche divergence?

Previous work using ecological niche-based models had uncovered distinct ecological requirements and non-overlapping distributions for pueriparous and larviparous populations of the *S. a. tingitana* subspecies (Beukema et al., 2010). However, this work was based on the assumption that pueriparity was restricted only to the northernmost lineage of this subspecies. The recent discovery of a pueriparous population in another lineage (as seen in the previous chapter of this work) adds an additional layer of complexity to the subject, and opens the non-exclusive possibilities of either multiple independent episodes of emergence of pueriparity, or a pattern of introgression promoting the spread of the trait across mitochondrial contact zones, both hypotheses having been previously proposed to explain the distribution of pueriparity among Iberian populations of the sister species *S. salamandra* (García-Paris et al., 2003; Velo-Antón et al., 2007). A deeper understanding of the biogeographic patterns and ecological requirements of *S. algira*, and particularly of its Rifean populations, is fundamental to provide further insight on these issues. In this context, the objectives of this chapter are to a) reconstruct the biogeographic history of *S. algira* in North Africa and in the Rif; b) characterize the potential distribution and assess the relative importance of distinct niche components for the Rif lineages; and c) estimate the degree of ecological niche divergence and its role on the evolutionary differentiation among subspecies and within the Rif.

3.2 Methods

3.2.1 Reconstruction of the biogeographic history of *S. algira* in North Africa and in the Rif

3.2.1.1 Data selection and preparation

A database of 329 geo-referenced presence points across the entire range of *S. algira* was compiled, including 84 previously published points collected between 1995 and 2016 (Donaire-Barroso & Bogaerts, 2003; Escoriza & Comas, 2007; Beukema et al., 2010; Vences et al., 2014; Velo-Antón et al., 2014; Merabet et al., 2016; Ben Hassine et al., 2016), as well as 245 new occurrence records collected during the year 2015 (61 of which were kindly provided by Wouter Beukema). Ocurrence records were verified to ensure their format was consistent across the entire database. The database was projected on ArcGIS 10.1 (ESRI, 2008) to confirm correct geographical placement of each occurrence record and eliminate redundant records. Records were assigned to the correct subspecies and sublineages based on their geographical location (assuming Oued Laou to be the border between subspecies *S. a. tingitana* and *S. a. splendens*), available morphological data and information on mitochondrial haplotype (Beukema et al., 2010; previous chapter of this thesis). Ocurrence records of uncertain membership and those belonging to subspecies *S. a. spelaea* (which due to this subspecies' highly restricted distribution and low number of records is unviable for construction of niche models) were eliminated.

The construction of a database based on all available occurrence records, rather than on a specific sampling design, opens the possibility of bias in sampling effort, which can dramatically affect ecological niche model predictions (Merow et al., 2013). Spatial filtering of occurrence records has been demonstrated to be one of the best solutions to account for sampling bias (Kramer-Schadt et al., 2013), and was implemented in this work by the widely accepted approach of reducing the level of clustering of the occurrence data (e. g. Martínez-Freiría et al., 2015, 2016; Vale et al., 2016). The degree of data clustering was first verified with the Nearest Neighbor Index (NNI), using the Average Nearest Neighbor tool on ArcGIS. For the subspecies and sublineages where clustering was identified, occurrence records were removed by superimposing

the occurrence records over a 5 x 5 km grid created using the Create Fishnet tool on ArcGIS, and eliminating random records in order to leave only one record per grid cell. The level of clustering was re-assessed following this procedure to confirm the effective decrease in the level of clustering. The final database consisted of 97 occurrence records: 15 for *S. a. algira*, 41 for *S. a. tingitana* and 41 for *S. a. splendens* (Figure 3.1).

To detect biogeographic patterns within the Rif, the 97 occurrence records available were further restricted to exclude populations outside the Rif. Occurrence points of uncertain membership were also excluded, particularly those located between Oued Laou and Oued Martil and for which no genetic information is available, as lack of more detailed molecular information hinders a complete clarification of the limits of the distribution of *S. a. tingitana* lineages 2 and 3 (See previous chapter). A total of 16 points for *S. a. tingitana* sublineage 1, 7 for *S. a. tingitana* sublineage 2, 11 for *S. a. tingitana* sublineage 3 and 21 for *S. a. splendens* sublineage 1 were considered (Figure 3.1).

3.2.1.2 Study area and variable selection

Nineteen climatic variable layers for present conditions, as well as reconstructions of the same variables for the Mid-Holocene (~ 6K years ago), Last Glacial Maximum (LGM; ~ 20K) and Last Inter-Glacial (LIG; ~ 120K), were obtained from the WorldClim database (http://www.worldclim.org; Hijmans et al., 2005). All climatic layers were obtained at a spatial resolution of 30 arc seconds (~ 1 x 1 km), except for the LGM, which were only available at 5 x 5 km. LGM scenarios accounted for three Global Circulation Models (MIROC-ESM (LGMme), Watanabe et al., 2011; CCSM4 (LGMcc), Gent et al., 2011; MPI-ESM (LGMmi), Giorgetta et al., 2013). While non-climatic variables are known to be relevant for the distribution of *S. algira* (Beukema et al., 2010), climate is expected to be the main factor shaping species distributions at large spatial scales (Mackey & Lindenmayer, 2001; Elith & Leathwick, 2009) and is known to have a major effect in the distribution and abundance of ectotherm species (Guisan & Hoffer, 2003; Pearson et al., 2004; Anadón et al., 2007, 2015). Moreover, the unavailability of non-climatic variables for past conditions hinders their usefulness in biogeographic studies using historical reconstructions.

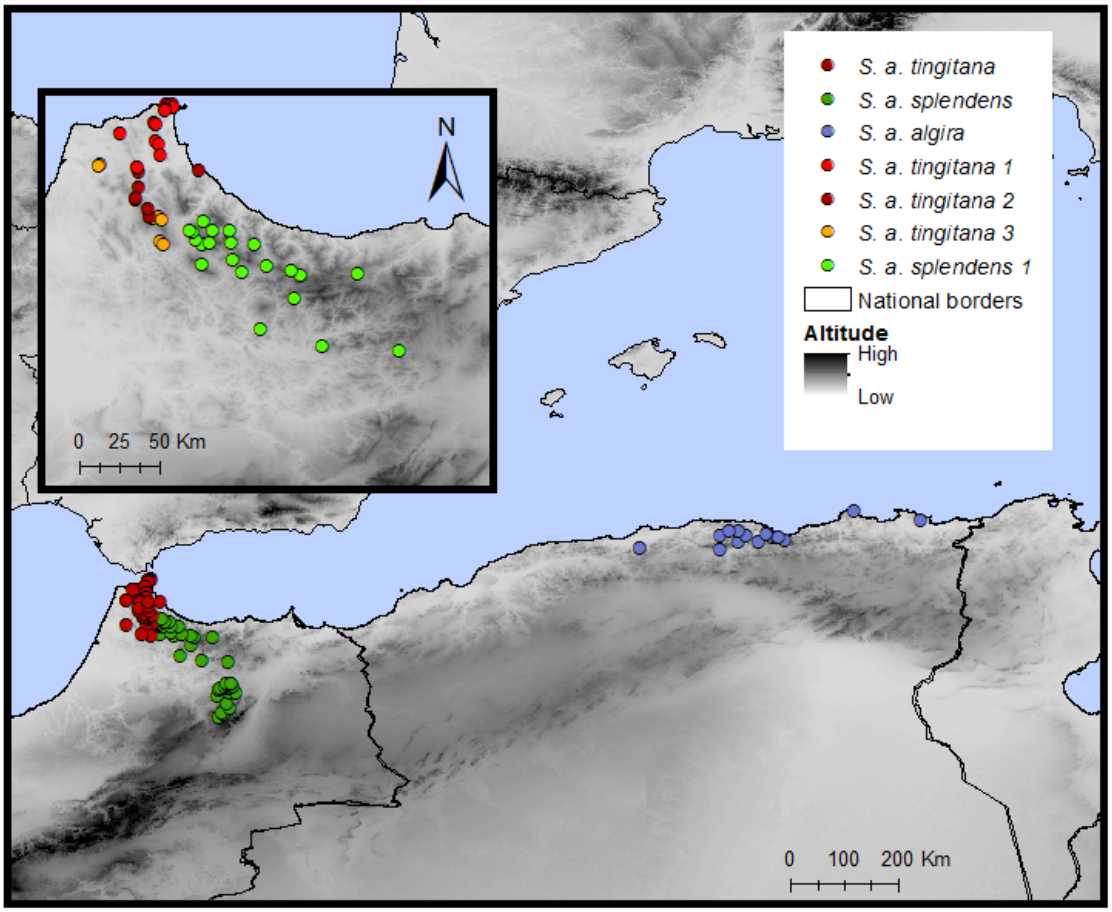

Figure 3.1 Location of occurrence records used for performing ecological niche-based models. Main image shows the presence data used for modeling subspecies, while inbox displays those used for modeling of Rif sublineages. Topography of the main mountain systems in the region is also represented.

Climatic variables were tested for spatial correlation using the Band Collection Statistics tool from ArcGIS and a set of seven not highly correlated variables ($R < 0.7$) was chosen to perform ecological niche-based models (ENM) and projections to past conditions (Table 3.1).

The limits of the study area for each lineage were defined by delimiting a 200 km buffer around the minimum convex polygon including all points assigned to the lineage. This intermediate area takes into consideration coarse distributional patterns, topography and vegetational zones, and was chosen to prevent biases in the sampling of background data, which are known to occur when using restricted or overly broad training areas (VanDerWal et al., 2009; Anderson & Raza, 2010). All steps were performed on ArcGIS, using the Minimum Bounding Geometry tool to create the

minimum convex polygon, Select By Location options to set the buffer and Extract By Mask tool to cut each variable to the buffer area.

3.2.1.3 Ecological niche modeling

Two regression-based and two machine learning algorithms were initially considered to model the geographic range of the subspecies and sublineages and project it to past conditions. However, low sample sizes hampered the development of accurate models and thus only models developed with the Maximum Entropy algorithm Maxent (Phillips et al., 2006), which has been shown to perform well even with low sample sizes (Elith et al., 2006; Hernandez et al., 2006), are considered in this chapter. Details on model construction and results from other modelling techniques can be consulted in Supplementary Materials.

The maximum entropy technique, as implemented in MAXENT (Phillips et al., 2006), was used to develop niche-based models and projections to past climatic conditions, using automatic limiting of feature types and a regularization multiplier of 1. 10,000 background points were generated randomly by MAXENT for each run. Each model was created by running 50 bootstraps, each time setting aside 30% of the available presence points for model testing. Forecasts of suitability were created by averaging the 50 replicates for each taxon, as consensus methods based on average functions increase the accuracy of species distribution forecasts (Marmion et al., 2009).

Model accuracy was verified by observing the training and test Area Under the Curve (AUC) of the Receiving Operator Characteristic (ROC). Observation of standard deviation plots was also taken into consideration when assessing model performance. The importance of environmental variables for each model was determined by the average percentage of contribution, permutation importance, and by jackknife analysis which consisted of performing model training first with each variable omitted, and then used in isolation (Phillips, 2006). Response curves for the most important variables were visually inspected to detect differences in ecological affinities between taxa.

Average consensus models of the replicates were projected to the area of the full species' distribution in the present to identify areas of overlap between subspecies, as well as to the same area under the climatic conditions of the LIG, Mid-Holocene, and LGM to identify areas of past climatic suitability and evaluate the responses of taxa to

past climatic oscillations at the regional scale. Projections used the Fade By Clamping option, to reduce the error associated with projecting to environmental conditions beyond the range used for training (Phillips, 2008a, b).

The probabilistic consensus models were converted to binary suitability models by applying the minimum probability threshold, reclassifying as suitable all probability values above that of the minimum probability where presence points occur, and all values below it as unsuitable. This task was performed using the Reclassify tool in ArcGIS.

Stable climatic areas were identified by detection of suitable areas that overlap between different time periods, using the Reclassify and Raster Calculator tools in ArcGIS. As three distinct projections were available for the LGM, first a consensus between the three LGM predictions was created. Only the areas where two or more LGM projections overlap were considered as suitable, and were then overlapped with the projections for the LIG, Mid-Holocene and present. The areas predicted to be suitable on all time periods were identified as stable.

3.2.2 Present distribution of Rif lineages and relative importance of their niche components

3.2.2.1 Data selection and preparation

In order to ensure comparability between different components of the environmental conditions relevant for *S. algira*, occurrence data and study area delimitation for *S. a. tingitana* sublineages 1, 2 and 3, as well as for *S. a. splendens* sublineage 1, were performed as described on section 3.2.1.1 Regarding variable selection, two distinct levels of niche modeling were performed: (1) using a set of variables related to habitat requirements of salamanders; and (2) using a combined dataset of the climatic and habitat variables found to contribute the most to the climate and habitat models previously created.

Vegetation availability is known to be an important requirement for *S. algira* (Ben Hassine & Escoriza, 2014), and there is evidence that populations in the North of the Tingitana peninsula may be less reliant on it than other populations, possibly due to availability of more stable climate in the region (Beukema et al., 2010; Escoriza & Ben

Hassine, 2014). It should, therefore, be a relevant variable in any potential differentiation between lineages. Temporal patterns of variation in vegetation productivity were represented by a time series of Normalized Difference Vegetation Index (NDVI) data. Pre-calculated NDVI layers at 250 m spatial resolution were obtained from the MOD13Q1 product of the MODIS Terra satellite, available at NASA's Land Processes Distributed Active Archive Center (LP DAAC, https://lpdaac/usgs.gov). NDVI layers were collected at an interval of 15 days for a period of time spanning the last 15 years (2000-2015), to allow characterization of annual and seasonal variation in vegetation cover, as well as to minimize the effect of extremes of vegetation productivity. Using the Cell Statistics tool on ArcGIS, two distinct vegetation layers were created, one for the average and another for the standard deviation of the NDVI for the period of salamander activity (October to May, corresponding to 240 distinct collection dates) over the entire temporal range considered.

Surface water is an important resource for larviparous salamanders, as it is fundamental for their reproductive cycle. In the case of pueriparous populations, the dry climate hypothesis dictates that being able to bypass the aquatic stage decreases the dependence on surface water (García-Paris et al., 2003; Velo-Antón et al., 2007; Beukema et al., 2010), making it a suitable variable for the detection of ecological differences between *S. algira* lineages. Identification of areas of surface water availability was performed by calculating the Normalized Difference Water Index (NDWI) for the study area. Landsat8 satellite images collected between 2013 and 2015 were obtained from the USGS Global Visualization Viewer (http://glovis.usgs.gov). Landsat8 images were chosen due to their high spatial resolution grain of 30 m, which was expected to be suitable for detection of ponds and other small water bodies which *S. algira* relies upon for reproduction. To include the entire training area of all groups to be modeled, Landsat8 images were collected for nine distinct Glovis path/row combinations (Table 7.3, Supplementary Materials). Images were selected based on Glovis' quality index (equal to or higher than 9) and cloud cover estimate (less than 10%), as well as visual inspection of images to exclude those with extensive cloud cover. Atmospheric corrections were performed on PCI Geomatica version 10 (PCIGE INC, 2010) to remove distortions caused by haze and clouds not detected in previous steps, and thus prevent color balancing issues when aggregating images into mosaics. Images were then sorted by whether they were collected in the dry or wet season, and

for each season images were aggregated into mosaics to cover the whole study area, using the Orthoengine Mosaic tools on PCI Geomatica. Average mosaics were then calculated for the dry and wet season, and NDWI's were calculated using Xu's $NDWI_{G/MIR}$ ((G-MIR)/(G+MIR)) (Xu, 2006) and Gao's $NDWI_{NIR/MIR}$ (NIR-MIR)/(NIR+MIR) (Gao, 1996), which have been described as being differentially suitable for the detection of permanent and seasonal water bodies, respectively (Campos et al., 2012). Image averaging and NDWI calculations were done on ArcGIS using the Cell Statistics and Raster Calculator tools, respectively.

Categorical maps of surface lithology (300 m of pixel size; Sayre et al., 2013) and land cover (GLOBCOVER 2006, 250 m; Bicheron et al., 2008) were converted to a set of binary grids for each relevant class. The lithological classes selected were carbonate and non-carbonate lithology, as they are predominant in the distribution of *S. algira*, and are expected to have distinct patterns of surface water availability, and consequently distinct importance for pueriparous and larviparous populations. Regarding land cover, all classes where *S. algira* records exist were considered. Conversion of categorical maps to continuous variables was performed on ArcGIS in a two-step process: first by using the Reclassify tool to create a binary map, with the variable of interest being classified as "1" and everything else as "No Data"; then, the Euclidean Distance tool was used to calculate the distance from each pixel in the study area to the category of interest. This process was repeated for each relevant variable.

Terrain ruggedness was obtained by calculating the Vector Ruggedness Measure (VRM) using the VRM extension for ArcGIS (http://www.arcgis.com/home/item.html?id=9e4210b3ee7b413bbb1f98fb9c5b22d4). This approach effectively captures variability in slope and aspect into a single measure, and appears to decouple terrain ruggedness from slope better than commonly used ruggedness indices such as TRI or LSRI (Sappington et al., 2007). VRM was calculated based on the SRTM Digital Elevation Map (90 m) (Jarvis et al., 2008).

All variables were extracted for the study area using the Extract By Mask tool and upscaled to the spatial resolution of the coarsest variable used (300 m), to avoid artifacts related with downscaling. A spatial correlation matrix was calculated to exclude highly correlated (R>0.7) variables, resulting in a set of nine not highly correlated variables (Table 3.2). Gao's $NDWI_{NIR/MIR}$ layers were excluded, as visual inspection

verified a lack of ability to predict known water sources and a tendency to overestimate NDWI values in urban areas, which might bias the models. High spatial correlation (>0.9) between Xu's $NDWI_{G/MIR}$ layers for the wet and dry season resulted in the exclusion of the layer for the dry season, as it is expected that conditions during the season of salamander activity are more important than those verified during periods of dormancy. All land cover layers were excluded due to high spatial correlation with the average NDVI layer, except for those representing closed-to-open shrubland and mosaics of vegetation/cropland and forest/shrubland.

Models were created on MAXENT and converted to binary suitability maps using the same parameters and approach described in section 3.2.1.3. All models were projected to a common area covering the entirety of the Rif, to detect potential areas of overlap beyond the range of the training areas of individual lineages.

3.2.2.2 Development of combined models and identification of areas of sympatry

Variable selection was performed by visualizing the individual variable contribution for each of the habitat and climate models created for the Rif lineages, and selecting those which were frequently classified as most important. Variables were upscaled to the coarsest spatial resolution (1 km). Correlation between variables, MAXENT model creation and projection to the entirety of the Rif area were handled as described in the previous section.

Combined models were developed using a set of four climate and four habitat variables (Table 3.2). High spatial correlation between two of the most important variables of the previous models (precipitation of the wettest quarter and average NDVI) led to the exclusion of the latter, as it is expected that at the coarser scale of 1 x 1 km (as opposed to the scale of 300 x 300 m used for the habitat models), climate should be a more suitable predictor of species distribution than habitat (Mackey & Lindenmaiyer, 2001; Elith & Leathwick, 2009).

Models were created on MAXENT and converted to binary suitability maps using the same parameters and approach described in section 3.2.1.3. All models were projected to a common area covering the entirety of the Rif, to detect potential areas of overlap

beyond the range of the training areas of individual lineages. The Raster Calculator tool of ArcGIS was used to sum the binary models, to obtain a map of areas of sympatry.

Table 3.1 Description, code, units and range (minimum and maximum) of the climatic and habitat variables used for model creation. Combined variables were the ones which contributed the most for climatic and habitat models and were thus used for the creation of combined models

Climatic variables	**Code**	**Units**	**Range**
Isothermality (BIO2/BIO7)	BIO3		26 - 52
Temperature Seasonality (SD*100)	BIO4		3459 - 8202
Max Temperature of Warmest Month	BIO5	º	25.7 - 45.8
Min Temperature of Coldest Month	BIO6	º	-13.2 - 9.4
Mean Temperature of Driest Quarter	BIO9	º	8.6 - 32.8
Precipitation of Wettest Quarter	BIO16	mm	38 - 707
Precipitation of Warmest Quarter	BIO18	mm	7 - 102
Habitat variables			
Average NDVI of the wet season	NDVIAV		- 0.3 - 0.87
Standard deviation of the wet season NDVI	NDVISD		0 - 0.53
Distance to carbonate lithology	GCARB	º	0 - 0.772
Distance to non-carbonate lithology	GNCARB	º	0 - 0.782
Distance to vegetation/cropland (50-70%/20-50%) mosaics	LVGCR	º	0 - 0.430
Distance to forest/shrubland mosaics	LFOSH	º	0 - 0.582
Distance to closed-to-open shrubland	LBNSH	º	0 - 1.751
Xu's $NDWI_{G/MIR}$ of the wet season	NDWIXW		-0.001 - 1
Vector Ruggedness Measure	VRM		0 - 0.998
Combined variables			
Temperature Seasonality (SD*100)	BIO4		3459 - 8202
Max Temperature of Warmest Month	BIO5	º	25.7 - 45.8
Precipitation of Wettest Quarter	BIO16	mm	38 - 707
Precipitation of Warmest Quarter	BIO18	mm	7 - 102
Distance to carbonate lithology	GCARB	º	0 - 0.772
Distance to non-carbonate lithology	GNCARB	º	0 - 0.782
Distance to forest/shrubland mosaics	LFOSH	º	0 - 0.582
Distance to closed-to-open shrubland	LBNSH	º	0 - 1.751

3.2.3 Ecological niche divergence and its role on the evolutionary differentiation among subspecies and within the Rif

ENMTools (Warren et al., 2008, 2010) was used to both quantify the degree of ecological niche overlap and test the contrasting hypotheses of niche conservatism versus niche divergence between pairs of lineages (subspecies), as well as between

pairs of sublineages in the Rif. Comparisons between subspecies were done only taking into account their responses to climatic variables, as biological distributions are mostly shaped by climate at large scales (Mackey & Lindenmaiyer, 2001; Elith & Leathwick, 2009), and it is therefore expected that any putative role of ecology in genetic differentiation at this scale would most likely express the effect of climate. For comparisons within the Rif, all sets of variables (climate, habitat and combined) were considered for tests of niche overlap, to obtain as complete a picture of the niche in its various components as possible. Niche overlap between each pair of models was calculated independently for each of the three sets of variables, using the models previously created as input. The hypotheses of niche equivalency and niche similarity were tested using identity tests and background tests, respectively. Niche similarity tests were performed to decouple the effects of differential habitat selection versus habitat availability on the niche overlap between lineages, by taking into account information on the geographic availability of environmental conditions (Warren et al., 2008). The same training areas used for the creation of niche models were used as background data for niche similarity tests. 50 pseudoreplicates were generated for each test. Due to the nonparametric nature of the data, significance of the difference between the empirical measurement of overlap and the null distributions of pseudoreplicates generated by identity and background tests was determined by Mann Whitney U tests on SPSS version 24.0 (IBM, 2016). Niche breadth was estimated using the inverse concentration index (Levins, 1968), with the previously developed models as input.

3.3 Results

3.3.1 Reconstruction of the biogeographic history

Overall model accuracy, as measured by the training and test Area Under the Curve (AUC) of the Receiving Operator Characteristic (ROC), was high (>0.94) for all climatic models (Table 3.2).

The most important variable related to the distribution of subspecies was the precipitation of the wettest season, with a contribution equal to or greater than 50 % on all models (Table 3.2). Minimum temperature of the coldest month also contributed importantly for the model for *S. a. splendens*. Regarding the models for the Rif

sublineages, precipitation of the wettest quarter was again the most important variable for all except *S. a. tingitana* 1, where temperature seasonality and maximum temperature of the warmest month were the variables with the most explanatory power (Table 3.2).

Table 3.2 Number of occurrence records, average (and SD) training/test AUC and average (and SD) variable percentage contribution for the climatic models of the three *S. algira* subspecies and four Rif sublineages. SAA: *S. a. algira;* SAS: *S. a. splendens*; SAT: *S. a. tingitana*; SAT1: *S. a. tingitana* 1; SAT2: *S. a. tingitana* 2; SAT3: *S. a. tingitana* 3; SAS1: *S. a. splendens* 1

		N	Performance metrics		Variable contribution						
			Training AUC	Test AUC	BIO3	BIO4	BIO5	BIO6	BIO9	BIO16	BIO18
Subspecies	**SAA**	15	0.971 (0.009)	0.956 (0.026)	5.6 (2.765)	6.2 (1.679)	9.8 (4.465)	7.1 (2.655)	0 (0.039)	**63 (7.155)**	8.8 (6.372)
	SAS	41	0.966 (0.010)	0.950 (0.026)	6 (4.536)	5.3 (2.554)	12 (6.701)	**26 (4.470)**	0.5 (6.591)	**50 (4.560)**	1.1 (1.177)
	SAT	41	0.975 (0.008)	0.961 (0.019)	4.9 (0.967)	11 (2.614)	15 (4.964)	2.9 (2.261)	1.3 (1.815)	**63 (8.196)**	2.2 (2.697)
Sublineages	**SAT1**	16	0.987 (0.006)	0.982 (0.011)	11.9 (3.484)	**24.9 (3.925)**	**45.3 (8.999)**	3.7 (3.009)	0.1 (0.355)	14 (5.688)	0.1 (0.104)
	SAT2	7	0.952 (0.010)	0.948 (0.027)	3.2 (3.123)	7.5 (12.153)	10.5 (5.854)	1 (1.295)	0 (0)	**77 (14.896)**	0.9 (1.360)
	SAT3	11	0.988 (0.004)	0.985 (0.010)	4.3 (3.827)	0.3 (1.123)	1.2 (2.360)	0.1 (0.330)	0.1 (0.519)	**93.9 (6.413)**	0 (0.045)
	SAS 1	21	0.975 (0.005)	0.965 (0.019)	1.8 (3.438)	0.8 (0.837)	4.1 (2.294)	18 (7.072)	6.7 (5.878)	**63.7 (7.605)**	4.8 (1.518)

In all models, precipitation of the wettest quarter show an overall direct response, with predicted suitability increasing as the precipitation increases, except for *S. a. splendens*, which has a bimodal response curve (Figure 3.2). The *S. a. tingitana* 1 model has an inverse relationship with its most important variables, reaching the highest predicted suitability at the lowest values of temperature seasonality and maximum temperature of the warmest month (Figure 3.2).

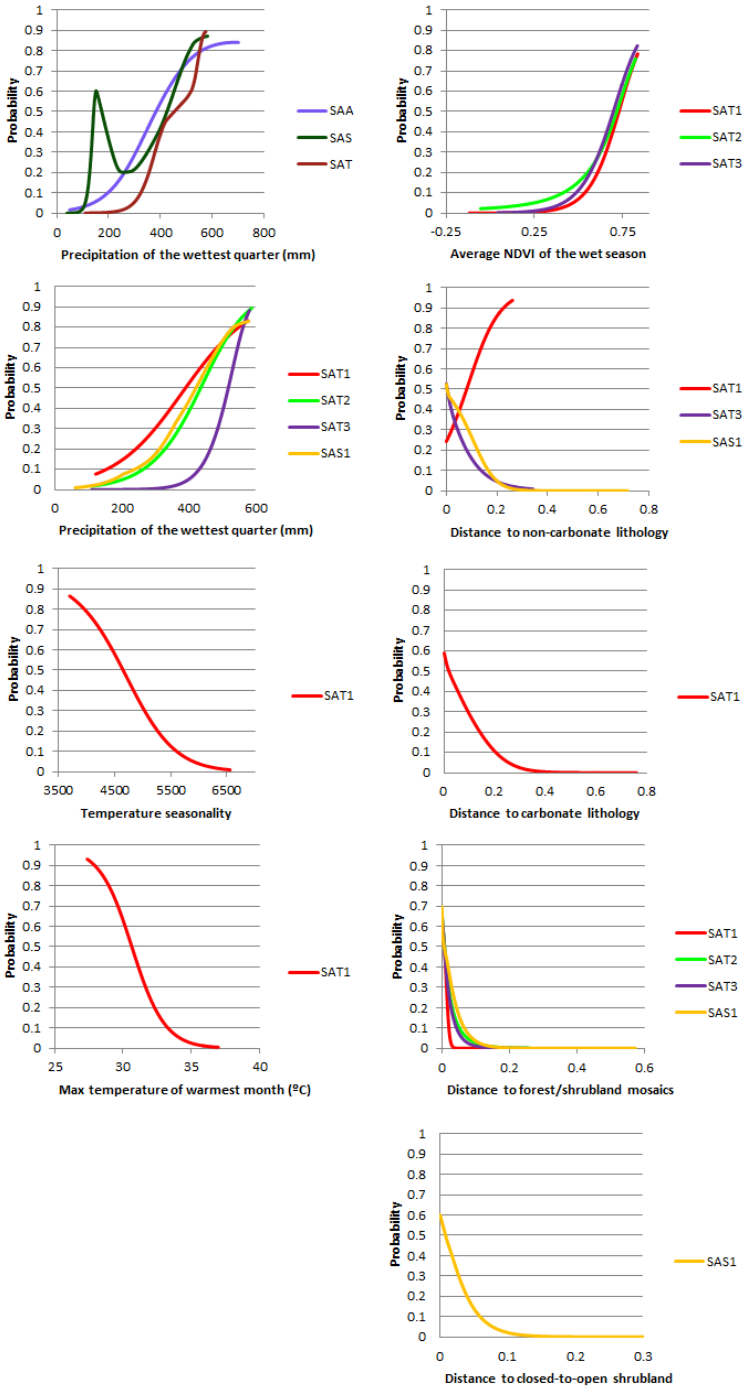

Figure 3.2 Response curves for the climate (left) and habitat (right) factors most relevant to the distribution of *S. algira* subspecies and sublineages. Curves depict the average predicted suitability of 50 model replicates along the environmental axes. SAA: *S. a. algira*; SAS: *S. a. splendens*; SAT: *S. a. tingitana*; SAT1: *S. a. tingitana* 1; SAT2: *S. a. tingitana* 2; SAT3: *S. a. tingitana* 3; SAS1: *S. a. splendens* 1

3.3.1.1 ENMs for subspecies

Probabilistic climatic models for the subspecies all predict areas of high suitability in the known range of the subspecies, yet also identify high suitability beyond the currently known distribution (Supplementary Materials, Figure 7.2). Binary models agree with this pattern, identifying suitable areas where the subspecies are not known to occur (Figure 3.3; Supplementary Materials, Figures 7.5-7.7). The model for *S. a. algira* predicts a mostly continuous distribution through the North of Algeria, with all occurrence records used in this study except the westernmost ones occupying the same continuous patch of suitable area (Supplementary Materials, Figure 7.5). Smaller isolated areas of suitability are identified in Tunisia, near the Morocco-Algeria border, and in the Rif (Supplementary Materials, Figure 7.5). The model for *S. a. splendens* identifies a large, almost continuous range that includes most of the Rif, Middle Atlas and the Algerian Tell Atlas, interrupted only in the arid Moulouya river basin (Figure 3.3; Supplementary Materials, Figure 7.6). The model for *S. a. tingitana* predicts a suitable area including the totality of the region north of Oued Laou, as well as an isolated area in Chefchaouen, and a portion of the Algerian and Tunisian coast similar to the one predicted by the *S. a. algira* model, though more restricted in area (Figure 3.3; Supplementary Materials, Figure 7.7).

Projections to the LIG show a similar pattern of severe range contraction for all subspecies, accompanied by a northwest range shift for *S. a. splendens*. For the LGM, all models predict drastic range expansion, which in the case of *S. a. splendens* and *S. a. tingitana* established connectivity between the Rif and the Algerian coastline, while for *S. a. algira* the expansion in Algeria is accompanied by the appearance of large isolated areas of suitability in the Rif and Middle Atlas. Projections to the Mid-Holocene are the most similar to the predicted present distribution, yet show distinct patterns among subspecies: while *S. a. tingitana* and *S. a. splendens* show a diminished range compared to the present, for *S. a. algira* a larger range is predicted (Figure 3.3; Supplementary Materials, Figures 7.5-7.7).

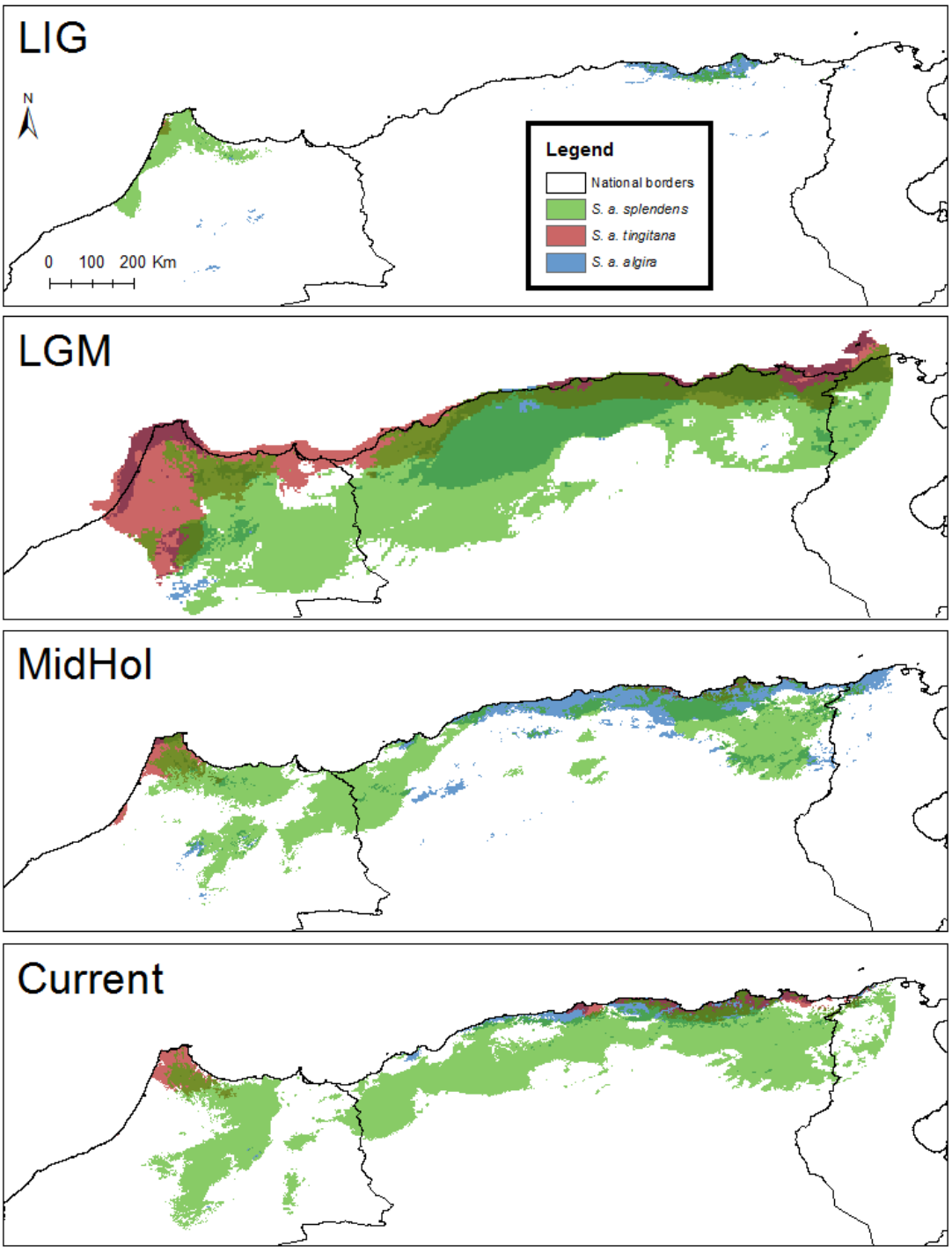

Figure 3.3 Binary models and projections to past conditions for the three subspecies of *S. algira*

Stable climatic areas are mostly restricted by the large range contractions experienced during the LIG, and are thus very similar to the predicted distributions for that period (Figure 3.4). An area of stability for *S. a. algira* was identified in the region of Kabylia,

but also some localized areas in the Middle Atlas of Moroco and western Tunisia. For *S. a. tingitana,* two stable areas were identified near Ceuta and in the western coast of the Tingitana peninsula, while for *S. a. splendens*, two isolated stable areas were identified along the Rif, on both sides of Oued Laou, as well as a third area in Algeria, which overlaps partially with that of *S. a. algira.*

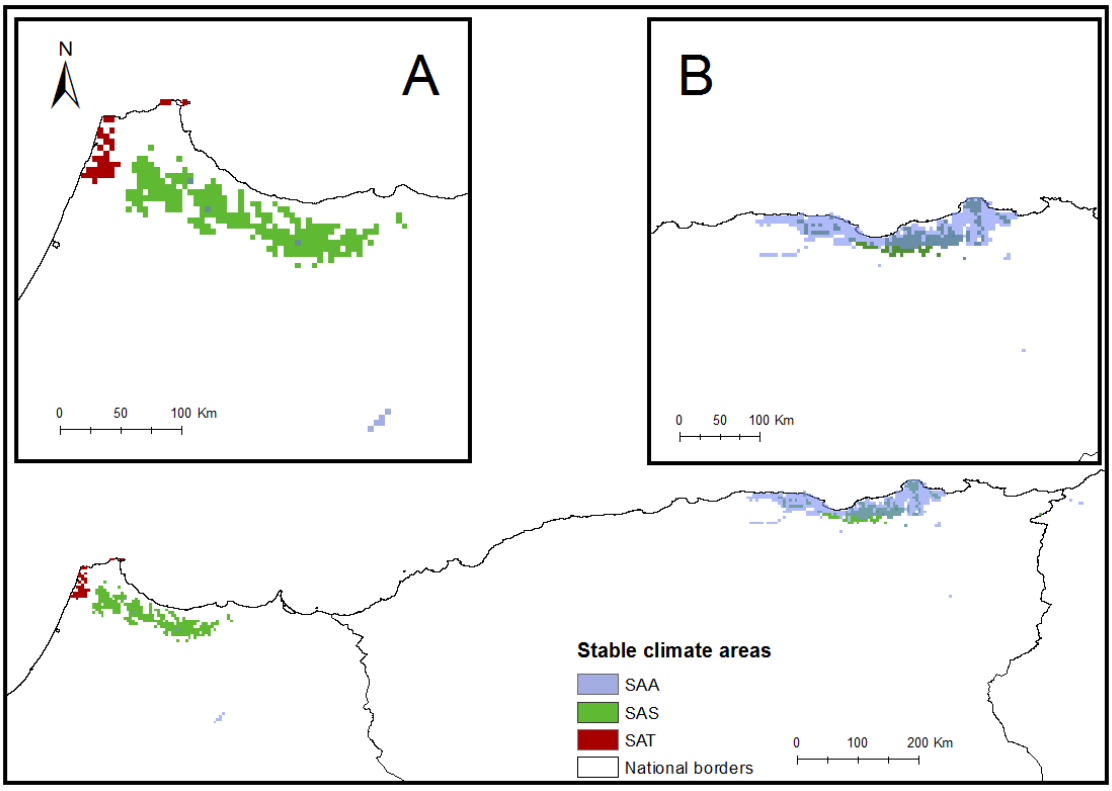

Figure 3.4 Predicted stable climatic areas identified by ecological models developed for subspecies *S. a. tingitana, S. a. splendens* and *S. a. algira* in North Africa. Bottom: Full North African projection; Inset A: Detail of the Moroccan Rif; inset B: detail of the Algerian stable areas. SAA: *S: a. algira*; SAS: *S. a. splendens;* SAT: *S. a. tingitana*

3.3.1.2 ENMs for Rif sublineages

Probabilistic climatic models for the Rif sublineages identified areas of high suitability predominantly in their known ranges, yet also detect highly suitable areas where *S. algira* is not known to occur (Supplementary materials, Figure 7.3) Binary climatic models for the sublineages in the Rif identified large suitable areas for *S. a. tingitana* 2 and *S. a. splendens* 1, with the former occupying most of the northern Tingitana peninsula and the latter most of the western and central Rif (Figure 3.5). *S. a. tingitana* 1 has suitable climatic conditions in most of the area north of Oued Martil, as well as in

some isolated areas near Moulay and Beni Maharone (Figu 3.5). *S. a. tingitana* 3 presents a distribution area that extends from near Beni Arous to Jebel Sugna, as well as isolated patches, including the populations of Dar Chaoui and Beni Maharone (Figure 3.5).

Projections to past climatic conditions predict distinct responses to climatic oscillations for each sublineage (Figure 3.5). For *S. a. tingitana* 1 no area was predicted as suitable during the LIG, while during the LGM a large continuous distribution extending into Algeria was identified, which then contracted to the north of the peninsula during the Mid-Holocene, and then expanded south into its present distribution. For *S. a. tingitana* 2 there was a range contraction during the LIG, followed by expansion in the LGM and successive contractions in the Mid-Holocene and in the present day. *S. a. tingitana* 3 had a wider distribution during the LIG than it does currently, after which it experienced expansion during the LGM, contraction in the Mid-Holocene, and further contraction to reach current conditions. *S. a. splendens* 1 presents a pattern of gradual southeastward range shifts along the Rif and Tingitana peninsula, coupled with range contraction during the LIG, expansion during the Mid-Holocene and subsequent contraction into present-day conditions. This pattern is interrupted, however, by a very large range expansion during the LGM. The identified stable climatic areas for each lineage are mostly similar to their current distributions, yet more restricted in area, and show extensive overlap which matches almost completely with the current suitable area for *S. a. tingitana* 3 (Figure 3.5).

3.3.2 Present distribution and relative importance of niche components

3.3.2.1 Habitat models

Overall model accuracy, as estimated by the training and test AUC, was high on all models (>0.93 and >0.87, respectively), though in all cases it was lower than in the climatic models (Table 3.3).

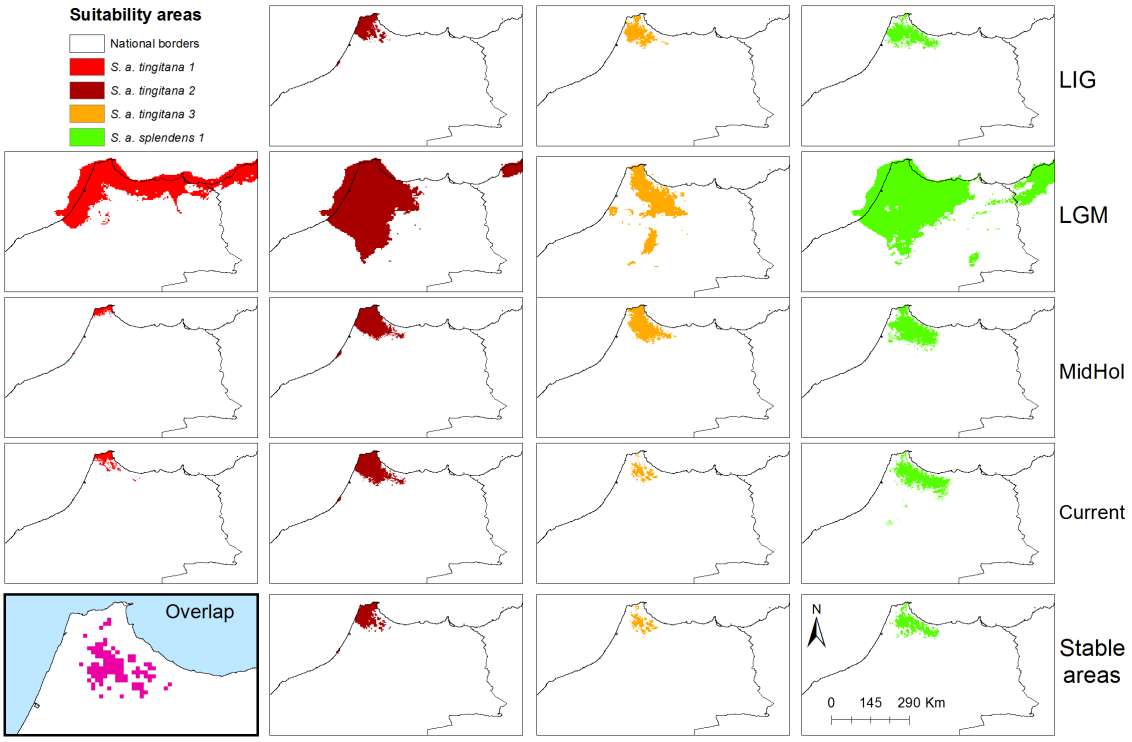

Figure 3.5 Binary models for current conditions and projections to past climatic conditions for the Rif sublineages. The absence of suitable area for the LIG prediction of *S. a. tingitana* 1 precludes the identification of stable areas for this lineage. The bottom left image displays the overlap between the stable areas for *S. a. tingitana* 2, *S. a. tingitana* 3 and *S. a splendens* 1.

All models placed an emphasis in the importance of vegetation, with average NDVI being the most important variable for all sublineages except *S. a. splendens* 1, and distance to forest/shrubland mosaics having a high contribution on all models. Distance to non-carbonate lithology also had an important contribution for all models except for *S. a. tingitana* 2. Uniquely among all sublineages, distance to closed-to-open shrubland was the most important variable for the *S. a. splendens* 1 model (23.4 %), and distance to carbonate lithology had an important contribution to the *S. a. tingitana* 1 model (21.5 %; Table 3.2).

Response curve profiles show similar patterns of close association with high NDVI values on all *S. a. tingitana* sublineages and with availability of forest/shrubland mosaics for all four sublineages (Figure 3.2). Regarding distance to non-carbonate lithology, *S. a. tingitana* 1 presented an opposite response to the other lineages, being generally excluded from this type of lithology. Regarding the responses of *S. a. tingitana* 1 and *S. a. splendens* 1 to carbonate lithology and closed-to-open shrubland,

respectively, both have the highest probabilities of occurrence at the shortest possible distances from these types of habitat features.

Habitat models show much larger and more scattered distributions than those observed with the climatic models, with several isolated patches of suitable habitat south of the Rif (Figure 3.6; Supplementary materials Figure 7.4). There is also a general tendency for avoidance of the northwestern shore of the Tingitana peninsula, particularly notable in the model for *S. a. tingitana* 1.

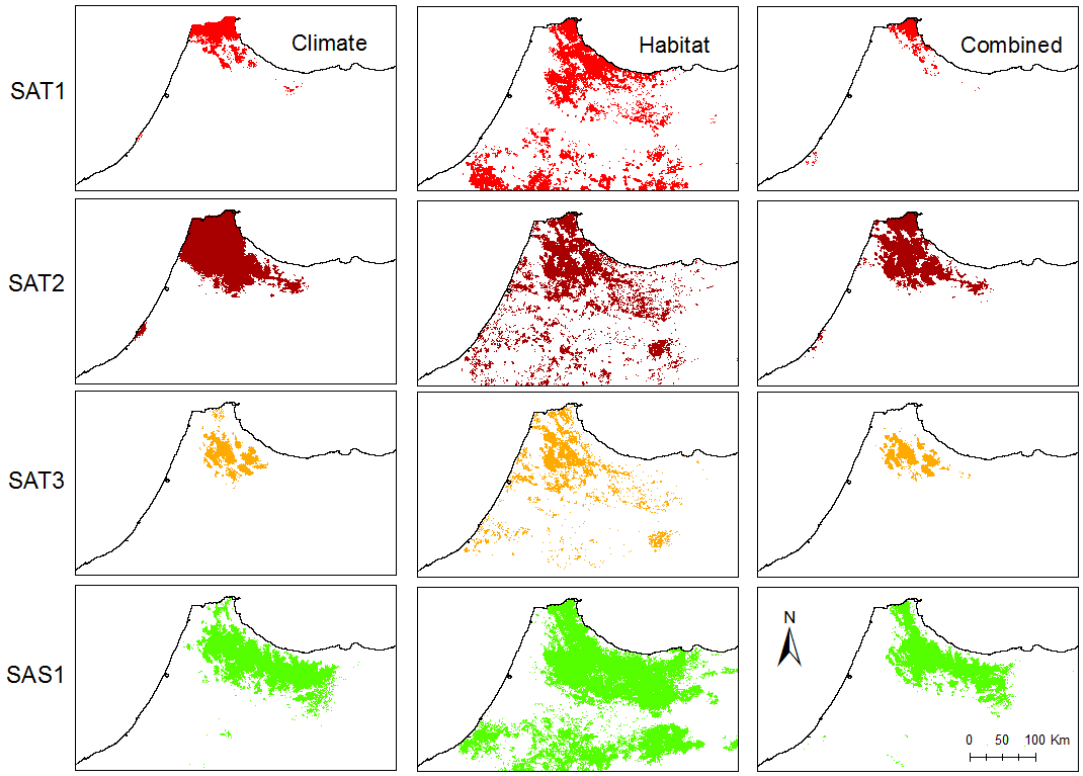

Figure 3.6 Side-by-side display of climate-only (left), habitat-only (center) and climate + habitat models (right) for the Rif sublineages. SAT1: *S: a. tingitana* 1; SAT2: *S. a. tingitana* 2; SAT3: *S. a. tingitana* 3; SAS1: *S. a. splendens* 1.

3.3.2.2 Combined models and areas of sympatry

Training and test AUC values were almost consistently higher than for either climate-only or habitat-only models, with the exception of the test AUC for *S. a. tingitana* 1, which was highest in the climate-only model (Table 3.3).

Precipitation of the wettest quarter was by far the most important variable for all sublineages except *S. a. tingitana* 1, for which maximum temperature of the warmest

month had the highest percent contribution, with important contributions of temperature seasonality, precipitation of the wettest quarter and distance to carbonate lithology as well (Table 3.3).

Table 3.3 Number of occurrence records, average (and SD) training/test AUC and average (and SD) variable percentage contribution for the habitat (top) and combined (bottom) models of the Rif sublineages. SAT1: *S. a. tingitana* 1; SAT2: *S. a. tingitana* 2; SAT3: *S. a. tingitana* 3; SAS1: *S. a. splendens* 1

	Sublineages			
	SAT1	**SAT2**	**SAT3**	**SAS1**
N	16	7	11	21
Habitat				
Training AUC	0.982 (0.008)	0.934 (0.043)	0.969 (0.016)	0.965 (0.015)
Test AUC	0.947 (0.046)	0.871 (0.108)	0.934 (0.094)	0.903 (0.039)
NDVIAV	**29.3 (10.242)**	**53.7 (24.522)**	**48.4 (17.238)**	10.4 (4.728)
NDVISD	2.2 (2.958)	0.3 (1.113)	3.8 (5.122)	5 (2.929)
GCARB	**21.5 (10.652)**	0.6 (1.620)	0.4 (0.939)	10.7 (4.741)
GNCARB	**19.2 (10.867)**	1.2 (4.098)	**13.5 (8.157)**	**16.1 (3.644)**
LVGCR	6 (4.926)	3.5 (5.856)	2.9 (4.213)	6.2 (6.042)
LFOSH	**16.2 (7.908)**	**26.3 (25.321)**	**16 (10.013)**	**19.5 (10.273)**
LBNSH	0.9 (1.520)	0.1 (0.292)	0.3 (0.705)	**23.4 (13.424)**
NDWIXW	3.1 (3.928)	3.8 (9.757)	6.2 (6.808)	4 (3.812)
VRM	1.6 (2.438)	10.4 (9.631)	8.5 (12.462)	4.5 (4.592)
Combined				
Training AUC	0.990 (0.003)	0.963 (0.013)	0.990 (0.004)	0.984 (0.008)
Test AUC	0.981 (0.021)	0.950 (0.025)	0.989 (0.009)	0.967 (0.018)
BIO4	**18.3 (4.335)**	3.5 (3.746)	0 (0.056)	4.2 (4.027)
BIO5	**31.9 (6.008)**	13.5 (8.117)	2.6 (3.317)	11.7 (5.569)
BIO16	**15.9 (4.929)**	**71.6 (13.894)**	**91.2 (7.513)**	**55.9 (11.656)**
BIO18	0 (0.119)	0.8 (1.443)	0.1 (0.360)	4.3 (3.960)
GCARB	**17.6 (7.523)**	1.5 (2.330)	0.9 (1.534)	9.1 (3.424)
GNCARB	6.2 (7.709)	0.5 (0.863)	1.2 (2.029)	6.5 (4.324)
LFOSH	9.5 (5.508)	8.4 (9.294)	3.7 (5.158)	3.5 (2.479)
LBNSH	0.5 (0.833)	0.2 (0.777)	0.4 (1.296)	4.9 (5.087)

Response curves to precipitation of the wettest quarter show a common pattern of positive response to higher precipitation for all sublineages, though the curve for *S. a.*

tingitana 1 is less steep than the others, suggesting a higher tolerance for intermediate values of precipitation (Figure 3.2).

All the combined models predict a more restrictive distribution than either climate-only or habitat-only models (Figure 3.6; Supplementary materials Figure 7.4). *S. a. tingitana* 1 is restricted to the northeastern corner of the Tingitana peninsula north of Oued Martil, save for some isolated patches in Beni Maharone and near Chefchaouen. *S. a. tingitana* 2 is predicted to have a very wide area of suitability, extending almost continuously through most of the northwestern Rif and into the Atlantic coastline. *S. a. tingitana* 3 shows the most restricted range, identifying an area of continuous suitability extending from Tazia to Jebel Sugna as well as isolated patches in Dar Chaoui, Beni Maharone, and immediately south of Oued Laou, in Chefchaouen and Fifi. *S. a. splendens* 1 is predicted to occur in most of the southwestern and central Rif, and to extend north of Oued Laou and Oued Martil into Beni Maharone and Taghramt.

Extensive overlap is observed between sublineages, even in the more conservative combined models, with predicted areas of sympatry in Ain Lahasen, Beni Maharone and Chefchaouen, where conditions are suitable for all sublineages, as well as secondary sympatry areas in Taghramt, Moulay, Jebel Sugna and Fifi, where suitability was predicted for three of the four lineages (Figure 3.7).

3.3.3 Niche divergence

Niche identity tests rejected niche equivalency of subspecies *S. a. tingitana* with both *S. a. splendens* and *S. a. algira*, but not between the latter two. Despite this, all background tests for among-subspecies comparisons indicate that niches are more similar than expected by chance, thus rejecting niche divergence on all cases (Table 3.4).

Regarding the Rif sublineages, niche equivalency was consistently rejected between *S. a. tingitana* 1 and 3, and between *S. a. tingitana* 1 and *S. a. splendens* 1, with all modeling approaches (climate-only, habitat-only and climate + habitat). Moreover, equivalency was rejected between *S. a. tingitana* 1 and 2 with both climate-only and climate + habitat models, and between *S.a. tingitana* 3 and *S. a. splendens* 1 with climate + habitat models. The majority of background tests indicate niche conservatism (by failing to reject similarity or by identifying more similarity than expected by chance),

except in the case of the combined models for *S. a. tingitana* 1 and 2, where the former was found to be less similar to the latter than randomly expected, though this result was not reciprocated in the opposite direction (Table 3.4). To test the possibility of *S. a. tingitana* 1 being restricted to a subset of the environmental conditions available to *S. a. tingitana* 2, niche breadth was measured for these lineages, identifying a narrower niche in *S. a tingitana* 1 (inverse concentration: 0.089; uncertainty: 0.819) than in *S. a. tingitana* 2 (inverse concentration: 0.297; uncertainty: 0.927).

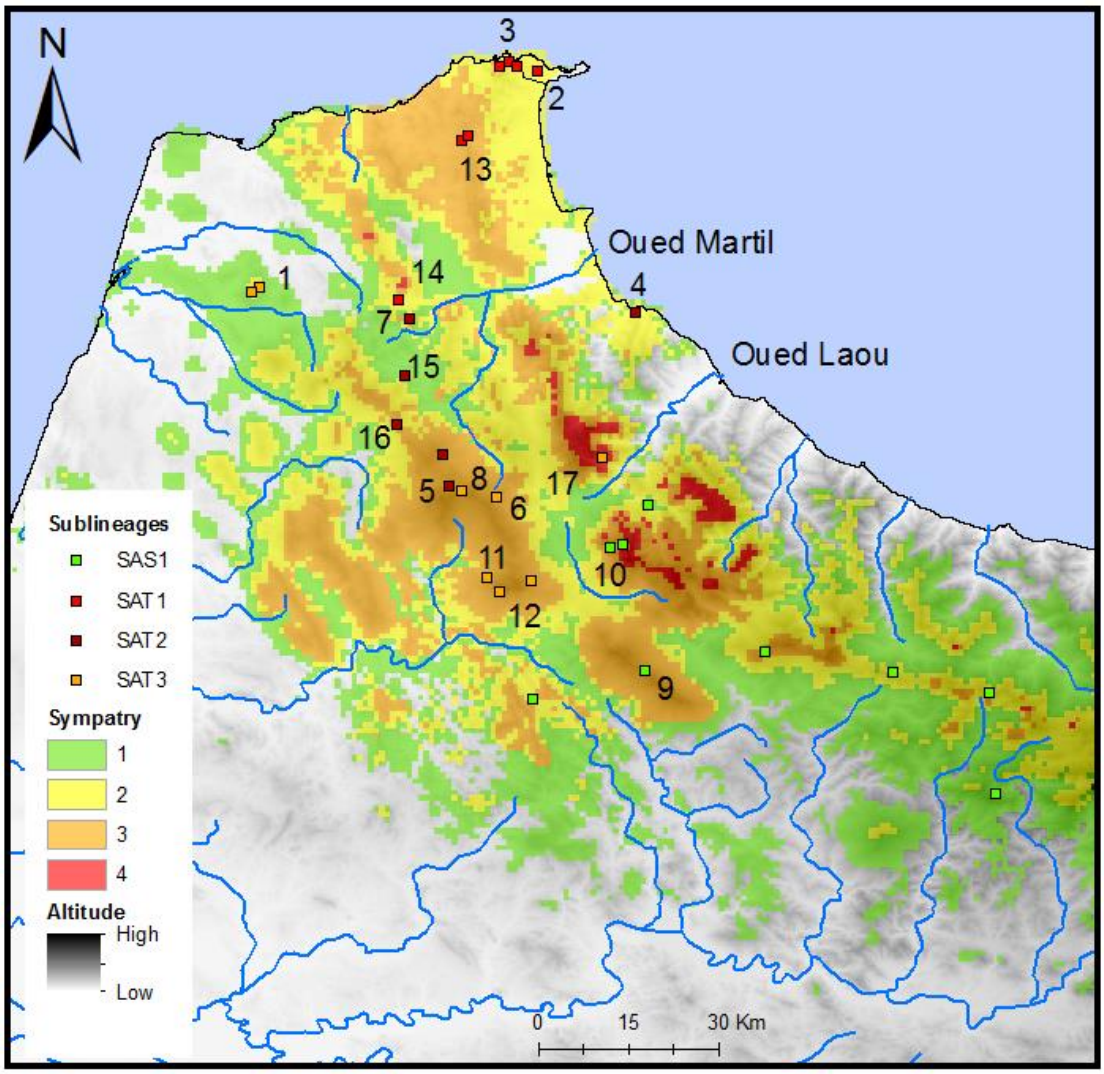

Figure 3.7 Areas of sympatry predicted by the combined models. The 1-4 numbers on the sympatry scale identify the number of sublineages predicted to have suitable habitat available at a given location. SAS1: *S. a. splendens* 1; SAT1: *S. a. tingitana* 1; SAT2: *S. a. tingitana* 2; SAT3: *S. a. tingitana* 3. Numbers correspond to localities: 1: Dar Chaoui, 2: Ceuta, 3: Jebel Musa, 4: Tetouan, 5: Moulay 1, 6: Adayourha, 7: Spirada, 8: Moulay 2, 9: Fifi, 10: Talassemtane, 11: Jebel Sugna 1, 12: Jebel Sugna 2, 13: Taghramt, 14: Ain Lahsen, 15: Jbel Hamziouat,16: Tazia, 17: Beni Maharone.

Table 3.4 Results of niche identity and background tests for all *S. algira* subspecies and for the Rif sublineages, using the climate-only, habitat-only and combined (climate + habitat) models. Significant results (<0.05) are outlined in bold. D: Schoener's D (Schoener, 1968); 1: background tests for which the empirical measurement of D is situated to the left of the null distribution. Alg: *S. a. algira*; spl: *S. a. splendens;* tin: *S. a. tingitana;* tin1: *S. a. tingitana* 1; tin2: *S. a. tingitana* 2; tin3: *S. a. tingitana* 3; spl1: *S. a. splendens* 1

	Pairwise comparisons	D	Identity tests (p-value)	Background tests (p-value)	
				A->B	B->A
Subspecies climate-only	alg/spl	0.47	0.078	**0.039**	**0.039**
	alg/tin	0.5	**0.039**	**0.039**	**0.039**
	tin/spl	0.35	**0.039**	**0.039**	**0.039**
Rif climate-only	tin1/tin2	0.57	**0.039**	0.235	**0.039**
	tin1/tin3	0.31	**0.039**	0.471	0.235
	tin2/tin3	0.48	0.157	0.588	0.078
	tin1/spl1	0.34	**0.039**	**0.039**	**0.039**
	tin2/spl1	0.55	0.196	**0.039**	**0.039**
	tin3/spl1	0.42	0.118	**0.039**	0.549
Rif habitat-only	tin1/tin2	0.55	0.471	1	0.706
	tin1/tin3	0.41	**0.039**	0.078	0.902
	tin2/tin3	0.71	0.745	**0.039**	0.275
	tin1/spl1	0.45	**0.039**	**0.039**	0.863
	tin2/spl1	0.63	0.078	**0.039**	0.902
	tin3/spl1	0.59	0.196	0.51	**0.039**
Rif combined (climate + habitat)	tin1/tin2	0.47	**0.039**	**0.039**[1]	0.078
	tin1/tin3	0.34	**0.039**	0.157	**0.039**
	tin2/tin3	0.54	0.118	0.392	0.353
	tin1/spl1	0.35	**0.039**	**0.039**	**0.039**
	tin2/spl1	0.58	0.275	**0.039**	0.078
	tin3/spl1	0.4	**0.039**	**0.039**	0.471

3.4 Discussion

3.4.1 General biogeographic patterns

The identification of non-overlapping stable areas for each subspecies, coupled with the lack of support for niche divergence (see below) on all between-subspecies and between-sublineages comparisons, suggests a model of allopatric divergence aided by niche conservatism, coupled with topographic and climatic barriers, as the main driver of diversification among *S. algira.* This pattern is in line with the predominantly vicariant mode of speciation among salamanders (e. g. Caccone et al., 1994; Kuchta, 2007; Veith et al., 2008), and with the widespread tendency for intraspecific patterns of deep divergence and spatially structured genetic diversity in North African species (reviewed in Husemann et al., 2014).

The predominant pattern of responses to climatic oscillations on all subspecies and sublineages of *S. algira* consisted of range contractions during the LIG and expansion during the LGM and (to a lesser extent) the Mid-Holocene. Species responses to Pleistocene glacial and interglacial periods were individualistic and were shaped by their biogeographic affinities (Hewitt, 2004; Stewart et al., 2010).

The pattern seen in *S. algira* is similar to other species located on the southernmost limits of distribution of their climatic affinities, such as *Vipera seoanei* in the Atlantic region of North Iberia (Martínez-Freiría et al., 2015) and *Alytes maurus* in the Mediterranean region of North Africa (de Pous et al., 2013). Species in these climatic transition zones may be particularly vulnerable to warmer and dryer conditions, responding with range contractions to mountain ranges, while milder and more humid periods may increase the availability of suitable habitat in the lowlands, promoting range expansion. Evidence for the occurrence of warm mixed forests at intermediate altitudes and temperate xerothermic woods and shrublands at low altitudes in North Africa during the Mid-Holocene (Jolly et al., 1998) supports the expansion of *S. algira* during this period due to greater availability of humid and vegetated habitat.

The large scale connectivity between the Moroccan and Algerian populations observed in the LGM is likely overly optimistic, as it doesn't consider the limitations to distribution resulting from biotic interactions and limitations to dispersal (Soberon, 2007; Sillero, 2011). The latter may be particularly important for *Salamandra* species with limited

dispersal capacity (Bonato & Fracasso, 2003; Bar-David et al., 2007; Schulte et al., 2007). Nonetheless, the predicted distribution reflects the overall species-level tendency towards range expansion during more humid periods, and may therefore mirror, to some extent, the distribution of the species prior to diversification of the current subspecies. The absence of predicted areas of suitability in the Moulouya River basin for all projections except those for the LGM supports an important role of this historically arid region in promoting isolation between the eastern and western clade of *S. algira*, a scenario already suggested for the species (Escoriza et al., 2006) and in agreement with similar patterns observed in other vertebrates (e. g. Alvarez et al., 2000; Barata et al., 2008; Velo-Antón et al., 2012a; Stuckas et al., 2014).

The occurrence of a single stable climatic refuge for *S. a. algira* supports previous assertions, prompted by the discovery of a shallow genetic structure in Algerian populations, of a continuous connectivity between populations driven by climatic stability in the area (Merabet et al., 2016; Ben Hassine et al., 2016), while the identification of multiple non-overlapping stable areas for each of the subspecies *S. a. tingitana* and *S. a. splendens* could be implicated not only in the vicariant divergence between these subspecies, but also in more recent patterns of vicariance related with their further divergence into the present sublineages. Particularly in the case of the model for *S. a. splendens*, it was unexpected to find no stable areas in the Middle Atlas, which would have supported prolonged vicariance as the source of the deep divergence found between sublineages 1 and 2 of this subspecies (as detailed in the previous chapter). It's possible that sampling bias hinders the representation of the full environmental variability of this subspecies' range, due to the sampling gaps still remaining in the Central Rif and, particularly, in the Middle Atlas. While the present work is predominantly aimed at establishing the biogeographic patterns of the Rif, a more detailed biogeographic analysis of the populations of the Middle Atlas is certainly a necessity to fully clarify the role of this mountain system in the evolution of *S. algira.*

3.4.2 Biogeographic patterns of the Rif

The role of habitat as a constraining factor to the distributions predicted by climate-only data, poses a challenge for the understanding of the biogeographic history of the Rif sublineages in a context of vicariant divergence, as a high degree of overlap has been found between all sublineages on all time periods considered. An undisclosed role of

dispersal constraints or non-climatic habitat variables may therefore be the driving force that has promoted divergence between these lineages. Like in the present, past distributions likely experienced similar restricting effects of vegetation and lithology which are not detectable by climate-only models but may have constrained distributions to more restrictive extents than observable using the biogeographic approach applied in this work. River systems, particularly Oued Martil and Oued Laou, may have been important geographical barriers to dispersal, as supported by the inability of present-day combined models to detect areas of suitability in these rivers and immediately adjacent areas.

The history of divergence between the sister sublineages *S. a. tingitana* 1 and 2 remains unclear, as the inability to identify a stable climatic area for the former hinders the formulation of hypotheses derived from spatial segregation patterns. The lack of suitable areas for sublineage 1 during the warmer conditions of the LIG is consistent with this sublineages' stronger relationship with mild, stable temperatures when contrasted with the other, predominantly precipitation-dependent sublineages of the Rif. Persistence of this sublineage during warmer periods may have been restricted to microclimatic refugia, mediated by the availability of porous karstic substrate coupled with climatic buffer effects of vegetation cover and the heterogeneous topography of the Rif, which would be capable of securing the cool, mesic environment thought to be relevant for interglacial microrefugia (Dobrowski, 2011), yet would be undetectable under the present framework.

Salamandra a. tingitana sublineage 3 has a predominantly precipitation-driven distribution, reflected in the high percent contribution of this variable to models and in the sharp response curve for this variable, which excludes this sublineage from intermediate levels of precipitation where all other sublineages have a predicted suitability greater than zero. This emphasis on a restricted range of precipitation levels is likely the main constraint responsible for the comparatively restricted historical and contemporary distribution of this sublineage. While connectivity between the populations in Jebel Sugna and Moulay has remained historically stable (in agreement with the shared population structure uncovered in the previous chapter), the populations of Beni Maharone and Dar Chaoui are located in isolated stable areas, and may therefore represent relict populations which have persisted through successive climate-related range contractions in isolated refugia. Nevertheless, the low number

and restricted distribution of occurrence records for this sublineage might be hampering the development of accurate models, therefore limiting any interpretation related to its biogeographical history.

The biogeographic history of *S. a. splendens* sublineage 1 remains difficult to clarify. Model projections to the past predict a more prevalent presence in the north-western Rif than what is found today. This would have greatly increased the overlap with *S. a. tingitana* and, given the absence of fully established reproductive isolation inferred from the evidence of admixture uncovered in the previous chapter, open up opportunities for gene flow with all *S. a. tingitana* sublineages. Our current understanding of the secondary contact zone dynamics of *S. algira* is insufficient to fully clarify the biogeographic history of secondary contact between the western subspecies. Future endeavours should strive to build upon the knowledge of current distribution and population structure uncovered in the previous chapter of this work, as well as to identify suitable markers for obtaining a clear picture of the nuclear genome.

3.4.3 Common ecological patterns

The overall lack of evidence for niche divergence supports previous assertions that all *S. algira* lineages have similar ecological requirements, and that differences found between populations are related to the evolutionary history of each lineage, isolation by distance and current availability of habitat rather than to distinct environmental tolerances (Ben Hassine et al., 2016). In this context, it is more poignant to focus the discussion on common ecological patterns than on the differences between lineages. There is a consistent pattern of association with high levels of wet-season precipitation on the majority of the climatic and combined models created in this study. Precipitation is expected to have a dual role in the delimitation of *S. algira* distribution: first, a causal relationship likely exists between precipitation and vegetation productivity (as attested by the high correlation found between precipitation and vegetation productivity in western Morocco), which is favourable for *S. algira* as it can benefit from the microclimatic buffer effects of vegetation (Escoriza and Ben Hassine, 2014); second, high precipitation likely favours *S. algira* larviparous populations directly by providing surface water for reproduction.

The role of precipitation as major factor affecting *S. algira* is indirectly supported by the ecological patterns found in the Rif, where the high contribution of vegetation productivity to habitat-only models further underlines a common reliance of all sublineages on forested habitats. This reliance on forests is further highlighted by the identification of areas of sympatry, as the areas where suitable habitat is found for all sublineages of the Rif (Beni Maharone and Chefchouen/Talassemtane, located on both sides of Oued Laou) overlap with the old, high altitude, conifer forests of the Talassemtane National Park. The fact that surface water availability importance is not reflected more directly in the form of a higher contribution of NDWI variables to our niche-based models likely reflects an inability to capture the role of the small water bodies required by salamander reproduction (Escoriza & Ben Hassine, 2015) at the scale used in the models presented here, as well as from the difficulty in detecting smaller water bodies hidden below the canopy using Remote Sensing techniques. Active and Very High Resolution Remote Sensing data have demonstrated an ability to penetrate the canopy (Nagendra et al., 2015), and may be better suited for future assessments of the relationship between *S. algira* and surface water.

Of all the environmental variable datasets used for modelling Rif sublineages, those employing a combination of climatic and habitat variables were the most reliable, followed by the climate-only models, while the habitat-only models had the poorest performance. Inspection of the models shows that combined datasets result in a more restricted and detailed prediction than that created by climate models, but with the same overall range limits. Conversely, habitat models produce more scattered predictions resulting from repetitive combinations of the same habitat conditions occurring often and stochastically in the training area. This fits the generally accepted model of biological distributions being predominantly shaped by climate at larger scales (Mackey & Lindenmaiyer, 2001; Elith & Leathwick, 2009), while habitat-based variables have a major effect at a more local scale, where their greater spatial heterogeneity further constraints the distribution of species. In this sense, the combined models can be thought of as representing two hierarchic levels of delimitation of species distribution: at large scales the distribution is constrained by a favourable climatic envelope, while subsequently, at finer scales, the area within this envelope is further constrained by availability of suitable habitat.

Nonetheless, this does not necessarily exclude the possibility of species persistence in microclimatic refugia on areas where the regional climate ceases to be climatically suitable. Persistence in microrefugia would be difficult to detect using ecological models based on typical climate predictors (e.g. Hijmans et al., 2005), and could account for the lack of suitable areas for *S. a. tingitana* sublineage 1 during the LIG. It could also account for the fact that, despite the overlap predicted between present-day models for the subspecies (which reflects the similarity between niches), none of them predict suitability in the Beni Snassen massif, where the highly localized and microclimate-dependent *S. a. spelaea* is distributed (Escoriza and Ben Hassine, 2014). Non-conventional modelling techniques and finer-scale environmental data (such as climate data derived from Very High Resolution Remote Sensing techniques) may be better suited for the identification of microrefugia (Ashcroft et al., 2012; Patsiou et al., 2014), and implementation of such methods may help clarify the role of microrefugia in the diversification and interglacial survival of *S. algira*

3.4.4 Current distribution of *S. algira*

The predicted present-day distribution of the subspecies *S. a. algira* identified a continuous range from Kabylia to Annaba, while also providing evidence for habitat discontinuity promoting the isolation of the westernmost population in Chrea from the remaining populations of this subspecies. These results are supported by the discovery of a shallow genetic structure in the Kabylia-Annaba region and greater differentiation for the Chrea population (Merabet et al., 2016). However, they are in contradiction with previous species-level niche-model-based attempts at characterizing the distribution of *S. algira*, which predicted connectivity between Chrea and Kabylia (Ben Hassine et al., 2016). Suitable areas were also identified in northwest Tunisia, suggesting that, despite previously reported inability to detect *S. algira* in the region (Bogaerts et al., 2013), climatic conditions are suitable for the occurrence of this species, and the possibility of its persistence in the area cannot be fully discarded.

The model for *S. a. splendens* extensively predicted suitability for this subspecies through the Algerian Tell Atlas. It is possible that the inclusion of Middle Atlas populations may have led the model to predict suitability in semi-arid conditions, as evidenced by the occurrence of a local maximum at low precipitation values in the response curve to wet-season precipitation. Nonetheless, the fact that this predicted

area of suitability is isolated from the known distribution of the subspecies by the arid lower Moulouya river basin makes it unlikely that *S. algira* occurs in the Tell Atlas. Also unexpected was the prediction of a continuous distribution between the Rif and Middle Atlas. Sampling difficulties in the Central Rif area, related with widespread cannabis cultivation (Labrousse and Romero, 2001; Chouvya and Afsahib, 2014), have so far precluded a detailed assessment of connectivity between these populations, which is necessary to fully confirm or disprove these results. Nonetheless, the aridity of the area between the Rif and Middle Atlas makes the occurrence of *S. algira* seem unlikely.

Detection of suitable areas for *S. a. tingitana* in western Algeria highlights the climatic similarities between the distributions of distinct subspecies. More importantly, extensive overlap between the models for *S. a. tingitana and S. a. splendens* was found in the Rif, supporting the existence of a contact zone between these subspecies. The increased level of detail provided by the models for the Rif sublineages supports this area, extending from Chefchaouen (south of Oued Laou) to Tagramth (north of Oued Martil), as a region of extensive overlap between all four sublineages that occur in the Rif. The validity of this sympatry area has been partially confirmed in the previous chapter, with the detection of contact zones across Oued Laou and in Moulay, yet the distribution of mitochondrial lineages is mostly circumscribed and non-overlapping. In light of the discovery of widespread potential sympatry and absence of niche differentiation between sublineages, it is likely that the current distributions reflect biotic or dispersal-related, rather than environmental, constraints.

The previously suggested role of Oued Martil and Oued Laou in the delimitation of the distribution of Rif sublineages (Beukema et al., 2010) had already been put into question in the previous chapter of this work by the identification of a population of *S. a. tingitana* sublineage 2 north of Oued Martil and by evidence of gene flow between populations on both sides of Oued Laou. While the combined models presented in this chapter provide evidence that the rivers and immediately adjacent areas are not suitable habitat for any of the sublineages except *S. a. splendens* sublineage 1, this does not preclude the possibility of dispersal being possible across the rivers. Another possibility is a continuous distribution around the rivers, which is observable for the widely distributed *S. a. tingitana* sublineage 2 and *S. a. splendens* sublineage 1, and would explain the patterns observed in the previous chapter.

3.4.5 Ecological implications for the evolution of pueriparity in *S. algira*

The unique relationship found between *S. a. tingitana* sublineage 1 and its environment (as expressed in present-day models including both climate and habitat variables) agrees with what is currently known about its microhabitat, characterized by a milder and more stable climate than other populations of *S. algira* (likely due to the effect of both Atlantic and Mediterranean maritime influence), which reduces the reliance on climatic buffer effects of vegetation, allowing persistence in the sparsely vegetated limestone outcrops that occur in the region (Escoriza & Ben Hassine, 2014). Previous attempts at characterizing the ecological differences between pueriparous and larviparous *S. algira* using ecological niche models, while erroneously assuming pueriparity to be restricted to *S. a. tingitana* sublineage 1, uncovered a reduced reliance of pueriparous populations on precipitation and vegetation, as well as a greater association with stable temperatures, when compared with larviparous populations (Beukema et al., 2010).

Present results for *S. a. tingitana* sublineage 1 effectively agree with a more loose association with precipitation than its counterparts, as well as a greater reliance on stable temperatures and carbonate lithology (which includes karst substrates, though not exclusively), mirrored by an overall avoidance of non-carbonate substrates, in marked contrast with the strictly larviparous Rif sublineages. The one-way rejection of niche similarity between *S. a. tingitana* sublineages 1 and 2, as well as the evidence for a more specialized niche in the former, suggest that despite the lack of true niche divergence, sublineage 1 may have become restricted to a subset of the environmental conditions available to sublineage 2, where the less water-dependent environments promoted the emergence of pueriparous reproduction. This is further supported by the overall independence from lithology for the more generalist sublineage 2, which may reflect an ability of this sublineage to occupy both dry/karstic and humid/non-karstic habitats by resorting to pueriparous or larviparous reproduction, respectively. Whether this is tied to evolutionary divergence or simply reflects plasticity of reproductive strategies within this sublineage remains unclear.

The absence of permanent surface water and the coastal location of the pueriparous population of sublineage 2 identified in this work support a set of environmental

affinities similar to sublineage 1. However, this population appears to be isolated on a patch of forest amidst a highly fragmented landscape. Moreover, the possibility of temporary surface water being available sporadically cannot be fully discarded. These factors do not allow us to reject with certainty the possibility of an affinity with vegetation and water availability similar to what is observable on larviparous populations. A deeper understanding of the distribution of reproductive strategies within this lineage, and of their genetic structure and ecological affinities, is required to fully clarify the context of pueriparity among *S. algira.*

Chapter 4: Impact of landscape-change on habitat availability in a Palearctic relict in northern Maghreb (Manuscript III)

4.1 Introduction

The shared biogeographic history of North Africa and Southern Europe has contributed to the remarkable biodiversity that can currently be found in the Global Biodiversity Hotspot of the Mediterranean Basin (Myers et al., 2000; Schmitt, 2007; Martínez-Freiría et al., 2013; Husemann et al., 2013). For Maghrebian taxa, the predominant biogeographic pattern seems to be that of an African centre of origin, with some species able to colonize Europe at later stages (Schmitt, 2007; Husemann et al., 2014). However, an opposite scenario also took place in this region, that is the colonization of North Africa by organisms of northern Palearctic origin, via south-west Asia (Dobson & Wright, 2000), by the land bridges that connected both continents during the Messinian Salinity Crisis (from 5.96 to 5.33 Mya; see Hsü et al., 1973; Krijgsman et al., 1999; Duggen et al., 2003), and in some cases by human introduction (e. g Michaux et al., 2003). Some of these Palaearctic relicts include insects (Ferreira et al., 2015), amphibians (*Alytes maurus*, Martínez-Solano et al., 2004; *Salamandra algira*, Beukema et al., 2010; *Bufo spinosus*, Recuero et al., 2012), reptiles (*Vipera latastei*, Velo-Antón et al., 2012a; *Emys orbicularis occidentalis*, Stuckas et al., 2014; *Natrix astreptophora*, Kindler et al., 2013) or mammals (*Apodemus sylvaticus*, Michaux et al., 2003).

Yet, the biogeographic affinities of these Palaearctic relicts often rely on relatively mild climate and on availability of appropriate vegetation cover (Bonz & Geniez, 1996; Escoriza et al., 2006; Brito et al., 2011, Ben Hassine & Escoriza, 2014; Ferreira et al., 2015), which may create a buffer effect promoting microclimatic stability (Escoriza & Ben Hassine, 2014). Such a reliance on vegetation is a shortcoming in North Africa, which through history has experienced periods of hyper-arid conditions (Dobson and Wright, 2000; Cosson et al., 2005), imposing constraints on the availability of suitable forest and shrubland habitat. As a result, many taxa of northern Palearctic origin are currently reduced to relict populations, strongly dependent on the relatively small habitat patches they occupy (Beja et al., 2009; Brito et al., 2011, de Pous et al., 2013; Escoriza et al., 2013; Stuckas et al., 2014; Velo-Antón et al., 2015c).

It is estimated that only 4.7 % of the original primary vegetation extent of the Mediterranean Basin remains (Myers et al., 2000; Allard et al., 2013). Climate change and the expansion of the Sahara Desert are, consequently, urgent threats for these species, as they may potentially cause a drastic reduction in the amount of dense-

vegetation habitats available. Besides increasing aridification, climate change carries additional risks for forest habitats, related with the possibility of colonization by invasive pests (Esteban et al., 2010). However, another pressing threat to habitat sustainability exists in the region. Human presence in North Africa has been associated with forest clearing and habitat degradation since at least 3,000 years ago (Cheddadi et al., 2015). Increasing human population in the last four centuries has resulted in a rapid global conversion of wilderness areas into human settlements, characterized by both an expansion and intensification of land use (Ellis et al., 2010). In the northern Maghreb, the predominant wildland and seminatural anthromes of 1700 had been almost completely replaced by rangelands, croplands, villages and dense settlements in 2000 (Ellis et al., 2010), with a documented detrimental effect on Palearctic relicts (Ferreira et al., 2015).

The consistent rise, in recent decades, of human population density in North Africa (Fargues 1986; Taboutin, Vilquin & Biraben, 2002; Allard et al., 2013) has continued this trend of human landscape modification, increasing pressure on ecosystems from forest clearing for agriculture and wood harvesting, as well as from overgrazing and changing fire regimes (Esteban et al., 2010; Allard et al., 2013). One particular concern in the Moroccan Rif is the cultivation of cannabis, which is increasingly being grown at mid-range altitudes (Esteban et al., 2010) and expanding along the western and central Rif (Labrousse & Romero, 2001; Chouvya & Afsahib, 2014). Considering that human population in North Africa is projected to increase in the next decades (Allard et al., 2013), an evaluation of the status of Palearctic relicts regarding habitat degradation should be prioritized, to allow the application of appropriate conservation action on the more vulnerable populations.

Salamandra algira is a North African endemic of northern Palearctic origin, classified as Vulnerable on the IUCN Red List of Threatened Species, due to its severely fragmented distribution and ongoing decline in the extent and quality of its forest habitat in Morocco and Algeria (Donaire-Barroso et al., 2009). It is often found associated with forest habitats, likely due to the microclimatic stability they provide (Escoriza et al., 2006; Escoriza & Ben Hassine, 2014; Ben Hassine & Escoriza, 2014). Salamanders are particularly reliant on moist habitats for respiration and surface activity, and the loss or degradation of forest cover reduces the effectiveness of the buffer effect responsible for the maintenance of a relatively high humidity environment

(Welsh & Droege, 2001). Currently *S. algira* is reduced to relict populations in the Rif, Middle Atlas and Beni Snassen, in Morocco, as well as in the regions of Annaba, Kabylia and Blida Atlas, in Algeria. Its genetic diversity, morphology and reproductive strategies show a high degree of geographic structure, as a result of its complex biogeographic history. Certain populations of this species represent unique phenotypes and evolutionary histories, and should therefore merit special attention from a conservation perspective. Therefore, *S. algira* is a suitable model for assessing how contemporary trends of habitat loss are affecting forest-dependent species in the region, and to identify the most vulnerable areas to habitat degradation and loss. The availability of Remote Sensing data makes it possible to obtain information on the temporal and spatial patterns of change in land use across the region.

This study aims to a) characterize temporal trends of variation in vegetation cover in North Africa in recent years (2006-2014); b) identify the natural areas most affected by vegetation loss; and c) identify at-risk populations of *S. algira*. It is expected that the methodological approach and the findings obtained for *S. algira* contribute to future assessments on conservation status of North African Palearctic relicts, by providing a better understanding of the impact of human-induced vegetation change on the viability of such populations.

4.2 Methods

4.2.1 Characterization of recent temporal trends in the variation of vegetation cover

The Normalized Differential Vegetation Index (NDVI) was used to characterize temporal patterns of vegetation change in North Africa. NDVI has been found to be well correlated with leaf area index, chlorophyll abundance, absorption of photosynthetically active radiation and gross primary production quantity, and is therefore a general measurement of plant productivity (Myneni et al., 1995; Goetz & Prince, 1999). Temporal trends of NDVI change have been previously shown to be a useful tool for detecting land degradation associated with human activity (e. g. Thiam, 2003; Wessels et al., 2004) and assessing climatic constraints to vegetation growth (e. g. Chen et al., 2016).

Pre-calculated NDVI layers at 250 x 250 m spatial resolution were obtained from the MOD13Q1 product of the MODIS Terra satellite, available at NASA's Land Processes Distributed Active Archive Center (LP DAAC, https://lpdaac/usgs.gov). A time series of NDVI layers was obtained which spanned the last nine years available (2006-2014), with images collected every 15 days, for a total of 216 independent collection dates. While NDVI data were available since 2000, the year 2006 was chosen as a starting point for analysis to allow characterization of vegetation loss by type of land cover, for which there is reliable information available for the year 2006 (details below). To include the full extent of the distribution of *S. algira*, as well as the entire Maghreb, temporal series were collected for two distinct MODIS tiles (H17V05 and H18V05) covering the area from the Atlantic Moroccan coast to Tunisia. All subsequent analyses were performed on ArcGIS version 10.1 (ESRI, 2008). Images were sorted by year of collection, and yearly NDVI layers for the wet season were obtained by selection of a NDVI layer for the peak of each year's wet season (mid-December). The maximum NDVI raster layers for each tile were then combined into a single layer per year using the Mosaic tool. Temporal patterns of vegetation change were assessed using Raster Calculator to compute, for each cell, the difference in absolute NDVI value between each year and the subsequent one.

To obtain a summary of fluctuations in vegetation productivity and control for sporadic and cyclic phenomena such as years of climatic extremes or crop rotation, the sum of the yearly variation maps was obtained in Raster Calculator. This raw NDVI loss layer was then reclassified to convert negative (net vegetation gain) and zero values (no net vegetation change) to zero and stratify the positive values (net vegetation loss) in 10 % increments, to provide a relative measurement of vegetation loss severity. While ideally control points would help establish thresholds to classify severity of vegetation loss into biologically meaningful classes, the logistic difficulties associated with field work in a study area which includes remote locations and crosses the national borders of four different nations make this approach unviable. Relative severity is therefore a compromise which is valuable to identify priority areas warranting further attention from conservationists, even if it fails to completely clarify what the situation may be in any particular location.

4.2.2 Identification of natural areas most affected by vegetation loss

To obtain information on vegetation loss by land cover class, the full vegetation loss layer obtained in the previous step was further reclassified to a binary vegetation loss-or-gain/stability map and summed to the GLOBCOVER 250 m land cover map for 2006 (Bicheron et al., 2008), using Raster Calculator. For each class of land cover, the percentage of the total subject to vegetation loss was obtained by dividing the number of cells within the land cover class where vegetation loss was detected by the total number of cells belonging to that land cover class. The percentage of total vegetation loss corresponding to loss in each particular land cover type was calculated by dividing the number of cells within the land cover class where vegetation loss was detected by the total number of cells of vegetation loss in the entire study area.

4.2.3 Identification of at-risk populations of *S. algira*

The impact of vegetation loss on distinct populations of *S. algira* was assessed by using the Extract Values To Points tool to extract values from the reclassified vegetation loss layer created previously to a shapefile containing occurrence records of *S. algira.*

Vegetation loss within the potential distribution of *S. algira* was identified by quantifying the degree of overlap between vegetation loss and the predicted distribution of the species, as assessed by the ecological niche models created in the previous chapter. This step was performed at the scale of subspecies, to allow an overview of the effects of vegetation loss across the entire distribution of *S. algira*, as well as for the sublineages of the Rif, which due to their strong population structure and restricted distribution may be particularly vulnerable to habitat loss. The models used were those created with a combined (climate + habitat) set of environmental variables, as they were more restrictive than those created solely with climatic data and should therefore be less prone to overprediction.

Summarizing the modeling approach detailed in the previous chapter, models were created on Maxent (Phillips et al., 2006) using occurrence-only data and a set of non-highly correlated variables, with a training area consisting of a 200 km buffer around the minimum convex polygon that includes all occurrence records belonging to a subspecies or sublineage. Each model was created by running 50 bootstraps, each time setting aside 30 % of the available presence points for model testing. Probabilistic

models were then converted to binary suitability models by applying the minimum training probability threshold. Combined models had not been previously created for the subspecies, and where therefore created using the same approach, using the same set of variables employed for the sublineage combined models, and the same training areas and occurrence data that were used for the subspecies climatic models. Models performance and predictions can be consulted in Supplementary Materials (Table 7.6; Figure 7.10).

The binary vegetation loss layer was reclassified using the Reclassify tool on ArcGIS, to change all values of “1” (vegetation loss) to “10”, to allow the distinction between unsuitable and non-degraded (0), suitable and non-degraded (1), unsuitable and degraded (10) and suitable and degraded (11) areas. The Extract By Mask tool was then used to cut the vegetation loss layer to the extent of each model. For the Rif sublineages this step was performed on projections of the models to the entirety of the Rif, while for subspecies it was performed on the training areas used to create the models, to avoid issues with prediction of suitability in areas where subspecies occurrence is unlikely due to dispersal constraints. To avoid artifacts caused by performing mathematical operations on rasters with distinct spatial resolution, the vegetation loss layer was upscaled to the resolution of the models (1 x 1 km) by setting the cell size to be identical to that of the extraction mask during the Extract By Mask procedure. Raster Calculator was used to obtain the sum between vegetation loss and the binary suitability models. Percentage of suitable area affected by vegetation loss for each subspecies and sublineage was determined by dividing the number of grid cells exhibiting both suitability and vegetation loss by the total number of suitable grid cells.

4.3 Results

4.3.1 Temporal patterns of vegetation change in North Africa

When restricting the temporal scale to observe vegetation fluctuations on a year-by-year basis (Figure 4.1; Supplementary Materials Figure 7.8), no clear signature of a geographically localized tendency for vegetation gain or loss is observable, as regions which have lost vegetation in one year may experience recovery in the next, and vice versa. Complete lack of vegetation change in either direction from one year to the next is rare and emphasizes the impact of yearly climatic fluctuations in vegetation

productivity (Supplementary Materials Figure 7.8). It should be noted that a persistent pattern of northwestern-oriented stretches of vegetation loss is observable in the southernmost portion of the study area. This may be an artifact of satellite data collection caused by dune shadows in the Sahara desert, suggesting that application of this type of analysis in more arid regions may be troublesome. For the northernmost, predominantly Mediterranean part of the study area, however, no such artifacts are observable. Alternatively, it may reflect disturbances resulting from cloud cover, or possibly sensor errors.

Net vegetation loss over the 9-year period considered (Figure 4.2) was observed in Morocco through most of the Rif, Middle Atlas and High Atlas, as well as along the northwestern coast and in the Moroccan portion of the High Plateau. In the Spanish province of Ceuta, vegetation loss was observed through most of the area. In Algeria, the westernmost part of the country had relatively little net vegetation loss, yet extensive loss was detected in the easternmost portion of the Tell Atlas and in the Aurès Mountains. In Tunisia, most vegetation loss was observed near the gulfs of Hammamet and Gabès, as well as in the Marjardah valley. Overall net vegetation loss is observable in c. 78 % of the study area, of which c. 75 % correspond to the lowest observed level of severity. Values of severity above 3 are rare and collectively comprise less than 0.2 % of the study area (Table 4.1).

The most severe vegetation loss in the Rif was observed near Chefchaouen, particularly in the south of the Talassemtane Natural Park and Botanical Reserve, and in the Central Rif locality of Targuist. More circumscribed foci of vegetation loss were located around Taghramt and Jebel Musa. Along the Atlantic coast of Morocco, severe vegetation loss was most apparent south of Tanger, east of Larache and in Ben Mansour (Figure 4.2 A, 4.3 A). Severe vegetation loss was detected in the Middle Atlas localities of Taffert and particularly south of the Ifrane National Park and south of Beni Melal (Figure 4.2 A, 4.3 B). In northeast Algeria, vegetation loss is widespread and several local peaks of severity occur scattered across the region, of which the four largest in extent and severity are located in the Djurdjura National Park, south of Skikda and both east and west of Biskra. In Tunisia, the regions of Bizerte and Sousse present the most severe vegetation loss (Figure 4.3 B, 4.4).

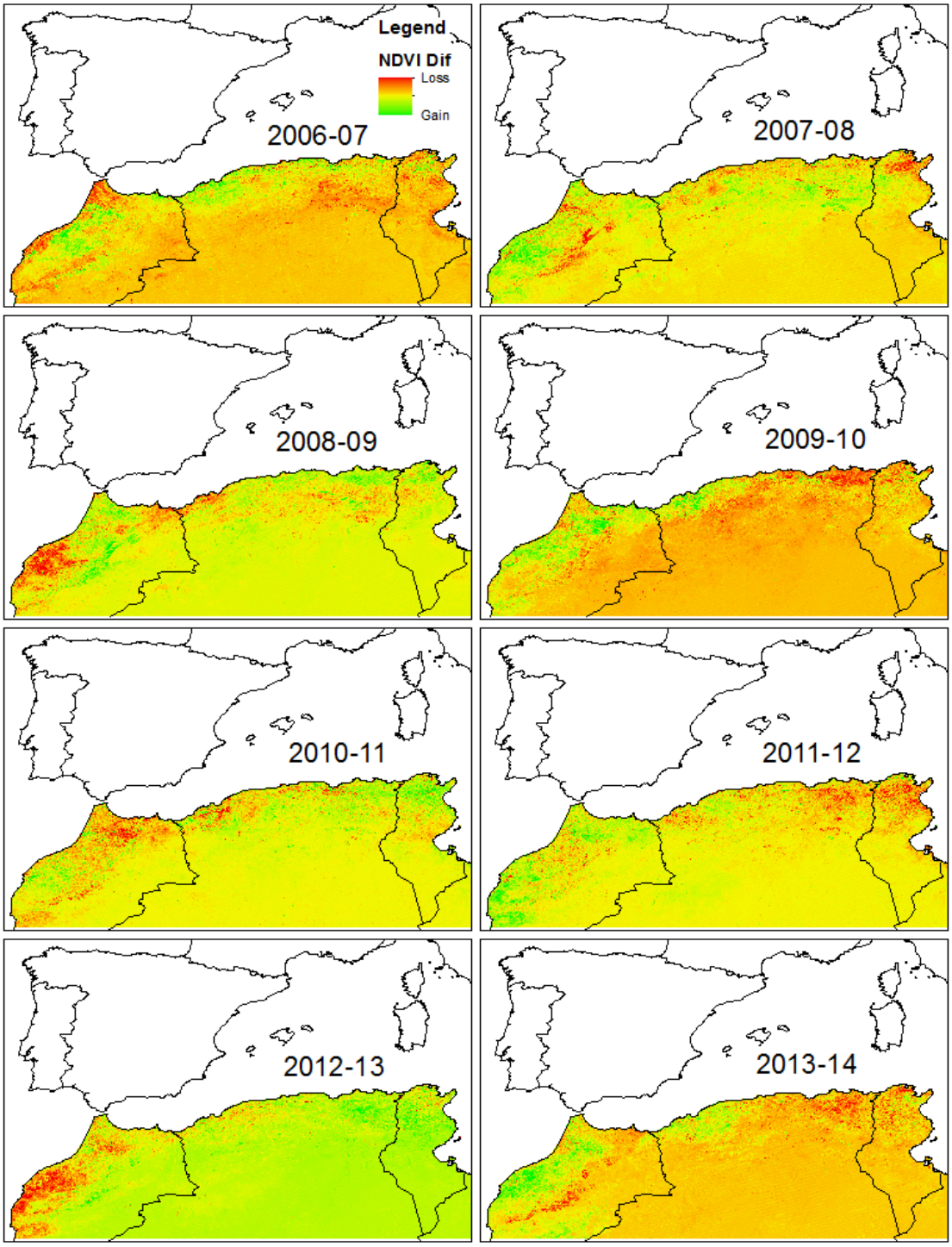

Figure 4.1 Maximum NDVI difference between each consecutive pair of years from 2006 to 2014. Positive differences (red) correspond to decreases in NDVI, while negative differences (green) correspond to increases.

Table 4.1 Percentage of the study area corresponding to distinct classes of relative net vegetation loss severity. Cumulative percentage is also displayed.

Severity	Percentage of study area	Cumulative percentage
0	22.02	22.02
1	74.648	96.667
2	2.736	99.404
3	0.431	99.835
4	0.086	99.921
5	0.027	99.948
6	0.014	99.962
7	0.012	99.974
8	0.01	99.985
9	0.013	99.998
10	0.002	100

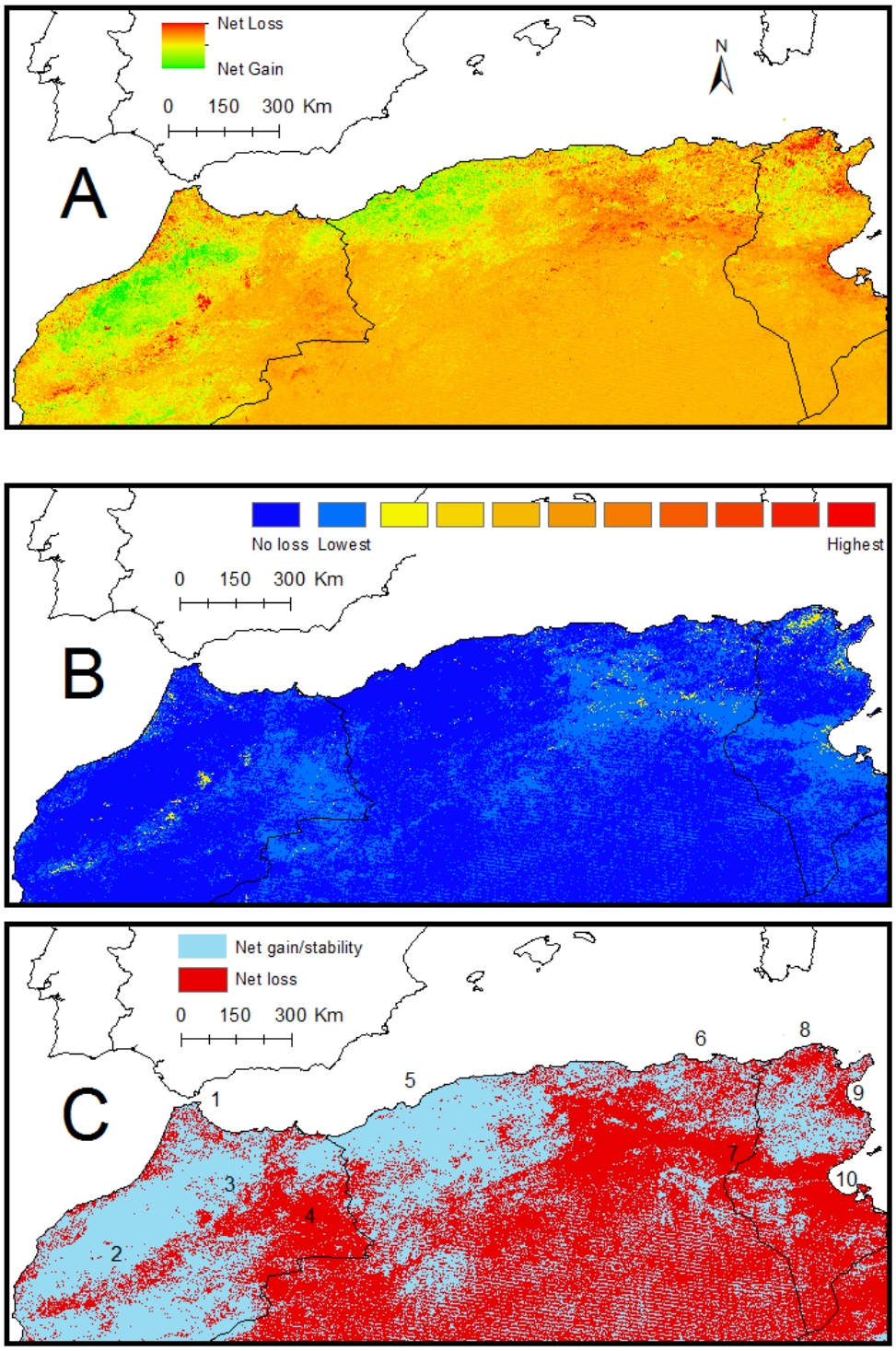

Figure 4.2 Net vegetation loss in northwest Africa between 2006-2014. Panel A displays net maximum NDVI change. Higher values (red) correspond to decreases in NDVI, while lower values (green) correspond to increases. Panel B details severity of vegetation loss. Panel C provides an overview of the total net vegetation loss observed in northwest Africa, regardless of severity. 1: Rif; 2: High Atlas; 3: Middle Atlas; 4: High Plateau; 5: western Tell Atlas; 6: eastern Tell Atlas; 7: Aurès Mountains; 8: Marjardah Valley; 9: Gulf of Hammamet; 10: Gulf of Gabés

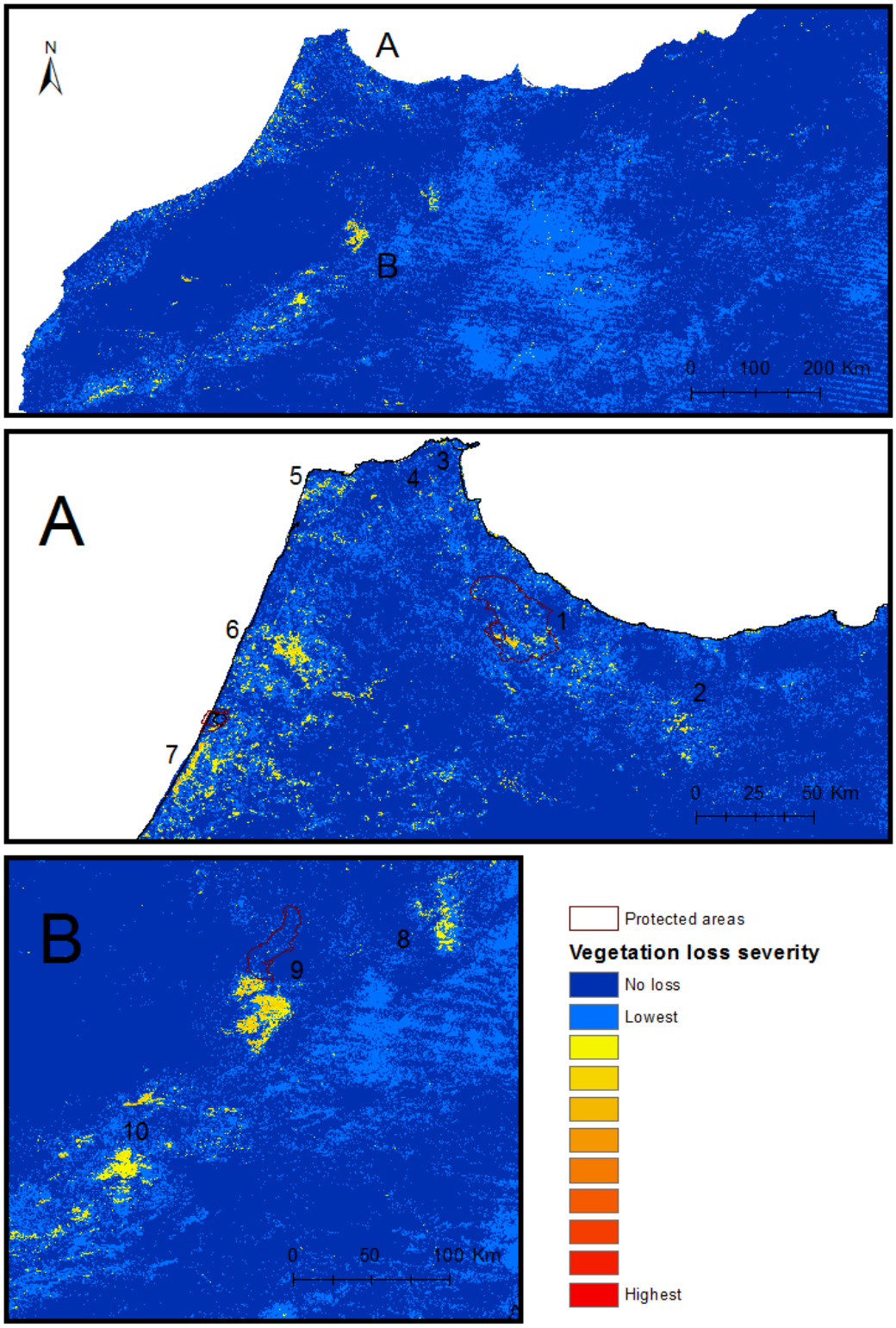

Figure 4.3 Vegetation loss severity in the western Maghreb. Top: Overview of the region; A: Tingitana peninsula; B: Middle Atlas; 1: Talassemtane National Park; 2: Targuist; 3: Jebel Musa; 4: Taghramt; 5: Tanger; 6: Larache; 7: Ben Mansour; 8: Taffert; 9: Iffrane National Park; 10: Beni Melal

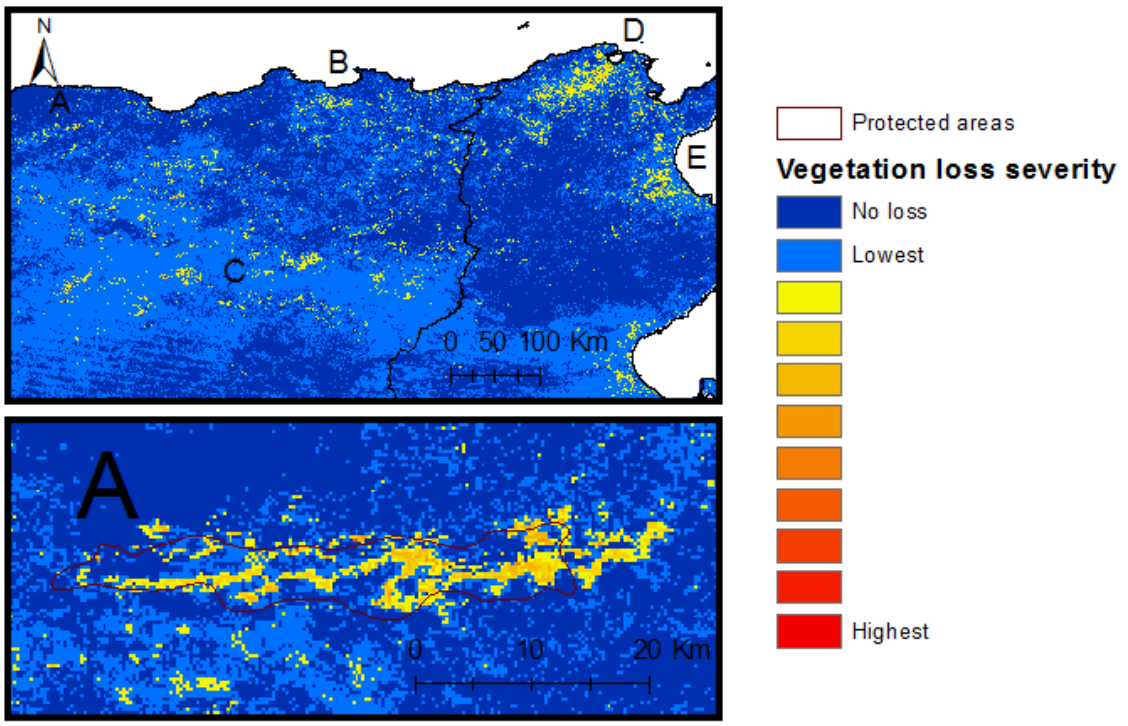

Figure 4.4 Vegetation loss severity in the eastern Maghreb. Top: Overview of the region; Bottom: Detail of the Djurdjura National Park, Algeria; A: Djurdjura National Park; B: Skikda; C: Biskra; D: Bizerte; E: Sousse

4.3.2 Vegetation loss by land cover class

After excluding areas of bare desert, urbanized areas and water bodies, the predominant land cover classes in the region are sparse vegetation (c. 40.4 %) and mosaics of farmland and natural vegetation (c. 42 %, divided among two classes). Collectively, natural vegetation classes comprise c. 49.5 % of the study area, or only 9 % if we exclude areas of sparse vegetation which are likely to be less suitable for Palearctic-origin organisms. Strictly agricultural land cover, either irrigated or rain-fed, comprises less than 9 % of the total study area (Table 4.2).

Overall, the percentage of total vegetation loss which corresponds to any land cover type is roughly of the same order of magnitude as the proportion of the landscape dedicated to that type of land cover, suggesting an even distribution of vegetation loss across land cover types. Nevertheless, land cover consisting of natural vegetation accounts for 58 % of all loss (49.5 % in areas of sparse vegetation and 8.5 % in other classes) despite only occupying 49.5 % of the study area, while areas partially or completely dedicated to agriculture account for 42 % of all loss while occupying 50.5 %

of the area. Despite the low contribution of non-sparse natural vegetation areas to total vegetation loss, their restricted extent means that vegetation loss in a small area translates to a large percentage of natural vegetation being lost, with each forest and shrubland class showing evidence of vegetation loss in more than 25 % of its extent, and a maximum percentage of vegetation loss of c. 43 % for closed broadleaved deciduous forests, the largest percent loss in habitats where *S. algira* is known to occur. Agricultural landscapes experienced vegetation loss in c. 28.5 % of their extent, most of which corresponds to mosaics of farmland and natural vegetation. The high percentage of *S. algira* records located in this type of land cover (c. 58.6 %), while likely disproportionate due to sampling bias related with greater ease of access when compared to less anthropocentric landscapes, reflects the importance of these mosaics for salamander persistence. Also noteworthy is the detection of vegetation loss in 42 % of the sparsely vegetated areas in the region (Table 4.2).

4.3.3 At-risk populations of *S. algira*

All *S. algira* populations currently known occur in grid cells with relatively low (0-3) vegetation loss severity (Figure 4.5). The Moroccan populations occupying areas of most concern are located in Taffert (Middle Atlas) and in the Talassemtane National Park (Rif). Populations in the Central Rif are located in areas of no vegetation loss, in contrast with those of the Western Rif, where low severity vegetation loss was identified for most of the populations. No net vegetation loss was detected in the only known location of *S. a. spelaea* in the Beni Snassen massif. In Algeria, the populations most severely affected by vegetation loss are located near Blida and in Boukhlifa. While less severe, vegetation loss has also been detected in the apparently isolated populations of Annaba and Tifiras Skikda.

Overlap between ecological niche-based models and binary vegetation loss ranges between 21-38 %, with the greatest overlap among subspecies occurring in the distribution of *S. a. algira* (32.11 %), followed by *S. a. tingitana* (29.83 %) and *S. a. splendens* (21.37 %). Among the sublineages of the Rif, overlap is greatest for *S. a tingitana* sublineage 1 (37.98 %), followed by sublineages 2 (31.32 %) and 3 (27.29 %) of the same subspecies, and is smallest for *S. a. splendens* sublineage 1 (25.51 %). Overlap between niche models and vegetation loss can be consulted in Supplementray Materials (Figure 7.9)

Table 4.2 Vegetation loss by type of land cover. All values are percentages. Total: percentage of study area occupied by land cover type; Loss LC: percentage of land cover type where vegetation loss was detected; Loss Total: percentage of the total vegetation loss corresponding to vegetation loss in the land cover type; *S. algira* occurrence records: percentage of *S. algira* occurrence records per land cover type. The last three lines summarize information for natural land cover excluding sparse vegetation areas, all natural land cover and non-natural (i.e. agricultural) land cover

Land cover	Total	Loss LC	Loss total	*S. algira* occurrence records
Sparse vegetation	40.433	42.054	49.521	4.505
Mosaic Cropland/vegetation	25.959	25.974	19.637	34.234
Mosaic Vegetation/Cropland	15.771	32.328	14.849	21.622
Rainfed Croplands	8.789	29.47	7.544	2.703
Closed to open shrubland	3.307	31.249	3.01	14.414
Mosaic Forest-Shrubland/Grassland	2.691	34.755	2.723	9.009
Mosaic Grassland/Forest-Shrubland	2.001	25.153	1.466	2.703
Closed Broadleaved deciduous forest	0.747	43.295	0.941	7.207
Closed needleleaved evergreen forest	0.281	35.409	0.289	3.604
Closed to open mixed broadleaved and needleleaved forest	0.019	31.668	0.018	0
Closed broadleaved forest permanently flooded (saline-brackish water)	0.001	75	0.002	0
Closed to open broadleaved evergreen or semi-deciduous forest	<0.001	50	<0.001	0
Irrigated croplands	<0.001	100	<0.001	0
Non-sparse natural vegetation	9.046	32.067	8.45	36.937
All natural vegetation	49.479	40.228	57.97	41.441
Non-natural vegetation	50.52	28.566	42.03	58.559

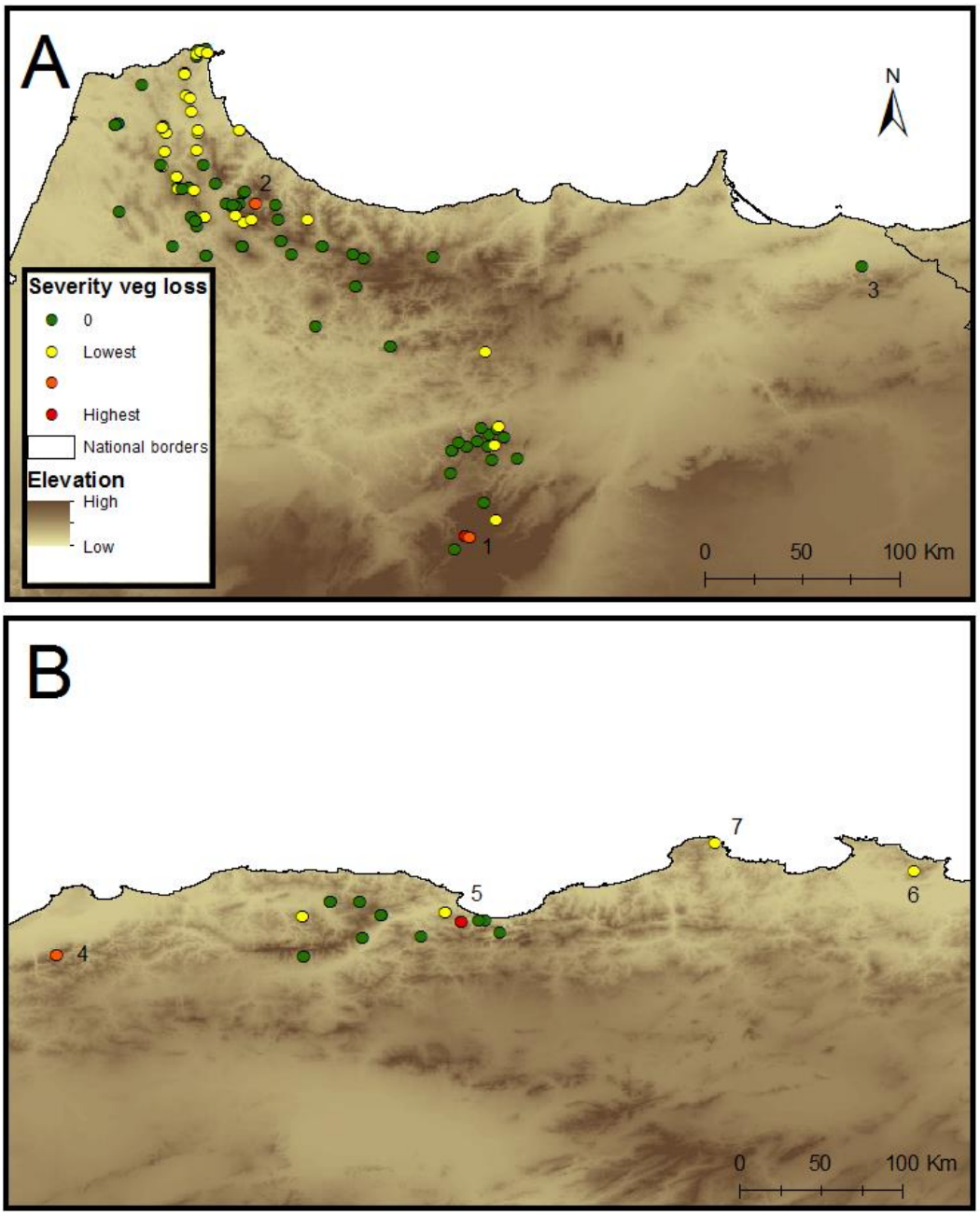

Figure 4.5 Severity of vegetation loss depicted for each occurrence locality of *S. algira*. Colors of points represent distinct degrees of relative severity of vegetation loss. A: Distribution of Moroccan populations; B: Distribution of Algerian populations. 1: Taffert; 2: Talassemtane; 3: Beni Snassen; 4: Blida; 5: Boukhlifa; 6: Annaba; 7: Tifiras Skikda

4.4 Discussion

4.4.1 Global patterns of vegetation change

Fluctuation in NDVI values were persistently observed during the nine year period monitored in this study, with areas where vegetation productivity remained stable from one year to the next being restricted to few scattered grid cells through the entire study area. Even where net vegetation change showed a predominant tendency towards gain or loss over the nine years, this tendency was often temporarily reversed in some years. This emphasizes the dynamic character of landscapes, and is likely associated with sporadic events, both natural and anthropogenic, such as climate extremes, fires, crop rotations and changes in land management. While the identification of specific disturbance events was not the main purpose of this work, future endeavours may benefit from looking into this subject in more detail. The identification of correlations between drastic vegetation changes and climatic anomalies may be particularly useful in discerning the effects of climate and human activities on the observed changes in vegetation.

Nonetheless, the analysis of net vegetation change allows us to minimize the obscuring effects of sporadic fluctuations and obtain information on the dominant trends of vegetation change in the Maghreb. A predominant tendency for decreasing NDVI was identified for the majority of the study area. The more economically vulnerable regions of the Mediterranean are currently undergoing a process of human demographic expansion, with the population of the southern and eastern Mediterranean (which includes the Maghreb) doubling in size between 1955 and 2010, and expected to continue to grow until 2060 (UNDP, 2011; Allard et al., 2013). For this reason, anthropogenic pressure on Mediterranean ecosystems has been increasing as the growth of rural populations has led to overuse of forests and farmland, resulting in habitat degradation (Allard et al., 2013).

Conversely, positive trends of vegetation growth were observed in ~ 20 % of the study area. Increases in vegetation productivity can be related to several phenomena expected to have a positive effect on biodiversity, such as reforestation efforts or ecological succession following disturbances. Yet, the relationship between increases in vegetation productivity and ecosystem function is not necessarily a direct one, as

vegetation productivity by itself is not informative on the type of vegetation growing at a location. For example, reforestation efforts in the Chefchaouen province of Morocco during the 1990's, while taking place at a rate identical to that of loss of natural forest, largely consisted of fast-growing coniferous monocultures for the production of timber (DPA, 1994). Positive trends of vegetation growth can, alternatively, be related with land abandonment, which has at times been associated with loss of biodiversity in Mediterranean landscapes due to loss of spatial heterogeneity (Blondel et al., 2010; Plieninger et al., 2014), and with the local extinction of *Vipera aspis* populations in central Europe (Jäggi & Baur, 1999). While land abandonment is not as problematic in North Africa as it is in Europe, due to the former's ongoing increase in rural population (Allard et al., 2013), the possibility of it being a local issue in some parts of North Africa cannot be fully discarded. For these reasons, trends of increased vegetation must be interpreted cautiously, and should be supported by field data.

A possible effect of climate change on trends of vegetation change must also be considered. The majority of the area included in this study is arid or semi-arid, and it is therefore expected that precipitation should be the main climatic constraint of vegetation growth as expressed in temporal trends of NDVI change (Chen et al., 2016). There is evidence for an ongoing decrease in number of wet days and annual precipitation, accompanied by an increase in dry episode duration and magnitude in the Maghreb (Tramblay et al., 2013). Though this discussion will primarily focus on the possible anthropogenic causes of habitat degradation, the effect of climate on vegetation trends in the Maghreb should be assessed in detail.

4.4.2 Landscape change and habitat degradation

Sparsely vegetated areas, the majority of which are located in the arid margin of the Sahara desert, account for nearly half of the total area where net vegetation loss has been registered. While severity of NDVI loss is predominantly low in the desert margin, suggesting local loss in productivity is relatively small when compared to other locations in the study area, it appears that widespread land degradation is taking place in the area. The arid environment may increase the vulnerability of this type of landscape to water scarcity and land overuse.

Vegetation loss was detected on a large portion of the closed broadleaved deciduous forests of the study area. This type of forest is predominantly distributed in the Moroccan Rif and Middle Atlas, and in eastern Algeria, all of which are characterized by the presence of rural populations, which is likely to be the source of pressure on these ecosystems. The predominant anthropogenic causes of forest degradation in North Africa are overgrazing, conversion to agriculture, and clearing (Allard et al., 2013). Wood and wood pulp harvesting represent a small portion of the economy of North African countries (Allard et al., 2013), and a more important driver of forest clearing seems to be the harvesting of fuelwood. In Morocco, the only nation in the study area for which data on fuelwood usage is available, it represents 30 % of energy consumption (Moroccan Centre for Development of Renewable Energies, 2007). This level of consumption exceeds the productive capacity of Moroccan forests and is identified by the Moroccan High Commission for Water and Forestry and Combat against Desertification as a major driver of deforestation and ecosystem degradation (Moroccan Centre for Development of Renewable Energies, 2007). The identification of areas of severe vegetation loss in the Talassemtane Natural Park and south of the Ifrane National Park is consistent with the particularly high reliance of the provinces of Chefchaouen, Ifrane and Khéfira on fuelwood, due to a lack of alternative energy sources (Moroccan Centre for Development of Renewable Energies, 2007).

The present work presents evidence for widespread degradation of forest areas in northeast Algeria between 2006 and 2014. These results agree with previous findings of a tendency towards forest loss in Algeria between 1990 and 2010 (FAO, 2010). While the causes for this degradation of Algerian forests are not entirely clear, the active rural population in Algeria experienced the greatest growth among Maghreb countries between 1990 and 2010, and by the end of this period had the largest active rural population in the region (Allard et al., 2013). Increased human pressure is therefore likely to be a driving force of habitat degradation in the country. Fire is likely to play an important role as well, as Algeria, out of all nations in the Maghreb, experienced the highest number of fires per every 1,000 ha between 2008-2010, the largest total burned area between 2000-2010, and the largest average fire extent in the majority of the years between 2000-2010 (Allard et al., 2013). While there is still a systemic lack of information on the prevailing causes of fire in the Mediterranean,

mostly caused by lack of proper post-fire investigation (Allard et al., 2013), the existing data suggests an important role of human activities (e. g. Meddour-Sahar et al., 2013).

The incidence of severe vegetation loss in protected areas, specifically in the Talassemtane National Park in Morocco and Djurdjura National Park in Algeria, suggests that current methods of protection may be insufficient to halt habitat degradation. Both protected areas occur in regions with dense rural populations (Moore et al., 1998; Allard et al., 2013) and are likely to be under pressure from human activities. Fire and cannabis cultivation at mid-range altitude have been identified as the main threats to the *Abies pinsapo* forests of the Talassemtane National Park (Esteban et al., 2010), though another threat may lie in forest clearing, as it is uncertain whether the prohibition of forest clearing established in the park is effective in preventing the locally important harvesting of fuelwood. The Algerian region of Kabylia, where the Djurdjura National Park is located, is the region of the country most severely affected by fires, most of which are deliberately set for pasture renewal or for security reasons (i.e. “security fires” set by the state in its fight against *jihadi* combatants; Meddour-Sahar et al., 2013). While this work didn’t test a causal link between these hypothesized threats and the observed loss in vegetation, the presented results suggest that these protected areas may retain a degree of vulnerability to habitat degradation. Therefore, a proper threat assessment should be performed soon, and management approaches adjusted accordingly.

Mosaics of farmland and natural vegetation represent a substantial component of the North African landscape. Heterogeneous landscapes provide a diversity of habitats and may help maximize biodiversity of Mediterranean communities (Blondel et al., 2010; Plieninger et al., 2014). The incidence of species adapted to agricultural habitats in North Africa (e. g. *Pleurodeles* sp., Ben Hassine & Escoriza, 2014) supports this ability of mosaics to maximize species richness by enabling the occurrence of both farmland-adapted and forest-adapted species in the same area. However, the spatial complexity of mosaics makes the interpretation of vegetation change in these areas problematic under the framework used in this work, as it is not possible to identify the type of natural vegetation present, or to distinguish between changes in the natural and agricultural components of vegetation. One particular threat to mosaic landscapes in North Africa is ongoing urban growth, which imperils peri-urban ecosystems (Allard et al., 2013). The locations of severe vegetation loss identified near the Algerian locality of

Skikda and in the Tunisian localities of Bizerte and Sousse all consist of mosaics situated on the outskirts of major population centres, and the trend of decreasing vegetation observed may reflect an increase in pressure from urban populations, either due to replacement of mosaics by urban areas or by intensification of local agricultural practices resulting in a reduction of natural vegetation.

4.4.3 Impact of vegetation loss on *S. algira*

The Moroccan Rif has historically been subject to forest loss due to human activities since at least 2,000 years ago (Cheddadi et al., 2015). Due to the high rainfall and relative erodibility of the local lithology (Moore et al., 1998), deforestation in the region has been conductive to further habitat degradation caused by soil erosion (Moore et al., 1998; Cheddadi et al., 2015). Through the 20th and early 21th centuries, the Rif has been characterized by a growing rural population, increasing the pressure caused by overgrazing and cannabis cultivation on forest systems (Moore et al., 1998; Labrousse & Romero, 2001; Chouvya & Afsahi, 2014). Starting in 2005, a shifting tendency in cannabis cultivation in the Rif has been reported, as a result of stronger state control, with a shift from cultivation of the traditional *kif* to new hybrid varieties which produce greater yields (Chouvy & Afsahi, 2014). While this shift has resulted in abandonment of cannabis cultivation in some areas of the central Rif, a proper assessment of the current extent of cannabis cultivation is still lacking (Chouvy & Afsahi, 2014). What seems apparent is that this can be seen as a transition from extensive to intensive cultivation methods, as the new varieties have greater water demands than the traditional *kif*, with unforeseen consequences for water management in the region (Chouvy & Afsahi, 2014). The expansion of cannabis cultivation has been previously proposed as a cause for loss of forest habitat for Palearctic vertebrates (*Vipera latastei*, Brito et al., 2011; *Emys orbicularis occidentalis*, Velo-Antón et al., 2015c), and is therefore expected to also have a negative impact on *S. algira*.

The assessment of threat levels among *S. algira* populations of the Rif, as reflected in the detection of vegetation loss severity per occurrence record, and in the overlap of vegetation loss with predicted distributions per sublineage, indicates that the northernmost populations of the Rif may be currently at more risk than those of the southwestern and central Rif. The sparsely vegetated limestone outcrops occupied by the pueriparous populations of the north may be more vulnerable to the effects of

overgrazing and soil erosion than other types of land cover. However, the effect on the local populations, which are less dependent on forest cover than larviparous populations of other sublineages (Beukema et al., 2010; Escoriza & Ben Hassine, 2014; Previous chapter of this thesis), remains unclear.

In the southwestern and central Rif, the majority of populations appear to be in stable areas of stable vegetation, though this may simply reflect persistence in areas so far unaffected by deforestation and cannabis cultivation. While *S. a. splendens* sublineage 1 (the sublineage with the largest suitable area in the southwestern and central Rif) exhibited the lowest percentage of overlap between distribution models and vegetation loss, 25.5 % of its distribution experienced some extent of habitat degradation, suggesting human pressure in the Rif is still strong. The western Rif includes the Talassemtane National Park, which is part of a contact zone between the Rif sublineages of *S. algira* (See chapters 2 and 3 of this thesis for details), and where severe vegetation loss was identified. In the central Rif, the identification of an area of severe vegetation loss in the region of Targuist may support a continued expansion of traditional cannabis cultivation in this region, where the more arid climate may limit the cultivation of the new water-demanding hybrid varieties in favour of the more resilient *kif* (Chouvy & Afsahi, 2014).

The Middle Atlas has been historically subject to human pressure for the last 3,000 years (Cheddadi et al., 2015). The major factors contributing to habitat degradation in the region are forest clearings and pastoral activities, with well documented effects on vertebrate populations such as the *Macaca sylvanus* of Ifrane (Camperio Ciani et al., 2005, 2006; van Lavieren et al., 2010). Further north, historical deforestation occurred in Taffert, and all *S. algira* populations known in the region seem restricted to small patches of *Cedrus atlantica* (Guillermo Velo-Antón, personal observation). Therefore, forest clearing appears to be the predominant threat to forest-dependent species in this region.

While low-severity vegetation loss was identified in the area of Beni Snassen, most of it is restricted to the lowlands, where the landscape is predominantly agricultural, and none of it overlaps with the occurrence records available for *S. a. spelaea*. While the restricted distribution and low genetic variability of this subspecies make it a priority target for conservation (Escoriza & Comas, 2007), the major threat to its survival

appears to be loss of suitable water bodies for reproduction due to habitat modification for human activities (Escoriza et al., 2006, 2013). Loss of forest habitat has been suggested as an additional threat for this subspecies (Escoriza et al., 2013), but hard data on vegetation loss in Beni Snassen is currently non-existent, and the present work supports only moderate vegetation loss which does not appear to interfere directly with *S. algira*. However, it should be taken into account that the threat assessment performed in this work was more limited for *S. a spelaea* than for the other subspecies of *S. algira*, as the low number of records precluded the prediction of the potentially suitable area of distribution by ecological niche models. For this reason, the full distribution of *S. a. spelaea* remains unknown, hindering a more detailed assessment of habitat degradation. Moreover, this work is unable to detect vegetation loss prior to 2006, and historical habitat modifications (Ellis et al., 2010) likely contributed to habitat loss and low genetic diversity of this isolated and endangered population. A proper clarification of the conservation status of *S. a. spelaea* is still lacking, and would require a better delimitation of the distribution of this subspecies, as well as a detailed assessment of landscape change in Beni Snassen, taking into account not only data on vegetation change but also on changes in water availability.

Salamandra algira algira has the greatest overlap between predicted suitable area and vegetation loss, out of all the three *S. algira* subspecies for which this assessment was performed. This is consistent with the greater impact of pressure from rural population growth and man-made fire in Algeria, as described above. All the populations of *S. a. algira* identified as being subject to any level of vegetation loss are situated in forest areas on the outskirts of important human population centres, which may reflect an impact of human activities on the degradation of these habitats. The population near Blida may be particularly affected by the reliance of the city on the nearby forests for water supply (Allard et al., 2013), which may impose hydric stress on these habitats.

4.4.4 Applicability to other Palearctic taxa

The framework applied in this study uncovered evidence of habitat degradation in areas where other Palearctic species co-occur with *S. algira*, specifically in the Rif (*Alytes maurus, Bufo spinosus*, *Emys orbicularis occidentalis, Natrix astreptophora, Vipera latastei*; Mediani et al., 2015), Middle Atlas (*Alytes maurus, Bufo spinosus, Vipera latastei*; Brito et al., 2011; Mediani et al., 2015) and the eastern Algeria localities

of Kabylia and Annaba (*Natrix astreptophora, Vipera latastei*; Schleich et al., 1996; Brito et al., 2011). Severe vegetation loss was also identified in coastal areas of northwest Morocco, in agreement with previous reports of possible local extinction, related with intensification of human activities, of coastal populations of *Emys orbicularis occidentalis* (Velo-Antón et al., 2015c) and *Vipera latastei* (Brito et al., 2011).

The approach used here for identifying vulnerable populations is limited by difficulties in the identification of the underlying causes of vegetation loss, yet it shows potential in the identification of priority areas where habitat degradation may be taking place. As exemplified by our results for the *S. algira* of the Rif, the reliance on occurrence data alone may be insufficient to obtain an accurate picture of habitat degradation, and should be complemented with data on the full distribution, which while difficult to assess empirically, can be predicted with ecological niche models.

Chapter 5: Final remarks

This work supports a predominantly allopatric model of diversification within *S. algira*, with wet-season precipitation acting as the main driver of vicariance, due to its influence on the distribution of suitable forested habitat and surface water.

The evolutionary history of the eastern clade of *S. algira*, which consists of the subspecies *S. a. algira* and *S. a. spelaea,* is still not fully clarified. There are doubts about the status of the latter as a full subspecies or simply a divergent branch of *S. a. algira*. Low sample size hampered the development of ecological niche based models for the restricted *S. a. spelaea,* hindering evolutionary reconstructions for the eastern clade, though we hypothesize a role of microrefugia on the differentiation of *S. a. spelaea*. Nonetheless, this work has provided insights into the origin of current population structure in *S. a. algira*, supporting a continuous or only recently fragmented distribution of the known populations of *S. a. algira* in eastern Algeria, as suggested previously (Merabet et al., 2015; Ben Hassine et al., 2016).

In the western clade, there is evidence for an early split between *S. a. tingitana* and *S. a. splendens*, driven by vicariance in independent climatic refugia. This work provides evidence for a deep divergence between the two *S. a. splendens* sublineages. Insufficient data on the distribution of *S. a. splendens* in the central Rif and Middle Atlas currently hinders a complete characterization of the full environmental variability available to the subspecies, which produces uncertainty regarding ecological niche model results.

Ample overlap between predicted climatic suitability for the *S. algira* sublineages of the Rif suggests that non-climatic environmental variables and barriers to dispersal, such as major river basins, likely played an important role in the divergence between sublineages of *S. a tingitana*. Persistence in microrefugia is hypothesized as an important driver for the differentiation of *S. a tingitana* sublineage 1.

This work uncovered evidence for secondary contact between the sublineages of *S. a. tingitana*, as well as between subspecies *S. a. tingitana* and *S. a. splendens*, supporting an absence of reproductive isolation and overlapping ecological requirements among *S. algira* in the Rif. A possible area of sympatry between all Rif sublineages was identified on the predominantly forested habitat surrounding Oued Laou. While not all sublineages are confirmed to occur in this area, evidence of gene flow between the two subspecies has been detected here. Closing the remaining

sampling gaps of *S. algira* in the Rif should be prioritized, to allow a full clarification of the population structure and contact zone dynamics in this region.

The discovery of pueriparous reproduction in a population of *S. a. tingitana* sublineage 2 marks the first observation of pueriparity south of Oued Martil and outside of sublineage 1, as well as the first evidence of distinct reproductive strategies within one sublineage of *S. algira*. Multiple events of pueriparity evolution or transference of the trait from one sublineage to another by mtDNA capture, as previously proposed for *S. salamandra* (García-París et al., 2003; Velo-Antón et al., 2007, 2012), are suggested as possible explanatory scenarios for the current distribution of pueriparity among *S. algira*.

The identification, for the pueriparous sublineage 1, of distinct ecological affinities from the larviparous sublineages (reduced association with precipitation and vegetation cover, increased affinity for karstic lithology) supports the “dry climate hypothesis” previously proposed as the ecological driver of pueriparity in the genus *Salamandra* (García-Paris et al., 2003; Velo-Antón et al., 2007; Beukema et al., 2010). A more detailed knowledge of the distribution of pueriparity within sublineage 2 is now required to clarify the evolutionary origin and ecological context of pueriparity in this sublineage.

New insights were gained on the amount and distribution of vegetation loss across North Africa for the 2006-2014 period, with the identification of areas presenting high pressure from human activities in the Rif, Middle Atlas and northeast Algeria. Vegetation loss is particularly widespread along the desert margins, on heterogeneous landscapes combining agriculture and natural vegetation, and on Mediterranean broadleaved forests, with the latter having severe implications for relict Palearctic species in North Africa. Populations of *S. algira* subject to recent vegetation loss were identified in the Talassemtane National Park in the Rif, suggesting that protective measures currently in place may be insufficient to safeguard this important area of sympatry for this species. The results obtained in this work identified the areas of most severe vegetation loss in North Africa and the populations of *S. algira* more vulnerable to habitat degradation, providing a valuable resource for prioritizing future conservation efforts for relict Palearctic species in North Africa, and for *S. algira* in particular.

Chapter 6: References

Allard, G., Berrahmouni, N., Besacier, C., Boglio, D., Briens, M., Brizay, A., Camia, A., Colletti, L., Conigliaro, M., D'Annunzio, R. & Ducci, F. (2013) *State of Mediterranean forests 2013*.

Allouche, O., Tsoar, A., & Kadmon, R. (2006). Assessing the accuracy of species distribution models: prevalence, kappa and the true skill statistic (TSS). *Journal of applied ecology*, *43*(6), 1223-1232.

Alvarez, Y., Mateo, J.A., Andreu, A.C., Diaz-Paniagua, C., Diez, A. & Bautista, J.M. (2000) Mitochondrial DNA haplotyping of Testudo graeca on both continental sides of the Straits of Gibraltar. *Journal of Heredity, 91*, 39–41.

Álvarez, D., Lourenço, A., Oro, D. & Velo-Antón, G. (2015). Assessment of census (N) and effective population size (N e) reveals consistency of N e single-sample estimators and a high N e/N ratio in an urban and isolated population of fire salamanders. *Conservation Genetics Resources*, *7*(3), 705-712.

Anadón, J. D., Giménez, A., Martínez, M., Palazón, J. A. & Esteve, M. A. (2007). Assessing changes in habitat quality due to land use changes in the spur-thighed tortoise Testudo graeca using hierarchical predictive habitat models. *Diversity and Distributions*, *13*(3), 324-331.

Anadón, J. D., Graciá, E., Botella, F., Giménez, A., Fahd, S. & Fritz, U. (2015). Individualistic response to past climate changes: niche differentiation promotes diverging Quaternary range dynamics in the subspecies of Testudo graeca. *Ecography*, *38*(9), 956-966.

Anderson, E.C. & Thompson, E.A. (2002) A model-based method for identifying species hybrids using multilocus genetic data. *Genetics,* 160: 1217—1229

Anderson, R. P.,& Raza A. (2010): The effect of the extent of the study region on GIS models of species geographic distributions and estimates of niche evolution: preliminary tests with montane rodents (genus Nephelomys) in Venezuela. *Journal of Biogeography, 37*(7) 1378-1393.

Elith, J., Graham, C.H., Anderson, R.P., Dudık, M., Ferrier, S., Guisan, A., Hijmans, R.J., Huettmann, F., Leathwick, J.R., Lehmann, A., Li, J., Lohmann, L. G., Loiselle, B.A. , Manion, G., Moritz, C., Nakamura, M., Nakazawa, Y, Overton, J.M , Peterson,

A.T., Phillips, S. J, Richardson, K., Scachetti-Pereira, R., Schapire, R.E., Soberon, J., Williams, S., Wisz, M.S. & Zimmermann, N.E. (2006). Novel methods improve prediction of species' distributions from occurrence data. *Ecography*, *29*(2), 129-151.

Araújo, M. B., Pearson, R. G., Thuiller, W. & Erhard, M. (2005). Validation of species–climate impact models under climate change. *Global Change Biology*, *11*(9), 1504-1513.

Ashcroft, M. B., Gollan, J. R., Warton, D. I. & Ramp, D. (2012). A novel approach to quantify and locate potential microrefugia using topoclimate, climate stability, and isolation from the matrix. *Global Change Biology*, *18*(6), 1866-1879.

Barata, M., Harris, D.J. & Castilho, R. (2008) Comparative phylogeography of northwest African Natrix maura (Serpentes: Colubridae) inferred from mtDNA sequences. *African Zoology, 43*,1–7.

Barata, M., Perera, A., Martínez-Freiría, F. & Harris, D.J. (2012) Cyryptic diversity within Morroccan endemic day geckos Quedenfeldtia (Squamata: Gekkonidae): a multidisciplinar approach using genetic, morphological and ecological data. *Biological Journal of the Linnean Society 106,* 828–850.

Bar-David, S., Segev, O., Peleg, N., Hill, N., Templeton, A.R., Schultz C.B. & Blaustein, L. (2007): Long-distance movements by fire salamanders (Salamandra infraimmaculata) and implications for habitat fragmentation. *Israel Journal of. Ecology and Evolution, 53*: 143-159.

Beja, P., Bosch, J., Tejedo, M., Edgar, P., Donaire-Barroso, D., Lizana, M., Martínez-Solano, I., Salvador, A., García-París, M., Gil, E.R., Slimani, T., El Mouden, E.H., Geniez, P. (2009). *Pleurodeles waltl. The IUCN Red List of Threatened Species 2009: e.T59463A11926338.* (http://dx.doi.org/10.2305/IUCN.UK.2009.RLTS.T59463A11926338.en. Downloaded on 05 August 2016).

Ben Hassine, J., Gutiérrez-Rodríguez, J., Escoriza, D., & Martínez-Solano, I. (2016). Inferring the roles of vicariance, climate and topography in population differentiation

in Salamandra algira (Caudata, Salamandridae). *Journal of Zoological Systematics and Evolutionary Research*.

Beukema, W., De Pous, P., Donaire, D., Escoriza, D., Bogaerts, S., Toxopeus, A. G., De Bie, C.A.J.M., Roca, J. & Carranza, S. (2010). Biogeography and contemporary climatic differentiation among Moroccan Salamandra algira. *Biological Journal of the Linnean Society*, *101*(3), 626-641.

Beukema, W., De Pous, P., Donaire-Barroso, D., Boaerts, S., Garcia-Porta, J., Escoriza, D., Arribas, O.J., El Mouden, E. H. & Carranza, S. (2012). Review of the systematics, distribution, biogeography and natural history of Moroccan amphibians. *Zootaxa*, *3661*, 1-60.

Bicheron, P., Defourny, P., Brockmann, C., Schouten, L., Vancutsem, C., Huc, M., Bontemps, S., Leroy, M., Achard, F., Herold, M., Ranera, F. & Arino, O. (2008). *GLOBCOVER. Products Description and Validation Report*, Medias-France, Toulouse, France.

Blondel, J., Aronson, J., Bodiou, J. & Boeuf, G., (2010). *The Mediterranean Region*. 2nd Edition, Oxford University Press.

Bogaerts, S., & Donaire-Barroso, D. (2003) Sobre el politipismo en Salamandra algira Bedriaga, 1883. *Boletin de la Asociacion. Herpetológica Española,* 14.1-2: 47-51.

Bogaerts, S., Donaire Barroso, D., Pasmans, F., Böhme, W., & Carranza, S. (2013). Do north African fire salamanders, Salamandra algira, occur in Tunisia?. *Herpetology. Notes*, *6*, 301-306.

Bonato, L. & Fracasso, G. (2003). Movements, distribution pattern and density in a population of Salamandraatra aurorae (Caudata: Salamandridae). *Amphibia-Reptilia, 24*: 251-260.

Bons, J., & Geniez. P. (1996). *Amphibians and reptiles of Morocco*. Barcelona, Asociación Herpetológica Española

Brito, J. C., Fahd, S., Martínez-Freiría, F., Tarroso, P., Larbes, S., Pleguezuelos, J. M., & Santos, X. (2011). Climate change and peripheral populations: predictions for a relict Mediterranean viper. *Acta Herpetologica*, *6*(1), 105-118.

Buckley, D., Alcobendas, M., García-París, M., & Wake, M. H. (2007). Heterochrony, cannibalism, and the evolution of viviparity in Salamandra salamandra. *Evolution & development*, *9*(1), 105-115.

Buckley, D. (2012). Evolution of viviparity in salamanders (Amphibia, Caudata). *eLS*. Wiley, Chichester.

Caccone A., Milinkovitch M.C., Sbordoni V. & Powell J.R. (1994) Molecular biogeography: Using the Corsica-Sardinia microplate disjunction to calibrate mitochondrial rDNA evolutionary rates in mountain newts (Euproctus). *Journal of Evolutionary Biology 7*, 227–245.

Camperio Ciani, A., & Mouna, M. (2006). Human and environmental causes of the rapid decline of Macaca sylvanus in the Middle Atlas of Morocco. *The Barbary macaque: biology, management and conservation.* Nottingham University Press, Nottingham, 257-275.

Campos, J.C., Sillero, N., & Brito, J.C. (2012). Normalized difference water indexes have dissimilar performances in detecting seasonal and permanent water in the Sahara–Sahel transition zone. *Journal of Hydrology, 464*, 438-446.

Carranza, S., Harris, D. J., Arnold, E. N., Batista, V. & Gonzalez de la Vega, J. P. (2006). Phylogeography of the lacertid lizard, Psammodromus algirus, in Iberia and across the Strait of Gibraltar. *Journal of biogeography*, *33*(7), 1279-1288.

Cheddadi, R., Nourelbait, M., Bouaissa, O., Tabel, J., Rhoujjati, A., López-Sáez, J. A., Alba-Sánchez, F., Khater, C., Ballouche, A., Dezileau, L. & Lamb, H. (2015). A history of human impact on Moroccan mountain landscapes. *African Archaeological Review*, *32*(2), 233-248.

Chen, B., Xu, G., Coops, N. C., Ciais, P. & Myneni, R. B. (2016). Satellite-observed changes in terrestrial vegetation growth trends across the Asia-Pacific region associated with land cover and climate from 1982 to 2011. *International Journal of Digital Earth*, 1-22.

Chouvy, P. A. & Afsahi, K. (2014). Hashish revival in Morocco. *International Journal of Drug Policy*, *25*(3), 416-423.

Ciani, A. C., Palentini, L., Arahou, M., Martinoli, L., Capiluppi, C., & Mouna, M. (2005). Population decline of Macaca sylvanus in the Middle Atlas of Morocco. *Biological Conservation, 121*(4), 635-641.

Cosson, J.F., Hutterer, R., Libois, R., Sara, M., Taberlet, P. & Vogel, P. (2005) Phylogeographical footprints of the Strait of Gibraltar and Quaternary climatic fluctuations in the western Mediterranean: a case study with the greater white-toothed shrew, Crocidura russula (Mammalia: Soricidae). *Molecular Ecology*, *14*, 1151–1162.

Coyne, J.A. & Orr, H.A. (2004) *Speciation*. Sinauer Associates, Sunderland, MA.

Darriba, D., Taboada, G. L., Doallo, R. & Posada, D. (2012). jModelTest 2: more models, new heuristics and parallel computing. *Nature methods*, *9*(8), 772-772.

Donaire-Barroso, D., Martínez-Solano, I., Salvador, A., García-París, M., Gil, E.R., Slimani, T., El Mouden, E.H., Geniez, P. & Mateo, J. (2009). *Salamandra algira. The IUCN Red List of Threatened Species 2009: e.T59464A11927380*. (http://dx.doi.org/10.2305/IUCN.UK.2009.RLTS.T59464A11927380.en. Downloaded on 04 August 2016).

de Pous, P., Metallinou, M., Donaire-Barroso, D., Carranza, S. & Sanuy, D. (2013). Integrating mtDNA analyses and ecological niche modelling to infer the evolutionary history of Alytes maurus (Amphibia; Alytidae) from Morocco. *The Herpetological Journal*, *23*(3), 153-160.

Dobrowski, S. Z. (2011). A climatic basis for microrefugia: the influence of terrain on climate. *Global change biology*, *17*(2), 1022-1035.

Dobson, M., & Wright, A. (2000). Faunal relationships and zoogeographical affinities of mammals in north-west Africa. *Journal of Biogeography*, *27*(2), 417-424.

Donaire-Barroso, D., & Bogaerts, S. (2003). A new subspecies of Salamandra algira Bedriaga, 1883 from northern Morocco. *Podarcis*, *4*(3), 84-100.

DPA (Direction Provinciale de l'Agriculture) (1994) *Potentialités et développement agricole dans la Province de Chefchaouen*. Unpublished internal report. Direction Provinciale de l'Agriculture, Chefchaouen: 18 pp.

Drummond, A.J., Suchard, M.A., Xie, D. & Rambaut, A. (2012). Bayesian phylogenetics with BEAUti and the BEAST 1.7. *Molecular Biology and Evolution*, *29*(8), 1969-1973.

Duggen, S., Hoernle, K., Van Den Bogaard, P., Rüpke, L., & Morgan, J. P. (2003). Deep roots of the Messinian salinity crisis. *Nature*, *422*(6932), 602-606.

Earl, D.A. (2012). STRUCTURE HARVESTER: a website and program for visualizing STRUCTURE output and implementing the Evanno method. *Conservation genetics Resources*, *4*(2), 359-361.

Elith, J., Graham, C.H., Anderson, R.P., DudÍk, M., Ferrier, S., Guisan, A., Hijmans, R.J., Huettmann, F., Leathwick, J.R., Lehmann, A., Li J., Lohmann, L.G., Loiselle, B.A., Manion, G., Moritz, C., Nakamura, M., Nakazawa, Y., Overton, J.M.C., Peterson, A.T., Phillips, S.J., Richardson, K.S., Scachetti-Pereira, R., Schapire, R.E., Soberón, J., Williams, S., Wisz, M.S. & Zimmermann, N.E.. (2006). Novel methods improve prediction of species' distributions from occurrence data. *Ecography 29*, 129–151.

Elith, J., & Leathwick, J.R. (2009). Species distribution models: ecological explanation and prediction across space and time. *Annual Review of Ecology, Evolution, and Systematics*, *40*(1), 677.

Ellis, E.C., Klein Goldewijk, K., Siebert, S., Lightman, D. & Ramankutty, N. (2010). Anthropogenic transformation of the biomes, 1700 to 2000. *Global ecology and Biogeography*, *19*(5), 589-606.

Escoriza, D., Comas, M.M., Donaire, D., & Carranza, S. (2006). Rediscovery oí Salamandra algira Bedriaga, 1833 from the Beni Snassen massif (Morocco) and phylogenetic relationships of North African Salamandra. *Amphibia-Reptilia*, *27*, 448-455.

Escoriza, D., & Ben Hassine, J. (2014). Microclimatic variation in multiple Salamandra algira populations along an altitudinal gradient: phenology and reproductive strategies. *Acta Herpetologica*, *9*(1), 33-41.

Escoriza, D., & Comas, M.D.M. (2007). Description of a new subspecies of Salamandra algira Bedriaga, 1883 (Amphibia: Salamandridae) from the Beni Snassen massif (Northeast Morocco). *SALAMANDRA-BONN-*, *43*(2), 77.

Esteban, L.G., De Palacios, P. & Aguado, L.R.L. (2010). Abies pinsapo forests in Spain and Morocco: threats and conservation. *Oryx*, *44*(2), 276.

Evanno, G., Regnaut, S., & Goudet, J. (2005). Detecting the number of clusters of individuals using the software STRUCTURE: a simulation study. *Molecular Ecology 14*, 2611–2620.

Fahd, S., & Pleguezuelos, J.M. (1996). Los Reptiles del Rif (norte de Marruecos), I: Quelonios, Saurios. *Revista Española de Herpetología*, *10*, 55-89.

Fahd, S., El Marnisi, B., Mediani, M., & Fritz, U. (2009). Zur Verbreitung und zum Bedrohungsstatus der Europäischen Sumpfschildkröte (Emys orbicularis) in Marokko. *Elaphe*, *17*, 30-33.

Falush, D., Stephens, M., & Pritchard, J.K. (2003). Inference of population structure using multilocus genotype data: linked loci and correlated allele frequencies. *Genetics, 164*, 1567–1587.

FAO. 2010. *Global forest resources assessment 2010. Main report*. FAO Forestry Paper No. 163. Rome.

Fargues, P. (1986). Un siècle de transition démographique en Afrique méditerranéenne 1885-1985. *Population (french edition)*, 205-232.

Ferreira, S., Martínez-Freiría, F., Boudot, J.P., El Haissoufi, M., Bennas, N., Alves, P.C., Watts, P.C., Thompson, D.J., Brito, J.C. (2015). Local extinctions and range contraction of the endangered Coenagrion mercuriale in North Africa. *International Journal of Odonatology*, *18*(2), 137-152.

Franchimont, J., Saadaoui, E. (2001): *Etude nationale sur la biodiversite, rapport de synthese.*

Fritz, U., Guicking, D., Kami, H., Arakelyan, M., Auer, M., Ayaz, D., Fernández, C.A., Bakiev, A. G., Celani, A., Džukic, G., Fahd, S., Havas, P., Joger, U., Khabibullin, G .,

Mazaneva, L.F., Široký, P., Tripepi, S., Vélez, A.V., Velo-Antón, G ., Wink, M.(2007). Mitochondrial phylogeography of European pond turtles (Emys orbicularis, Emys trinacris)–an update. *Amphibia-Reptilia*, *28*(3), 418-426.

Fromhage, L., Vences, M., & Veith, M. (2004). Testing alternative vicariance scenarios in Western Mediterranean discoglossid frogs. *Molecular phylogenetics and evolution*, *31*(1), 308-322.

Frost, D. R. (2011). *Amphibian species of the world: an online reference*. *Version*, *5*(31),01. (http:// www.research.amnh.org/herpetology/amphibia/index.html)

Futuyma, D.J. (1998) *Evolutionary Biology*, 3rd ed. Sinauer Associates, Sunderland, MA.

Gao, B., (1996). NDWI—a normalized difference water index for remote sensing of vegetation liquid water from space. *Remote Sensing.of Environment*. *58*, 257–266.

GARCÍA-PARÍS, M., Alcobendas, M., Buckley, D., & Wake, D.B. (2003). Dispersal of viviparity across contact zones in Iberian populations of fire salamanders (Salamandra) inferred from discordance of genetic and morphological traits. *Evolution*, *57*(1), 129-143.

Gent, P. R., Danabasoglu, G., Donner, L. J., Holland, M. M., Hunke, E. C., Jayne, S. R., Lawrence, D.M., Neale, R.B., Rasch, P.J., Vertenstein, M., Worley, P. H., Yang, Z., Zhang, M. (2011). The community climate system model version 4. *Journal of Climate*, *24*(19), 4973-4991.

Giorgetta, M.A., Jungclaus, J., Reick, C.H., Legutke, S., Bader, J., Böttinger, M., Brovkin, V., Crueger, T., Esch, M., Fieg, K., Glushak, K., Gayler, V., Haak, H., Hollweg, H., Ilyina, T., Kinne, S., Kornblueh, L., Matei, D., Mauritsen, T., Mikolajewicz, U., Mueller, W., Notz, D., Pithan, F., Raddatz, T., Rast, S., Redler, R., Roeckner, E., Schmidt, H., Schnur, R., Segschneider, J., Six, K.D., Stockhause, M., Timmreck, C., Wegner, J., Widmann, H., Wieners, K., Claussen, M., Marotzke, J., Stevens, B. (2013). Climate and carbon cycle changes from 1850 to 2100 in MPI-ESM simulations for the Coupled Model Intercomparison Project phase 5. *Journal of Advances in Modeling Earth Systems*, *5*(3), 572-597.

Goetz, S., & Prince, S.D. (1999). Modelling Terrestrial Carbon Exchange and Storage: Evidence and Implications of Functional Convergence in Light-use Efficiency. *Advances in Ecological Research, 28*, 57–92.

Gómez, A., & Lunt, D.H. (2007) Refugia within refugia: patterns of phylogeographic concordance in the Iberian Peninsula. *Phylogeography of Southern European Refugia*. Springer Netherlands, 155-188.

Gómez, J. M. P., Fahd, S., & del Castellar, S. C. G. D. (2008). El papel del Estrecho de Gibraltar en la conformación de la actual fauna de anfibios y reptiles en el Mediterráneo Occidental. *Boletín de la Asociación Herpetológica Española*, *19*, 2-17.

Greven, H. (1998). Survey of the oviduct of salamandrids with special reference to the viviparous species. *Journal of Experimental. Zoology*. *282*, 507–525.

Greven, H., & Guex, G.D. (1994). Structural and physiological aspects of viviparity in Salamandra salamandra. *Mertensiella, 4*, 139–160.

Guisan, A. & Hofer, U. 2003. Predicting reptile distributions at the mesoscale: relation to climate and topography. *Journal of Biogeography*, *30*, 1233–1243.

HASSINE, J.B., & ESCORIZA, D. (2014). New ecological data on the family Salamandridae in the Maghreb. *Herpetological Review*, *45*(2), 1-5.

Hendrix, R., Susanne Hauswaldt, J., Veith, M., & Steinfartz, S. (2010). Strong correlation between cross-amplification success and genetic distance across all members of 'True Salamanders'(Amphibia: Salamandridae) revealed by Salamandra salamandra-specific microsatellite loci. *Molecular Ecology Resources*, *10*(6), 1038-1047.

Hernandez, P.A., Graham, C.H., Master, L.L., & Albert, D.L. (2006). The effect of sample size and species characteristics on performance of different species distribution modeling methods. *Ecography*, *29*(5), 773-785.

Hewitt, G.M. (2004). Genetic consequences of climatic oscillations in the Quaternary. *Philosophical Transactions of the Royal Society of London B: Biological Sciences*, *359*(1442), 183-195.

Hewitt, G. M. (1999). Post-glacial re-colonization of European biota. *Biological journal of the Linnean Society*, *68*(1-2), 87-112.

Hewitt, G. (2000). The genetic legacy of the Quaternary ice ages. *Nature*, *405*(6789), 907-913.

Hijmans, R. J., Cameron, S. E., Parra, J. L., Jones, P. G., & Jarvis, A. (2005). Very high resolution interpolated climate surfaces for global land areas. *International journal of Climatology*, *25*(15), 1965-1978.

Hodges, W. L. (2004). Evolution of viviparity in horned lizards (Phrynosoma): testing the cold-climate hypothesis. *Journal of Evolutionary Biology*, *17*(6), 1230-1237.

Hsü, K. J., Ryan, W. B. F., & Cita, M. B. (1973). Late Miocene desiccation of the Mediterranean. *Nature*, *242*(5395), 240-244.

Husemann, M., Schmitt, T., Zachos, F. E., Ulrich, W., & Habel, J. C. (2014). Palaearctic biogeography revisited: evidence for the existence of a North African refugium for Western Palaearctic biota. *Journal of Biogeography*, *41*(1), 81-94.

Jaggi, C., & Baur, B. (1999). Overgrowing forest as a possible cause for the local extinction of Vipera aspis in the northern Swiss Jura mountains. *Amphibia-Reptilia*, *20*(1), 25-34.

Jakobsson, M., & Rosenberg, N.A. (2007). CLUMPP: a cluster matching and permutation program for dealing with label switching and multimodality in analysis of population structure. *Bioinformatics*, *23*(14), 1801-1806.

Jarvis, A., Reuter, H.I., Nelson, A., & Guevara, E. (2008). *Hole-filled SRTM for the globe Version 4*. available from the CGIAR-CSI SRTM 90m Database (http://srtm.csi.cgiar.org).

Jedoui, Y., Davaud, E., Ismail, H.B. & Reyss, J.L. (2002) Sedimentological analysis of marine Pleistocene deposits of southeastern Tunisia: evidence of two positive eustatic pulsations during the marine isotopic substage 5e (Eemian, Tyrrhenian). *Bulletin de la Societe Geologique de France*, *173*, 255–264.

Jolly, D., Prentice, I.C., Bonnefille, R., et al. (1998). Biome reconstruction from pollen and plant macrofossil data for Africa and the Arabian peninsula at 0 and 6000 years. *Journal of Biogeography*, *25*(6), 1007-1027.

Kindler, C., Boehme, W., Corti, C., Gvoždík, V., Jablonski, D., Jandzik, D., Metalinou, M., SIROKY, P. & Fritz, U. (2013). Mitochondrial phylogeography, contact zones and taxonomy of grass snakes (Natrix natrix, N. megalocephala). *Zoologica Scripta*, *42*(5), 458-472.

Kramer-Schadt, S., Niedballa, J., Pilgrim, J. D., Schröder, B., Lindenborn, J., Reinfelder, V. Stillfried, M., Heckmann, I., Scharf, A.K., Augeri, D.M., Cheyne, S.M., Hearn, A.J., Ross, J., Macdonald, D.W., Mathai, J., Eaton, J., Marshall, A.J., Semiadi, G., Rustam,R., Bernard, H., Alfred, R., Samejima, H., Duckworth, J.W., Breitenmoser-Wuersten ,C., Belant, J.L., Hofer H., & Wilting, A. (2013). The importance of correcting for sampling bias in MaxEnt species distribution models. *Diversity and Distributions*, *19*(11), 1366-1379.

Krijgsman, W., Hilgen, F.J., Raffi, I., Sierro, F.J., & Wilson, D. S. (1999). Chronology, causes and progression of the Messinian salinity crisis. *Nature*, *400*(6745), 652-655.

Kuchta, S.R. (2007). Contact zones and species limits: hybridization between lineages of the California Newt, Taricha torosa, in the southern Sierra Nevada. *Herpetologica*, *63*(3), 332-350.

Kumar, S., Stecher, G., & Tamura, K. (2016). MEGA7: Molecular Evolutionary Genetics Analysis version 7.0 for bigger datasets. *Molecular Biology and Evolution*, msw054.

Labrousse, A., & Romero, L. (2001). *Rapport sur la situation du cannabis dans le Rif marocain*. Paris: Observatoire français des drogues et toxicomanies (OFDT). Retrieved from http://www.ofdt.fr/BDD/publications/docs/epbxalhc.pdf

Leigh, J. W., & Bryant, D. (2015). popart: full-feature software for haplotype network construction. *Methods in Ecology and Evolution*, *6*(9), 1110-1116.

Levins, R. (1968). *Evolution in changing environments: some theoretical explorations.* No. 2. Princeton University Press.

Mackey, B.G., & Lindenmayer, D.B. (2001). Towards a hierarchical framework for modelling the spatial distribution of animals. *Journal of Biogeography*, *28*(9), 1147-1166.

Marmion, M., Parviainen, M., Luoto, M., Heikkinen, R.K., & Thuiller, W. (2009). Evaluation of consensus methods in predictive species distribution modelling. *Diversity and Distributions*, *15*(1), 59-69.

Martínez-Freiría, F., Argaz, H., Fahd, S. & Brito, J.C. (2013). Climate change is predicted to negatively influence Moroccan endemic reptile richness. Implications for conservation in protected areas. *Naturwissenschaften, 100*, 877-889

Martínez-Freiría, F., Tarroso, P., Rebelo, H., & Brito, J.C. (2016). Contemporary niche contraction affects climate change predictions for elephants and giraffes. *Diversity and Distributions 22*: 432-444

Martínez-Freiría, F., Velo-Antón, G., & Brito, J.C. (2015). Trapped by climate: interglacial refuge and recent population expansion in the endemic Iberian adder Vipera seoanei. *Diversity and Distributions*, *21*(3), 331-344.

Martínez-Medina, F.J. (2007). Aproximación a la corología, autoecología y estado de conservación de las subpoblaciones de Salamandra algira en Marruecos. *Munibe*, (25), 140-147.

Martínez-Solano, I., Gonçalves, H.A., Arntzen, J.W., & García-París, M. (2004). Phylogenetic relationships and biogeography of midwife toads (Discoglossidae: Alytes). *Journal of Biogeography*, *31*(4), 603-618.

Meddour-Sahar, O., Lovreglio, R., Meddour, R., Leone, V., & Derridj, A. (2013). Fire and people in three rural communities in Kabylia (Algeria): results of a survey. *Open Journal of Forestry*, *3*(01), 30.

Mediani, M., Brito, J.C., & Fahd, S. (2015). Atlas of the amphibians and reptiles of northern Morocco: updated distribution and patterns of habitat selection. *Basic and Applied Herpetology,* 29.

Merabet, K., Sanchez, E., Dahmana, A., Bogaerts, S., Donaire, D., Steinfartz, S., Joger, U., Vences, M., Karar, M. & Moali, A. (2016). Phylogeographic relationships

and shallow mitochondrial divergence of Algerian populations of Salamandra algira. *Amphibia-Reptilia*, *37*(1), 1-8.

Merow, C., Smith, M.J., & Silander, J.A. (2013). A practical guide to MaxEnt for modeling species' distributions: what it does, and why inputs and settings matter. *Ecography*, *36*(10), 1058-1069.

Michaux, J.R., Magnanou, E., Paradis, E., Nieberding, C., & Libois, R. (2003). Mitochondrial phylogeography of the woodmouse (Apodemus sylvaticus) in the Western Palearctic region. *Molecular Ecology*, *12*(3), 685-697.

Moore, H.M., Fox, H.R., Harrouni, M.C., & Alami, A.E. (1998). Environmental challenges in the Rif mountains, northern Morocco. *Environmental Conservation*, *25*(04), 354-365.

Moroccan Centre for Development of Renewable Energies. 2007. *Studies on the management of resource and consumption profile of woodfuel in the rural environment*. Summary report.

Mouret, V., Guillaumet, A., Cheylan, M., Pottier, G., Ferchaud, A.L., & Crochet, P.A. (2011). The legacy of ice ages in mountain species: post-glacial colonization of mountain tops rather than current range fragmentation determines mitochondrial genetic diversity in an endemic Pyrenean rock lizard. *Journal of Biogeography*, *38*(9), 1717-1731.

Myers, N., Mittermeier, R.A., Mittermeier, C.G., Da Fonseca, G.A., & Kent, J. (2000). Biodiversity hotspots for conservation priorities. *Nature*, *403*(6772), 853-858.

Myneni, R.B., Hall, F.G., Sellers, P.J., & Marshak, A.L. (1995). The interpretation of spectral vegetation indexes. *IEEE Transactions on Geoscience and Remote Sensing*, *33*(2), 481-486.

Nagendra, H., Mairota, P., Marangi, C., Lucas, R., Dimopoulos, P., Honrado, J. P., Niphadkar, M., Mücher, C.A., Tomaselli,V., Panitsa, M., Tarantino, C., Mannakos, I. & Blonda, P. (2015). Satellite Earth observation data to identify anthropogenic pressures in selected protected areas. *International Journal of Applied Earth Observation and Geoinformation*, *37*, 124-132.

Nei, M. (1977). F-statistics and analysis of gene diversity in subdivided populations. *Annals of human genetics*, *41*(2), 225-233.

Nicolas, V., Mataame, A., Crochet, P.A., Geniez, P., & Ohler, A. (2015). Phylogeographic patterns in north African water frog Pelophylax saharicus (Anura: Ranidae). *Journal of Zoological Systematics and Evolutionary Research*, *53*(3), 239-248.

Patsiou, T.S., Conti, E., Zimmermann, N.E., Theodoridis, S., & Randin, C.F. (2014). Topo-climatic microrefugia explain the persistence of a rare endemic plant in the Alps during the last 21 millennia. *Global Change Biology*, *20*(7), 2286-2300.

Paulo, O.S., Pinheiro, J., Miraldo, A., Bruford, M.W., Jordan, W.C., & Nichols, R.A. (2008). The role of vicariance vs. dispersal in shaping genetic patterns in ocellated lizard species in the western Mediterranean. *Molecular Ecology*, *17*(6), 1535-1551.

Peakall, R.O.D., & Smouse, P.E. (2006). GENALEX 6: genetic analysis in Excel. Population genetic software for teaching and research. *Molecular Ecology Notes*, *6*(1), 288-295.

Pearson, R.G., Dawson, T.P., & Liu, C. (2004). Modelling species distributions in Britain: a hierarchical integration of climate and land-cover data. *Ecography*, *27*(3), 285-298.

Phillips, S.J., (2008). Transferability, sample selection bias and background data in presence-only modelling: a response to Peterson et al. (2007). *Ecography, 31*, 272–278.

Phillips, S.J. (2005). A brief tutorial on Maxent. *AT&T Research*.

Plieninger T, Hui C, Gaertner M, Huntsinger L, (2014). The impact of land abandonment on species richness and abundance in the Mediterranean basin: a meta-analysis. *PLoS ONE, 9*(5).

Pritchard, J.K., Stephens, M., & Donnelly, P. (2000). Inference of population structure using multilocus genotype data. *Genetics*, *155*(2), 945-959.

Puechmaille, S.J. (2016). The program structure does not reliably recover the correct population structure when sampling is uneven: subsampling and new estimators alleviate the problem. *Molecular ecology resources*, *16*(3), 608-627.

Quezel, P. & Barbero, M. (1993) Variations climatiques au Sahara et en Afrique sèche depuis le Pliocene: enseignements de la flore et de la végétation actuelles. *Revue d'Ecologie – la Terre et la Vie*, *24*, 191–202.

Raymond, M., & Rousset, F. (1995). GENEPOP (version 1.2): population genetics software for exact tests and ecumenicism. *Journal of Heredity*, *86*(3), 248-249.

Recuero, E., Canestrelli, D., Vörös, J., Szabó, K., Poyarkov, N.A., Arntzen, J.W., Crnobrnja-Isailovic, J., Kidov, A.A., Cogalniceanu, D.,Caputo, F.P.,Nascetti, G. & Martínez-Solano, I. (2012). Multilocus species tree analyses resolve the radiation of the widespread Bufo bufo species group (Anura, Bufonidae). *Molecular Phylogenetics and Evolution*, *62*(1), 71-86.

Reinig, W. (1950). Chorologische voraussetzungen für die analyse von formenkreisen. *Syllegomena Biologica, Festschrift für O. Kleinschmidt*, 364-378.

Rice, W.R. (1989). Analyzing tables of statistical tests. *Evolution 43*: 223–225.

Rissler, L.J., & Apodaca, J.J. (2007). Adding more ecology into species delimitation: ecological niche models and phylogeography help define cryptic species in the black salamander (Aneides flavipunctatus). *Systematic Biology*, *56*(6), 924-942.

Rousset, F. (2008). genepop'007: a complete re-implementation of the genepop software for Windows and Linux. *Molecular Ecology Resources*, *8*(1), 103-106.

Sappington, J., Longshore, K.M., & Thompson, D.B. (2007). Quantifying landscape ruggedness for animal habitat analysis: a case study using bighorn sheep in the Mojave Desert. *The Journal of Wildlife Management*, *71*(5), 1419-1426.

Sayre, R., Comer, P., Warner, H., & Cress, J. (2009). *A new map of standardized terrestrial ecosystems of the conterminous United States* (p. 17). US Department of the Interior. US Geological Survey.

Schleich, H.H., Kästle, W., & Kabisch, K. (1996). Amphibians and reptiles of North Africa. *Koeltz, Koenigstein*, *627*.

Schmitt, T. (2007). Molecular biogeography of Europe: Pleistocene cycles and postglacial trends. *Frontiers in zoology*, *4*(1), 1.

Schulte, U., Küsters, D., & Steinfartz, S. (2007). A PIT tag based analysis of annual movement patterns of adult fire salamanders (Salamandra salamandra) in a Middle European habitat. *Amphibia-Reptilia*, *28*(4), 531-536.

Sillero, N. (2011). What does ecological modelling model? A proposed classification of ecological niche models based on their underlying methods. *Ecological Modelling*, *222*(8), 1343-1346.

Soberón, J. (2007). Grinnellian and Eltonian niches and geographic distributions of species. *Ecology letters*, *10*(12), 1115-1123.

Stebbins, R.C., & Cohen, N.W. (1995). *A natural history of amphibians*. Princeton University Press.

Steinfartz, S., Kuesters, D., & Tautz, D. (2004). Isolation and characterization of polymorphic tetranucleotide microsatellite loci in the Fire salamander Salamandra salamandra (Amphibia: Caudata). *Molecular Ecology Notes*, *4*(4), 626-628.

Steinfartz, S., Veith, M., & Tautz, D. (2000). Mitochondrial sequence analysis of Salamandra taxa suggests old splits of major lineages and postglacial recolonizations of Central Europe from distinct source populations of Salamandra salamandra. *Molecular Ecology*, *9*(4), 397-410.

Stewart, J.R., Lister, A.M., Barnes, I., & Dalén, L. (2010). Refugia revisited: individualistic responses of species in space and time. *Proceedings of the Royal Society of London B: Biological Sciences*, *277*(1682), 661-671.

Stöck, M., Sicilia, A., Belfiore, N.M., Buckley, D., Brutto, S L., Valvo, M.L., & Arculeo, M. (2008a). Post-Messinian evolutionary relationships across the Sicilian channel: Mitochondrial and nuclear markers link a new green toad from Sicily to African relatives. *BMC Evolutionary Biology*, *8*(1), 1.

Stöck, M., Dubey, S., Klütsch, C., Litvinchuk, S.N., Scheidt, U., & Perrin, N. (2008b). Mitochondrial and nuclear phylogeny of circum-Mediterranean tree frogs from the Hyla arborea group. *Molecular Phylogenetics and Evolution*, *49*(3), 1019-1024.

Street, A., & Gasse, F. (1981). Recent developments in research into the Quaternary climatic history of the Sahara. *Sahara: Ecological Change and Early Economic History.* Menas Press Ltd, 7-28.

Stuckas, H., Velo-Antón, G., Fahd, S., Kalboussi, M., Rouag, R., Arculeo, M., Marrone, F., Sacco, F., Vamberger, M & Fritz, U. (2014). Where are you from, stranger? The enigmatic biogeography of North African pond turtles (Emys orbicularis). *Organisms Diversity & Evolution*, *14*(3), 295-306.

Tabutin, D., Biraben, J.N., & Vilquin, E. (2002). *L'histoire de la population de l'Afrique du Nord pendant le deuxième millénaire*. Louvain-la-Neuve: Université catholique de Louvain, Département des sciences de la population et du développement.

Thiam, A.K. (2003). The causes and spatial pattern of land degradation risk in southern Mauritania using multitemporal AVHRR-NDVI imagery and field data. *Land Degradation & Development*, *14*(1), 133-142.

Thiesmeier, B. (2004). *Der Feuersalamander*. Bielefeld: Laurenti Verlag.

Thuiller, W., Georges, D., & Engler, R. (2012). *Package "biomod 2" version 2.1.15*.

Thuiller, W., Lafourcade, B., Engler, R. & Araújo, M.B. (2009) BIOMOD—a platform for ensemble forecasting of species distributions. *Ecograph*y, *32*, 369–373.

Tramblay, Y., El Adlouni, S., & Servat, E. (2013). Trends and variability in extreme precipitation indices over Maghreb countries. *Natural Hazards and Earth System Sciences*, *13*(12), 3235-3248.

UNDP (United Nations Development Programme) - Human Development Report Office (2011). *The Human Development Index (HDI)*. New York. (available at http://hdr.undp.org/en/statistics/hdi/.

Vale, C.G., Campos, J.C., Silva, T L., Gonçalves, D.V., Sow, A.S., Martínez-Freiría, F., Boratynski, Z. & Brito, J.C. (2016). Biogeography and conservation of mammals

from the West Sahara-Sahel: an application of ecological niche-based models and GIS. *Hystrix, the Italian Journal of Mammalogy*, *27*(1).

van Lavieren, E., & Wich, S.A. (2010). Decline of the Endangered Barbary macaque Macaca sylvanus in the cedar forest of the Middle Atlas Mountains, Morocco. *Oryx*, *44*(01), 133-138.

Van Oosterhout, C., Hutchinson, W.F., Wills, D.P., & Shipley, P. (2004). MICRO-CHECKER: software for identifying and correcting genotyping errors in microsatellite data. *Molecular Ecology Notes*, *4*(3), 535-538.

VanDerWal, J., Shoo, L.P., Graham, C., & Williams, S.E. (2009). Selecting pseudo-absence data for presence-only distribution modeling: How far should you stray from what you know? *Ecological modelling*, *220*(4), 589-594.

Veith, M., Lipscher, E., Öz, M., Kiefer, A., Baran, I., Polymeni, R.M., & Steinfartz, S. (2008). Cracking the nut: Geographical adjacency of sister taxa supports vicariance in a polytomic salamander clade in the absence of node support. *Molecular Phylogenetics and Evolution*, *47*(3), 916-931.

Veith, M., Mayer, C., Samraoui, B., Barroso, D.D., & Bogaerts, S. (2004). From Europe to Africa and vice versa: evidence for multiple intercontinental dispersal in ribbed salamanders (Genus Pleurodeles). *Journal of Biogeography*, *31*(1), 159-171.

Velo-Antón, G., García-París, M., Galán, P., & Cordero Rivera, A. (2007). The evolution of viviparity in holocene islands: ecological adaptation versus phylogenetic descent along the transition from aquatic to terrestrial environments. *Journal of Zoological Systematics and Evolutionary Research*, *45*(4), 345-352.

Velo-Antón, G., Godinho, R., Harris, D.J., Santos, X., Martínez-Freiria, F., Fahd, S., Larb, S., Pleguezuelos, J.M. & Brito, J. C. (2012a). Deep evolutionary lineages in a Western Mediterranean snake (Vipera latastei/monticola group) and high genetic structuring in Southern Iberian populations. *Molecular Phylogenetics and Evolution*, *65*(3), 965-973.

Velo-Antón, G., Zamudio, K.R., & Cordero-Rivera, A. (2012b). Genetic drift and rapid evolution of viviparity in insular fire salamanders (*Salamandra salamandra*). *Heredity*, *108*(4), 410-418.

Velo-Antón, G., Cardenete, L.G., Cazalla, F.J., & Martínez-Freiría, F. (2014). New record of *Salamandra algira* isolated on the north-western Tingitana peninsula, with some notes on the reproductive modes within the species. *Zer: Revista de estudios de comunicación= Komunikazio ikasketen aldizkaria*, *25*(1), 46-50.

Velo-Antón, G., Pereira, P., Fahd, S., Teixeira, J., & Fritz, U. (2015a). Out of Africa: did Emys orbicularis occidentalis cross the Strait of Gibraltar twice?. *Amphibia-Reptilia*, *36*(2), 133-140.

Velo-Antón, G., Santos, X., Sanmartín-Villar, I., Cordero-Rivera, A., & Buckley, D. (2015b). Intraspecific variation in clutch size and maternal investment in pueriparous and larviparous Salamandra salamandra females. *Evolutionary Ecology*, *29*(1), 185-204.

Velo-Antón, G., el Marnisi, B., Fritz, U., & Fahd, S. (2015c). Distribution and conservation status of Emys orbicularis in Morocco. *Vertebrate Zoology*, *65*, 131-135.

Vences, M., Sanchez, E., Hauswaldt, J.S., Eikelmann, D., Rodríguez, A., Carranza, S., Donaire, D., Gehara, M., Helfer, V., Lötters, S., Werner, P., Schulz, S. & Steinfartz, S. (2014). Nuclear and mitochondrial multilocus phylogeny and survey of alkaloid content in true salamanders of the genus Salamandra (Salamandridae). *Molecular Phylogenetics and evolution*, *73*, 208-216.

Veríssimo, J., Znari, M., Stuckas, H., Fritz, U., Pereira, P., Teixeira, J., Arculeo, M., Marrone, F., Sacco, F., Naimi, M., Kehlmaier, C. & Velo-Antón, G. (2016). Pleistocene diversification in Morocco and recent demographic expansion in the Mediterranean pond turtle Mauremys leprosa. *Biological Journal of the Linnean Society*.

Wake, M.H. (1993). Evolution of oviductal gestation in amphibians. *Journal of Experimental Zoology*, *266*(5), 394-413.

Warren, D.L., Glor, R.E., & Turelli, M. (2008). Environmental niche equivalency versus conservatism: quantitative approaches to niche evolution. *Evolution*, *62*(11), 2868-2883.

Warren, D.L., Glor, R.E., & Turelli, M. (2010). ENMTools: a toolbox for comparative studies of environmental niche models. *Ecography*, *33*(3), 607-611.

Watanabe, S., Hajima, T., Sudo, K., Nagashima, T., Takemura, T., Okajima, H., Nozawa, T., Kawase, H., Abe, M., Yokojata, T., Ise, T., Sato, H., Kato, E., Takata, K., Emori, S. & Kawamiya, M. (2011). MIROC-ESM 2010: model description and basic results of CMIP5-20c3m experiments, *Geoscientific. Model Development*, *4*, 845–872, doi: 10.5194.

Weiss, S. & Ferrand, N. (2007). *Phylogeography of southern European refugia* (341-357). Dordrecht (Netherlands): springer.

Welsh, H.H., & Droege, S. (2001). A case for using plethodontid salamanders for monitoring biodiversity and ecosystem integrity of North American forests. *Conservation Biology*, *15*(3), 558-569.

Wessels, K.J., Prince, S.D., Frost, P.E., & Van Zyl, D. (2004). Assessing the effects of human-induced land degradation in the former homelands of northern South Africa with a 1 km AVHRR NDVI time-series. *Remote Sensing of Environment*, *91*(1), 47-67.

Wiens, J.A., Stralberga, D., Jongsomjita, D., Howella, C.A. & Snyder, M.A. (2009) Niches, models, and climate change: assessing the assumptions and uncertainties. *PNAS*, *106*, 19729–19736.

Xu, H. (2006). Modification of normalised difference water index (NDWI) to enhance open water features in remotely sensed imagery. *International Journal of Remote Sensing*, *27*(14), 3025-3033.

Chapter 7: Supplementary materials

Table 7.1 Characteristics of the 13 microsatellites used in this study. Information regarding multiplex arrangement, original published primer forward and reverse sequences, fluorescently labelled oligonucleotides used as template for modified forward primers and the concentration of primer forward and reverse used to construct multiplex mixes and on 10 µl PCR reactions are represented. (Adapted from Álvarez et al., 2015)

Locus	Multiplex	Label *	Primer forward (5' – 3')	Primer reverse (5' – 3')	PF concentration multiplex/PCR (µM)	PR concentration multiplex/PCR (µM)
SalE14 [1]	Panel S1.2	VIC	GCTGCCCTCTC TGCCTACTGAC CAT	GCCAAGACATG GAACACCCTCC CGC	0.08 / 0.008	0.8 / 0.08
Sal29 [1]	Panel S1.2	6-FAM	CTCTTTGACTG AACCAGAACCC C	GCCTGTCGGCT CTGTGTAACC	0.8 / 0.08	8.0 / 0.8
SST-B11 [2]	Panel S2	PET	TCAAACGGTGC CAAAGTTATTA G	TTAATTGGCAGT TTTCTTTCCAG	0.2 / 0.02	2.0 / 0.2
SalE12 [1]	Panel S2	VIC	CTCAGGAACAG TGTGCCCCAAA TAC	CTCATAATTTAG TCTACCCTCCCA C	0.08 / 0.008	0.8 / 0.08
Sal23 [1]	Panel S2	6-FAM	TCACTGTTTATC TTTGTTCTTTTA T	AATTATTTGTTT GAGTCGATTTT CT	0.92 / 0.092	9.2 / 0.92
SST-C3 [2]	Panel S3	PET	CCGTTTGAGTC ACTTCTTTCTTG	TTGCTTTACCAA CCAGTTATTGTC	0.14 / 0.014	1.4 / 0.14
SalE7 [1]	Panel S3	NED	TTTCAGCACCA AGATACCTCTTT TG	CTCCCTCCATAT CAAGGTCACAG AC	0.08 / 0.008	0.8 / 0.08
SalE5 [1]	Panel S3	6-FAM	CCACATGATGC CTACGTATGTTG TG	CTCCTGTTTACG CTTCACCTGCT CC	0.06 / 0.006	0.6 / 0.06
SalE2 [1]	Panel S3	VIC	CACGACAAAAT ACAGAGAGTGG ATA	ATATTTGAAATT GCCCATTTGGTA	0.3 / 0.03	3.0 / 0.3
SalE06 [1]	Panel S4	VIC	GGACTCATGGT CACCCAGAGGT TCT	ATGGATTGTGTC GAAATAAGGTA TC	0.12 / 0.012	1.2 / 0.12
Sal3 [1]	Panel S4	6-FAM	CTCAGACAAGA AATCCTGCTTCT TC	ATAAATCTGTCC TGTTCCTAATCA G	0.12 / 0.012	1.2 / 0.12
SalE8 [1]	Panel S4	NED	GCAAAGTCCAT GCTTTCCCTTTC TC	GACATACCAAA GACTCCAGAAT GGG	0.08 / 0.008	0.8 / 0.08
SST-G9 [2]	Panel S4	NED	CCTCGTCAGGG GTTGTAGG	CTTTCCAGGAA GAAACTGAGAT G	0.08 / 0.008	0.8 / 0.08

*An extra number of base pairs were added at 5' end of the original sequence of forward primers in order to allow binding of four different fluorescent labelled oligonucleotides (6-FAM - TGT AAA ACG ACG GCC AGT; VIC - TAA TAC GAC TCA CTA TAG GG; NED - TTT CCC AGT CAC GAC GTT G; PET - GAT AAC AAT TTC ACA CAG G);

[1] Steinfartz S, Kuesters D, Tautz D (2004) Isolation and characterization of polymorphic tetranucleotide microsatellite loci in the fire salamander Salamandra salamandra (Amphibia: Caudata). Mol Ecol Notes 4: 626–628.

[2] Hendrix R, Hauswaldt JS, Veith M et al (2010) Strong correlation between cross-amplification success and genetic distance across all members of 'True salamanders' (Amphibia: Salamandridae) revealed by Salamandra salamandra-specific microsatellite loci. Mol Ecol Resour 10: 1038–1047.

Table 7.2 Identification and location of all samples collected and cytochrome b (*cyt-b*) and β-fibrinogen (*β-fibint7*) sequence data used in this work. Mitochondral haplotype and samples included in microsatellite (SSR) analyses are identified. TBS: To be submitted to Genbank. SAT1: *S. a. tingitana* sublineage 1; SAT2: *S. a. tingitana* sublineage 2; SAT3: *S. a. tingitana* sublineage 3; SAS1: *S. a. splendens* sublineage 1; SAS2: *S. a. splendens* sublineage 2; SAA: *S. a. algira;* SASA: *S. a. spelaea*

Location						genbank accession			
Country	**Locality**	**Latitude**	**Longitude**	**Code**	**Origin**	**cytB**	**Bfib**	**mt Haplotype**	**SSR**
Spain	Ceuta	35.8938	-5.3556	GVA5740	New data				X
		35.8938	-5.3556	GVA5741	New data				X
		35.8938	-5.3556	GVA5742	New data				
		35.8938	-5.3556	GVA5743	New data				X
		35.8938	-5.3556	GVA5744	New data				X
		35.8938	-5.3556	GVA5745	New data				X
		35.8938	-5.3556	GVA5746	New data				X
		35.8938	-5.3556	GVA5747	New data				
		35.8938	-5.3556	GVA5748	New data				X
		35.8938	-5.3556	GVA5749	New data	TBS		SAT1	X
		35.8938	-5.3556	GVA5750	New data		TBS		X
		35.8938	-5.3556	GVA5751	New data		TBS		X
		35.8938	-5.3556	GVA5809	New data				
		35.8938	-5.3556	GVA5810	New data				
		35.8938	-5.3556	GVA5811	New data				X
		35.8938	-5.3556	GVA5812	New data				X
Morocco	Adayourha	35.2553	-5.4166	GVA5773	New data	TBS	TBS	SAT3	X
	Ain Lahsen (Ain el Hesn)	35.5497	-5.5641	E3009.9	Beukema et al. 2010	HQ190886		SAT1	
	Akchur (near Talembot)	35.2434	-5.1892	E1712.9	Donaire-Barroso & Bogaerts 2003	AY247734		SAS1	
	Beliunech (near Ceuta)	35.9080	-5.3980	Sei1	Vences et al. 2014	KF645934		SAT1	
		35.9080	-5.3980	SS214	Vences et al. 2014	KF645931		SAT1	
		35.9080	-5.3980	UK2	Vences et al. 2014	KF645933		SAT1	
	Beni Maharone	NA	NA	E13053.13	Beukema et al. 2010	HQ190881		SAT3	
	Beni Snassen	35.00	-2.3	IMS5220	Ben Hassine et al. 2016	KT995252		SASA	
		35.00	-2.3	IMS5221	Ben Hassine et al. 2016	KT995253		SASA	
		35.00	-2.3	IMS5222	Ben Hassine et al. 2016	KT995254		SASA	
		NA	NA	E220362	Escoriza and Comas 2007	DQ901442		SASA	
		NA	NA	E220363	Escoriza and Comas 2007	DQ901443		SASA	
		NA	NA	E220364	Escoriza and Comas 2007	DQ901444		SASA	
		NA	NA	E9035.1	Escoriza and Comas 2007	DQ221247		SASA	
	Bou Iblane - Taffert refuge	33.6501	-4.1626	GVA4173	New data	TBS		SAS2	
		33.6501	-4.1626	GVA4172	New data	TBS		SAS2	
	Bouadelle	34.5335	-4.5049	E15124.6	Beukema et al. 2010	HQ190900		SAS1	

Location						genbank accession			
Country	**Locality**	**Latitude**	**Longitude**	**Code**	**Origin**	**cytB**	**Bfib**	**mt Haplotype**	**SSR**
	Bouhachem	NA	NA	GVA5808	New data				
	Chefchaouen (= Xauen)	35.1791	-5.2463	E1712.14	Donaire-Barroso & Bogaerts 2003	AY247735		SAS1	
	Cudia Sbaa (= Sebaa)	35.0234	-5.0154	E15124.3	Beukema et al. 2010	HQ190899		SAS1	
	Dar Chaoiu 1	35.5681	-5.7722	GVA1938	Velo-Antón et al. 2014	TBS		SAT3	X
		35.5681	-5.7722	GVA1939	Velo-Antón et al. 2014	TBS		SAT3	X
		35.5681	-5.7722	GVA1940	Velo-Antón et al. 2014	TBS		SAT3	X
		35.5681	-5.7722	GVA1941	Velo-Antón et al. 2014	TBS		SAT3	
		35.5681	-5.7722	GVA1942	Velo-Antón et al. 2014	TBS		SAT3	
	Dar Chaoiu 2	35.5620	-5.7835	GVA4136	Velo-Antón et al. 2014	TBS		SAT3	X
		35.5620	-5.7835	GVA4137	Velo-Antón et al. 2014	TBS		SAT3	X
		35.5620	-5.7835	GVA4138	Velo-Antón et al. 2014	TBS		SAT3	X
		35.5620	-5.7835	GVA4139	Velo-Antón et al. 2014	TBS		SAT3	X
		35.5620	-5.7835	GVA4140	Velo-Antón et al. 2014	TBS		SAT3	X
	east of Bab Azhar	34.0511	-4.2203	E15124.5	Beukema et al. 2010	HQ190895		SAS2	
	east of Bab Berred	34.9933	-4.8228	E11113.2	Beukema et al. 2010	HQ190897		SAS1	
	Fifi 2	34.9956	-5.1947	GVA6175	New data	TBS		SAS1	X
		34.9956	-5.1947	GVA6176	New data	TBS		SAS1	X
		34.9956	-5.1947	GVA6177	New data				X
		34.9956	-5.1947	GVA6178	New data	TBS		SAS1	X
		34.9956	-5.1947	GVA6179	New data	TBS		SAS1	X
		34.9956	-5.1947	GVA6180	New data	TBS		SAS1	X
	Ighagdaren/Jebel Aoul	34.8093	-4.6694	E11113.6	Beukema et al. 2010	HQ190901		SAS1	
		34.8093	-4.6694	E11113.7	Beukema et al. 2010	HQ190902		SAS1	
	Jabal Mousa	35.9000	-5.3873	IMS3800	Ben Hassine et al. 2016	KT995212		SAT1	
		35.9000	-5.3873	IMS3801	Ben Hassine et al. 2016	KT995213		SAT1	
	Jabel el Fahies	35.0916	-5.4032	E309.13	Beukema et al. 2010	HQ190883		SAT1	
		35.0916	-5.4032	E1712.7	Donaire-Barroso & Bogaerts 2003	AY247732		SAT1	
	Jbel Hamziouat (near Beni Arous)	35.4370	-5.5541	E3009.11	Beukema et al. 2010	HQ190879		SAT2	
		35.4370	-5.5541	E30092.8	Beukema et al. 2010	HQ190880		SAT2	
	Jebel Musa	35.9000	-5.3873	GVA6016	New data				
		35.9000	-5.3873	GVA6017	New data	TBS		SAT1	X
		35.9000	-5.3873	GVA6018	New data	TBS		SAT1	X
		35.9000	-5.3873	GVA6237	New data	TBS		SAT1	X
	Jebel Suna 1	35.1337	-5.4303	GVA6181	New data	TBS		SAT3	X

Location						genbank accession			
Country	Locality	Latitude	Longitude	Code	Origin	cytB	Bfib	mt Haplotype	SSR
		35.1337	-5.4303	GVA6182	New data	TBS		SAT3	X
		35.1337	-5.4303	GVA6183	New data	TBS		SAT3	X
	Jebel Suna 2	35.1128	-5.4117	GVA6184	New data				
		35.1128	-5.4117	GVA6185	New data	TBS		SAT3	X
		35.1128	-5.4117	GVA6186	New data	TBS		SAT3	X
		35.1128	-5.4117	GVA6187	New data	TBS		SAT3	X
		35.1128	-5.4117	GVA6188	New data	TBS		SAT3	X
		35.1128	-5.4117	GVA6189	New data	TBS		SAT3	X
		35.1128	-5.4117	GVA6190	New data	TBS		SAT3	X
		35.1128	-5.4117	GVA6191	New data	TBS		SAT3	X
	Jebel Suna 3	35.1297	-5.3652	E13053.16	Beukema et al. 2010	HQ190882		SAT3	
	Jebel Sugna	NA	NA	GVA5804	New data				X
	Jebel Tazeka	34.0509	-4.2206	GVA5805	New data		TBS		
		34.0509	-4.2206	GVA5806	New data				
		34.0509	-4.2206	GVA5807	New data	TBS	TBS	SAS2	
	Mokrisset	34.9516	-5.3632	E1113.4	Beukema et al. 2010	HQ190889		SAS1	
		34.9516	-5.3632	E1113.5	Beukema et al. 2010	HQ190887		SAS1	
		34.9516	-5.3632	E13053.14	Beukema et al. 2010	HQ190888		SAS1	
	Moulay - Chefchaouen	35.2705	-5.4882	GVA5757	New data	TBS	TBS	SAT2	X
		35.2705	-5.4882	GVA5758	New data	TBS	TBS	SAT2	X
		35.2705	-5.4882	GVA5759	New data	TBS		SAT2	X
		35.2705	-5.4882	GVA5760	New data	TBS		SAT2	X
		35.2705	-5.4882	GVA5761	New data	TBS		SAT2	X
		35.2705	-5.4882	GVA5762	New data	TBS		SAT2	X
		35.2705	-5.4882	GVA5763	New data				X
		35.2705	-5.4882	GVA5764	New data				X
		35.2705	-5.4882	GVA5765	New data				X
		35.2705	-5.4882	GVA5766	New data				X
		35.2705	-5.4882	GVA5767	New data				
		35.2705	-5.4882	GVA5768	New data				
		35.2705	-5.4882	GVA5769	New data				
	Moulay Abdesalam	35.2650	-5.4701	GVA6247	New data	TBS		SAT3	X
	Near Taza	NA	NA	Sei4	Vences et al. 2014	KF645930		SAS2	
	S. Moulay Abdessalam	35.3174	-5.4976	E2909.20	Beukema et al. 2010	HQ190876		SAT2	
		35.3174	-5.4976	E2909.21	Beukema et al. 2010	HQ190877		SAT2	
	Souk Tleta Taghramt	35.7969	-5.4598	SAUK1	Vences et al. 2014	KF645932		SAT1	
	South of Taza, Ras el Ma	34.1474	-4.0093	E15124.8	Beukema et al. 2010	HQ190896		SAS2	

Location						genbank accession			
Country	**Locality**	**Latitude**	**Longitude**	**Code**	**Origin**	**cytB**	**Bfib**	**mt Haplotype**	**SSR**
		34.1474	-4.0093	E17121.11	Beukema et al. 2010	HQ190890		SAS2	
		34.1474	-4.0093	E17121.13	Beukema et al. 2010	HQ190891		SAS2	
	South Tetouan	35.5239	-5.3958	GVA4156	New data				
	Spirada	35.5224	-5.5482	GVA5792	New data				
		35.5224	-5.5482	GVA5793	New data	TBS	TBS	SAT2	X
	Taffert (Middle Atlas)	33.6434	-4.1412	E13124.6	Beukema et al. 2010	HQ190892		SAS2	
		33.6434	-4.1412	E13124.7	Beukema et al. 2010	HQ190893		SAS2	
		33.6434	-4.1412	E15124.1	Beukema et al. 2010	HQ190894		SAS2	
	Tagramt (= Taghramt)	NA	NA	E309.10	Donaire-Barroso & Bogaerts 2003	AY247733		SAT1	
		35.7956	-5.4596	E309.10	Beukema et al. 2010	HQ190884		SAT1	
		35.7956	-5.4596	E309.12	Beukema et al. 2010	HQ190885		SAT1	
	Talassemtane	35.1834	-5.2270	GVA5797	New data	TBS	TBS	SAS1	X
		35.1834	-5.2270	GVA5798	New data				X
		35.1834	-5.2270	GVA5799	New data	TBS		SAS1	X
		35.1834	-5.2270	GVA5800	New data	TBS		SAS1	X
		35.1834	-5.2270	GVA5801	New data				
	Targuist	NA	NA	GVA5803	New data				
		NA	NA	GVA5813	New data				
		NA	NA	GVA5814	New data				
		NA	NA	GVA5815	New data				
	Tazia crossing	35.3646	-5.5664	E1305.15	Beukema et al. 2010	HQ190878		SAT2	
	Tetouan: Amsa	35.5321	-5.2093	GVA6102	New data	TBS		SAT2	X
		35.5321	-5.2093	GVA6103	New data	TBS		SAT2	X
		35.5321	-5.2093	GVA6104	New data	TBS		SAT2	X
		35.5321	-5.2093	GVA6105	New data	TBS		SAT2	X
		35.5321	-5.2093	GVA6106	New data	TBS		SAT2	X
		35.5321	-5.2093	GVA6107	New data	TBS		SAT2	X
		35.5321	-5.2093	GVA6108	New data				X
		35.5321	-5.2093	GVA6109	New data				X
		35.5321	-5.2093	GVA6110	New data				X
		35.5321	-5.2093	GVA6111	New data				X
		35.5321	-5.2093	GVA6112	New data				X
		35.5321	-5.2093	GVA6113	New data				X
		35.5321	-5.2093	GVA6114	New data				X
		35.5321	-5.2093	GVA6115	New data				X
		35.5321	-5.2093	GVA6116	New data				X
		35.5321	-5.2093	GVA6117	New data				X
		35.5321	-5.2093	GVA6118	New data				X

Location						genbank accession			
Country	Locality	Latitude	Longitude	Code	Origin	cytB	Bfib	mt Haplotype	SSR
		35.5321	-5.2093	GVA6119	New data				X
		35.5321	-5.2093	GVA6120	New data				X
		35.5321	-5.2093	GVA6121	New data				X
		35.5321	-5.2093	GVA6122	New data				X
		35.5321	-5.2093	GVA6123	New data				X
		35.5321	-5.2093	GVA6124	New data				X
		35.5321	-5.2093	GVA6125	New data				X
		35.5321	-5.2093	GVA6126	New data				X
		35.5321	-5.2093	GVA6127	New data				
		35.5321	-5.2093	GVA6128	New data				
		35.5321	-5.2093	GVA6129	New data				
		35.5321	-5.2093	GVA6130	New data				
		35.5321	-5.2093	GVA6131	New data				
		35.5321	-5.2093	GVA6132	New data				
		35.5321	-5.2093	GVA6133	New data				
		35.5321	-5.2093	GVA6134	New data				
		35.5321	-5.2093	GVA6135	New data				
		35.5321	-5.2093	GVA6136	New data				
		35.5321	-5.2093	GVA6137	New data				
		35.5321	-5.2093	GVA6138	New data				
		35.5321	-5.2093	GVA6139	New data				
		35.5321	-5.2093	GVA6140	New data				
		35.5321	-5.2093	GVA6141	New data				
		35.5321	-5.2093	GVA6142	New data				
		35.5321	-5.2093	GVA6143	New data				
		35.5321	-5.2093	GVA6144	New data				
		35.5321	-5.2093	GVA6145	New data				
		35.5321	-5.2093	GVA6146	New data				
		35.5321	-5.2093	GVA6147	New data				
		35.5321	-5.2093	GVA6148	New data				
		35.5321	-5.2093	GVA6149	New data				
		35.5321	-5.2093	GVA6150	New data				
		35.5321	-5.2093	GVA6151	New data				
		35.5321	-5.2093	GVA6152	New data				
		35.5321	-5.2093	GVA6153	New data				
		35.5321	-5.2093	GVA6154	New data				
		35.5321	-5.2093	GVA6155	New data				
		35.5321	-5.2093	GVA6156	New data				
		35.5321	-5.2093	GVA6157	New data				
		35.5321	-5.2093	GVA6158	New data				

Location						genbank accession			
Country	Locality	Latitude	Longitude	Code	Origin	cytB	Bfib	mt Haplotype	SSR
		35.5321	-5.2093	GVA6159	New data				
		35.5321	-5.2093	GVA6160	New data				
		35.5321	-5.2093	GVA6161	New data				
		35.5321	-5.2093	GVA6162	New data				
		35.5321	-5.2093	GVA6163	New data				
		35.5321	-5.2093	GVA6164	New data				
		35.5321	-5.2093	GVA6165	New data				
		35.5321	-5.2093	GVA6166	New data				
		35.5321	-5.2093	GVA6167	New data				
		35.5321	-5.2093	GVA6168	New data				
		35.5321	-5.2093	GVA6169	New data				
		35.5321	-5.2093	GVA6170	New data				
		35.5321	-5.2093	GVA6194	New data				
		35.5321	-5.2093	GVA6195	New data				
		35.5321	-5.2093	GVA6196	New data				
		35.5321	-5.2093	GVA6197	New data				
		35.5321	-5.2093	GVA6198	New data				
		35.5321	-5.2093	GVA6199	New data				
		35.5321	-5.2093	GVA6200	New data				
		35.5321	-5.2093	GVA6201	New data				
		35.5321	-5.2093	GVA6202	New data				
		35.5321	-5.2093	GVA6203	New data				
		35.5321	-5.2093	GVA6204	New data				
		35.5321	-5.2093	GVA6205	New data				
		35.5321	-5.2093	GVA6206	New data				
		35.5321	-5.2093	GVA6207	New data				
		35.5321	-5.2093	GVA6208	New data				
		35.5321	-5.2093	GVA6209	New data				
		35.5321	-5.2093	GVA6210	New data				
		35.5321	-5.2093	GVA6211	New data				
		35.5321	-5.2093	GVA6212	New data				
		35.5321	-5.2093	GVA6213	New data				
		35.5321	-5.2093	GVA6214	New data				
		35.5321	-5.2093	GVA6215	New data				
		35.5321	-5.2093	GVA6216	New data				
		35.5321	-5.2093	GVA6217	New data				
		35.5321	-5.2093	GVA6218	New data				
		35.5321	-5.2093	GVA6219	New data				
		35.5321	-5.2093	GVA6220	New data				
		35.5321	-5.2093	GVA6221	New data				

Location						genbank accession			
Country	Locality	Latitude	Longitude	Code	Origin	cytB	Bfib	mt Haplotype	SSR
		35.5321	-5.2093	GVA6222	New data				
		35.5321	-5.2093	GVA6223	New data				
		35.5321	-5.2093	GVA6224	New data				
		35.5321	-5.2093	GVA6225	New data				
		35.5321	-5.2093	GVA6226	New data				
		35.5321	-5.2093	GVA6227	New data				
		35.5321	-5.2093	GVA6228	New data				
		35.5321	-5.2093	GVA6229	New data				
		35.5321	-5.2093	GVA6230	New data				
		35.5321	-5.2093	GVA6231	New data				
		35.5321	-5.2093	GVA6232	New data				
		35.5321	-5.2093	GVA6233	New data				
		35.5321	-5.2093	GVA6234	New data				
		35.5321	-5.2093	GVA6235	New data				
	West of Ketama	34.9607	-4.6806	E11113.3	Beukema et al. 2010	HQ190898		SAS1	
		34.9607	-4.6806	E13124.4,	Beukema et al. 2010	HQ190903		SAS1	
		34.9607	-4.6806	E13124.5	Beukema et al. 2010	HQ190904		SAS1	
Algeria	Seraïdi	36.92	7.71	IMS5169	Ben Hassine et al. 2016	KT995214		SAA	
	Adekkar	36.7281	4.5439	KHA2014.25	Merabet et al. 2016	KT335655		SAA	
		36.7281	4.5439	KHA2014.62	Merabet et al. 2016	KT335656		SAA	
	Aïn Boumendjel	36.91	7.68	IMS5181	Ben Hassine et al. 2016	KT995221		SAA	
	Ait Bouhni	36.7294	4.3853	KHA2014.34	Merabet et al. 2016	KT335652		SAA	
		36.7294	4.3853	KHA2014.58	Merabet et al. 2016	KT335653		SAA	
		36.7294	4.3853	KHA2014.71	Merabet et al. 2016	KT335654		SAA	
	Chrea NP - Blida, Atlas	36.4308	2.8769	KHA2014.44	Merabet et al. 2016	KT335642		SAA	
		36.4308	2.8769	KHA2014.55	Merabet et al. 2016	KT335643		SAA	
		36.4308	2.8769	KHA2014.60	Merabet et al. 2016	KT335644		SAA	
	Elmharka	36.77	6.14	IMS5212	Ben Hassine et al. 2016	KT995246		SAA	
		36.77	6.14	IMS5213	Ben Hassine et al. 2016	KT995247		SAA	
	Ettahra	36.9	6.4	IMS5192	Ben Hassine et al. 2016	KT995229		SAA	
		36.9	6.4	IMS5193	Ben Hassine et al. 2016	KT995230		SAA	
		36.9	6.4	IMS5194	Ben Hassine et al. 2016	KT995231		SAA	
		36.9	6.4	IMS5195	Ben Hassine et al. 2016	KT995232		SAA	
		36.9	6.4	IMS5196	Ben Hassine et al. 2016	KT995233		SAA	
		36.9	6.4	IMS5197	Ben Hassine et al. 2016	KT995234		SAA	

Location						genbank accession			
Country	**Locality**	**Latitude**	**Longitude**	**Code**	**Origin**	**cytB**	**Bfib**	**mt Haplotype**	**SSR**
		36.9	6.4	IMS5198	Ben Hassine et al. 2016	KT995235		SAA	
	Jnan el Bey	36.92	7.66	IMS5182	Ben Hassine et al. 2016	KT995222		SAA	
		36.92	7.66	IMS5183	Ben Hassine et al. 2016	KT995223		SAA	
		36.92	7.66	IMS5184	Ben Hassine et al. 2016	KT995224		SAA	
		36.92	7.66	IMS5185	Ben Hassine et al. 2016	KT995225		SAA	
		36.92	7.66	IMS5186	Ben Hassine et al. 2016	KT995226		SAA	
		36.92	7.66	IMS5187	Ben Hassine et al. 2016	KT995227		SAA	
		36.92	7.66	IMS5188	Ben Hassine et al. 2016	KT995228		SAA	
	Kabylie 1	36.71	5.61	IMS5200	Ben Hassine et al. 2016	KT995236		SAA	
		36.71	5.61	IMS5201	Ben Hassine et al. 2016	KT995237		SAA	
		36.71	5.61	IMS5202	Ben Hassine et al. 2016	KT995238		SAA	
		36.71	5.61	IMS5203	Ben Hassine et al. 2016	KT995239		SAA	
		36.71	5.61	IMS5204	Ben Hassine et al. 2016	KT995240		SAA	
		36.71	5.61	IMS5205	Ben Hassine et al. 2016	KT995241		SAA	
	Kabylie 2	36.74	5.63	IMS5208	Ben Hassine et al. 2016	KT995242		SAA	
		36.74	5.63	IMS5209	Ben Hassine et al. 2016	KT995243		SAA	
		36.74	5.63	IMS5210	Ben Hassine et al. 2016	KT995244		SAA	
		36.74	5.63	IMS5211	Ben Hassine et al. 2016	KT995245		SAA	
	Larba Nait Irathen	36.6489	4.2264	KHA2014.35	Merabet et al. 2016	KT335645		SAA	
		36.6489	4.2264	KHA2014.46	Merabet et al. 2016	KT335646		SAA	
		36.6489	4.2264	KHA2014.51	Merabet et al. 2016	KT335647		SAA	
		36.6489	4.2264	KHA2014.61	Merabet et al. 2016	KT335648		SAA	
		36.6489	4.2264	KHA2014.64	Merabet et al. 2016	KT335649		SAA	
	Sahli Hocine	36.71	4.55	IMS5215	Ben Hassine et al. 2016	KT995248		SAA	
		36.71	4.55	IMS5216	Ben Hassine et al. 2016	KT995249		SAA	
		36.71	4.55	IMS5217	Ben Hassine et al. 2016	KT995250		SAA	
		36.71	4.55	IMS5218	Ben Hassine et al. 2016	KT995251		SAA	
	Seraïdi	36.92	7.71	IMS5170	Ben Hassine et al. 2016	KT995215		SAA	
		36.92	7.71	IMS5171	Ben Hassine et al. 2016	KT995216		SAA	
		36.92	7.71	IMS5172	Ben Hassine et al. 2016	KT995217		SAA	
		36.92	7.71	IMS5173	Ben Hassine et al. 2016	KT995218		SAA	
		36.92	7.71	IMS5174	Ben Hassine et al. 2016	KT995219		SAA	
		36.92	7.71	IMS5175	Ben Hassine et	KT995220		SAA	

Location						genbank accession			
Country	Locality	Latitude	Longitude	Code	Origin	cytB	Bfib	mt Haplotype	SSR
					al. 2016				
	Tala Rana	36.4239	4.2339	KHA2014.26	Merabet et al. 2016	KT335650		SAA	
		36.4239	4.2339	KHA2014.27	Merabet et al. 2016	KT335651		SAA	

Table 7.3 Number of Landsat8 images selected for calculation of NDWI layers, sorted by season. Path and Row correspond to the eponymous identifiers on the Glovis interface

Path	Row	Final number of images	
		Wet season	Dry season
199	36	2	12
	37	4	11
200	36	4	9
	37	4	8
201	35	2	8
	36	3	7
	37	5	9
202	36	3	7
	37	5	5

BIOMOD

BIOMOD 2 (Thuiller et al., 2009, 2012) was initially used to create models for the analysis of biogeographic patterns of *S. algira* subspecies. Two regression-based (Generalized Linear Model (GLM) and Generalized Additive Model (GAM)) and two machine-learning-based algorithms (Artificial Neural Networks (ANN) and Maximum Entropy (MAXENT) were chosen, in order to reduce uncertainties associated with particular modeling techniques (Wiens et al., 2009). Model algorithms were set to default parameters. Five distinct datasets of 1,000 pseudoabsences each were created using the "random" function of BIOMOD 2, and each pseudo-absence dataset was fitted to each algorithm ten times. Presence data was selected randomly for each replicate by cross-validation, using 70/30 % of data for training/testing, respectively. While ideally, training and testing data should be statistically independent (Araújo et al., 2005), data-splitting is a viable alternative when independent datasets are not available (Thuiller et al., 2009). Replicates were rescaled using a binomial GLM to ensure that they were comparable in terms of scale (Thuiller et al., 2009, 2012). Individual replicate performance was evaluated using the True Skill Statistic (TSS), as its independence of species prevalence prevents it from introducing statistical artifacts to estimates of predictive accuracy (Allouche et al., 2006). Replicates with TSS below 0.7 were excluded, and the remaining replicates were projected into the climatic conditions of the present, Mid-Holocene, LIG and LGM. Projections for each period were then assembled into independent consensus projections per algorithm, and the probabilistic consensus models were converted to binary suitability models by applying the minimum probability threshold, reclassifying as suitable all probability values above that of the minimum probability where presence points occur, and all values below it as unsuitable. This task was performed using the Reclassify tool in ArcGIS.

Logistic regression-based model creation in BIOMOD exhibited performance issues, likely related with low sample sizes, which resulted in low accuracy in GLM (as reflected in low TSS and specificity) and failure to create most models using GAM. Consequently, BIOMOD-based model creation was abandoned in favor of a MAXENT-only approach. Model evaluation, variable contribution and past and current projections of the GLM-based models for the three subspecies are presented below as example (Table 7.4, Table 7.5 and Figure 7.1, respectively).

Table 7.4 Average (Avg) and Standard deviation (SD) TSS values, number of replicates with TSS >0.7 and avg/SD (in parenthesis) values for sensitivity and specificity for the climatic GLM models for the subspecies

ID	Avg (SD)	N replicates	Sensitivity	Specificity
S. a. algira	0.84 (0.08)	34	92.94 (9.70)	77.32 (36.47)
S. a. splendens	0.80 (0.05)	42	97.36 (5.08)	82.68 (4.51)
S. a. tingitana	0.88 (0.05)	49	98.78 (3.84)	84.4 (22.16)

Table 7.5 Average (and standard deviation) permutation importance of variables to each climatic GLM model for the subspecies. The most important variables to each average model are outlined in bold. See table 3.1 for variable names

Variables	*S. a. tingitana*	*S. a. splendens*	*S. a. algira*
BIO3	0.400 (0.112)	0.379 (0.073)	0.316 (0.306)
BIO4	**0.568 (0.239)**	0.126 (0.199)	0.276 (0.253)
BIO5	0.346 (0.272)	**0.650 (0.231)**	**0.568 (0.240)**
BIO6	0.404 (0.351)	0.317 (0.089)	0.400 (0.295)
BIO9	**0.560 (0.449)**	0.139 (0.204)	0.304 (0.287)
BIO16	**0.791 (0.090)**	0.466 (0.099)	**0.732 (0.171)**
BIO18	0.062 (0.098)	0.039 (0.064)	0.450 (0.278)

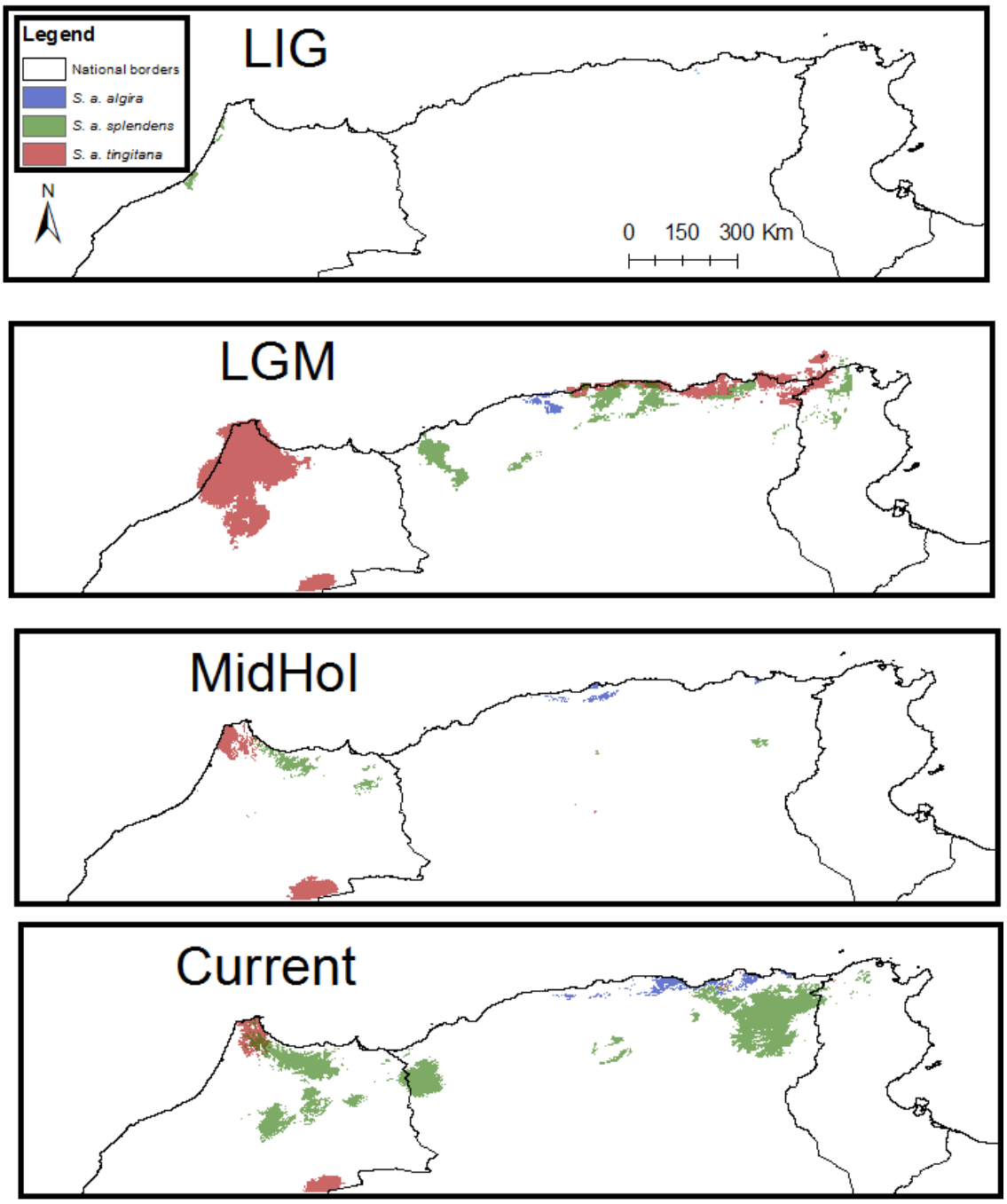

Figure 7.1 Binary GLM climate models and projections to past conditions for the three subspecies of *S. algira*

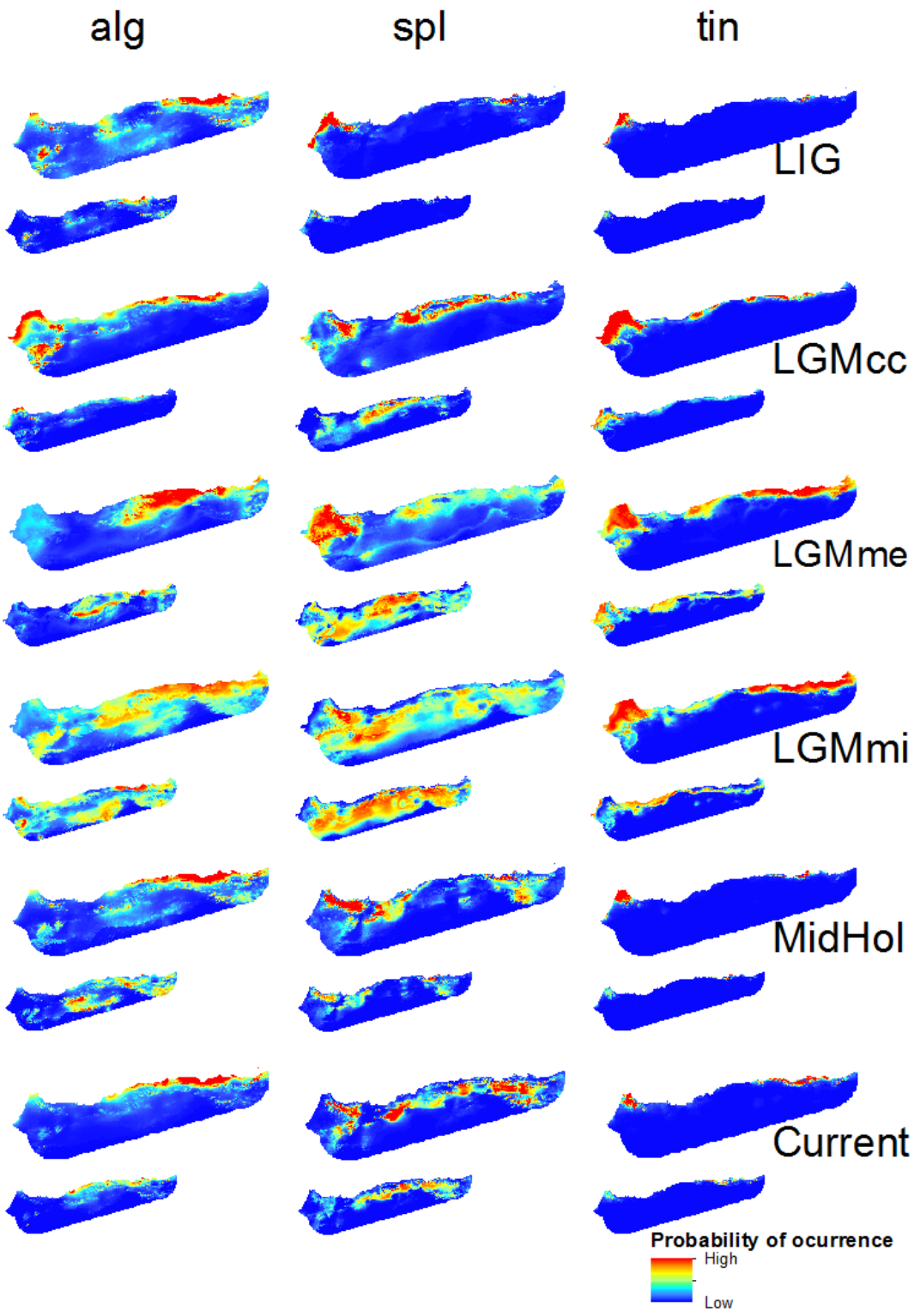

Figure 7.2 Average probabilistic climatic MAXENT model and projections to the past for the *S. algira* subspecies. Small insets represent standard deviation. alg: *S. a. algira*; spl: *S. a. splendens;* tin: *S. a. tingitana*

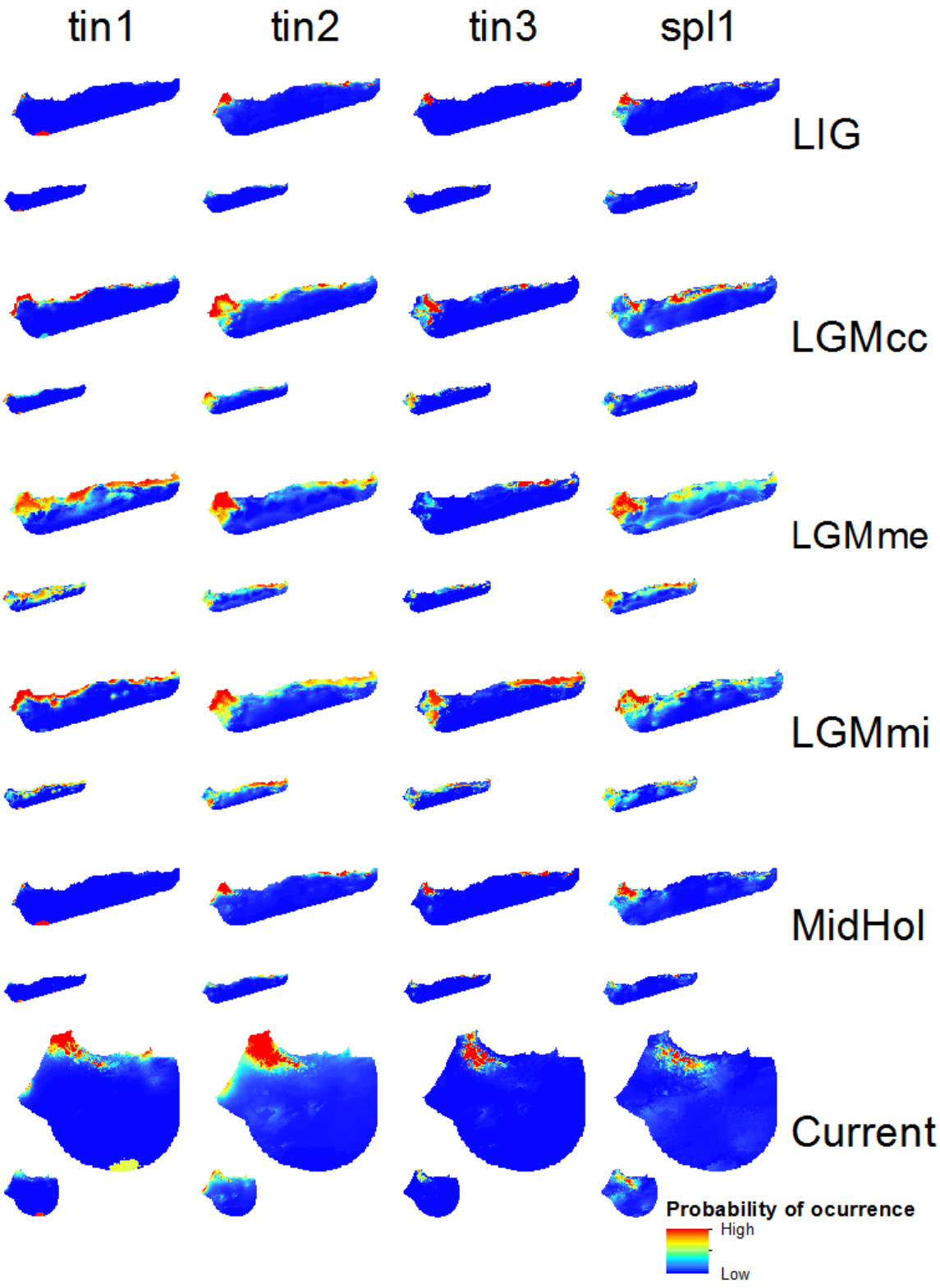

Figure 7.3 Average probabilistic climatic MAXENT model and projections to the past for the Rif sublineages. Small insets represent standard deviation. tin1: *S. a. tingitana* sublineage 1; tin2: *S. a. tingitana* sublineage 2; tin3: *S. a. tingitana* sublineage 3; spl1: *S. a. splendens* sublineage 1

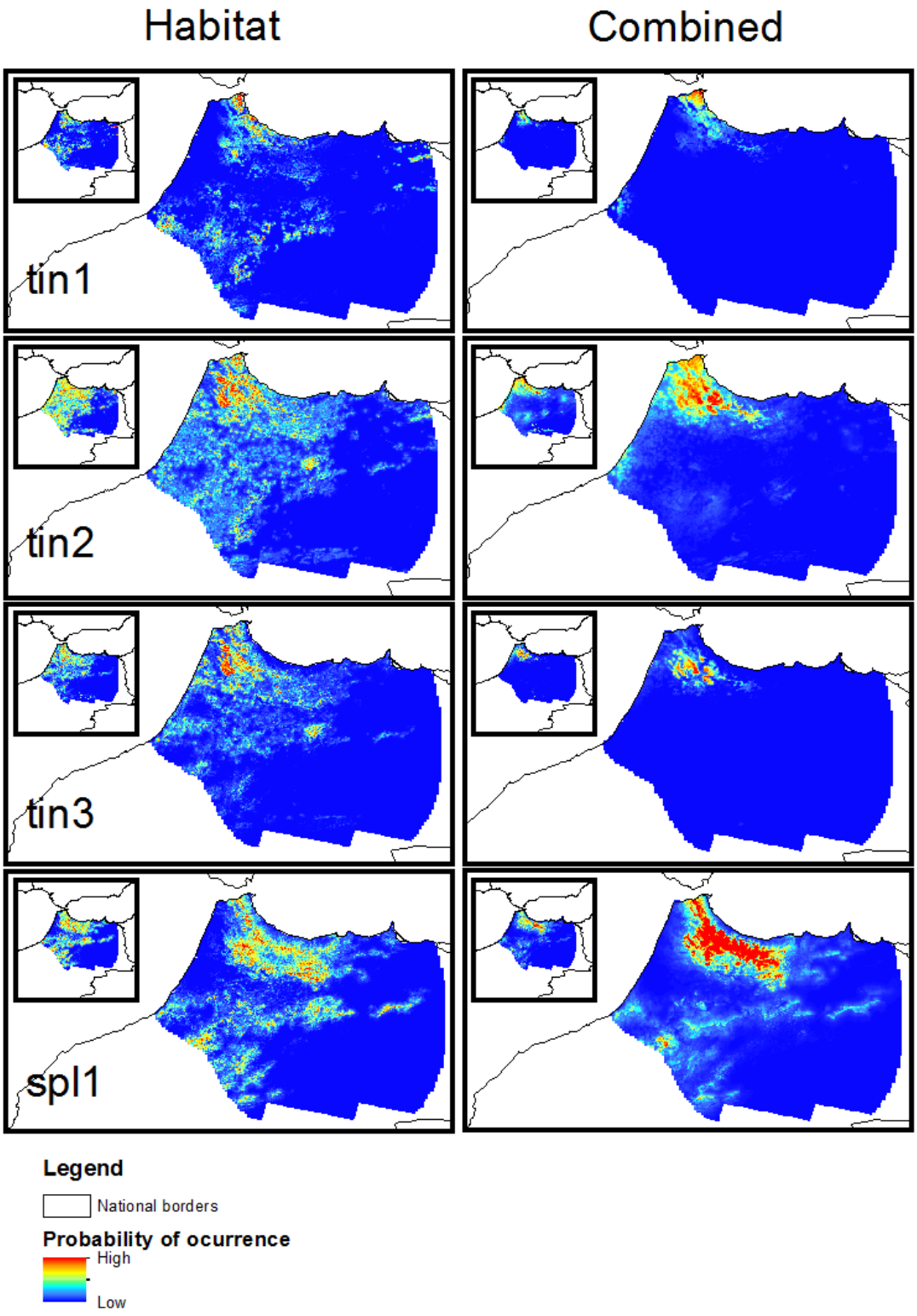

Figure 7.4 Average probabilistic habitat (left) and combined (right) MAXENT models for the Rif sublineages. Small insets represent standard deviation. tin1: *S. a. tingitana* sublineage 1; tin2: *S. a. tingitana* sublineage 2; tin3: *S. a. tingitana* sublineage 3; spl1: *S. a. splendens* sublineage 1

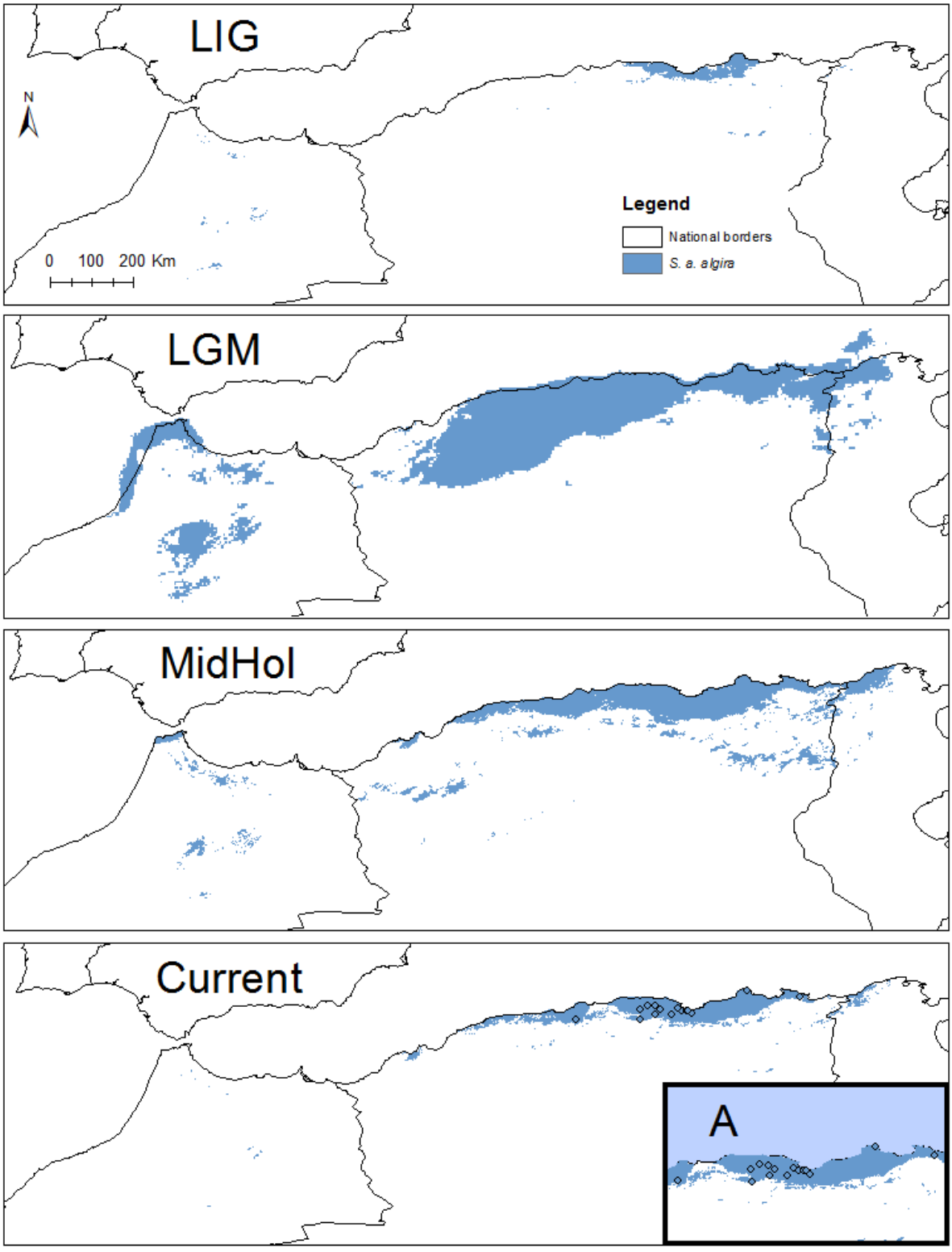

Figure 7.5 Binary climatic model and projections to the past for subspecies *S. a. algira*. Ocurrence records are displayed over the model for current conditions. Inset A displays the occurrence records in detail

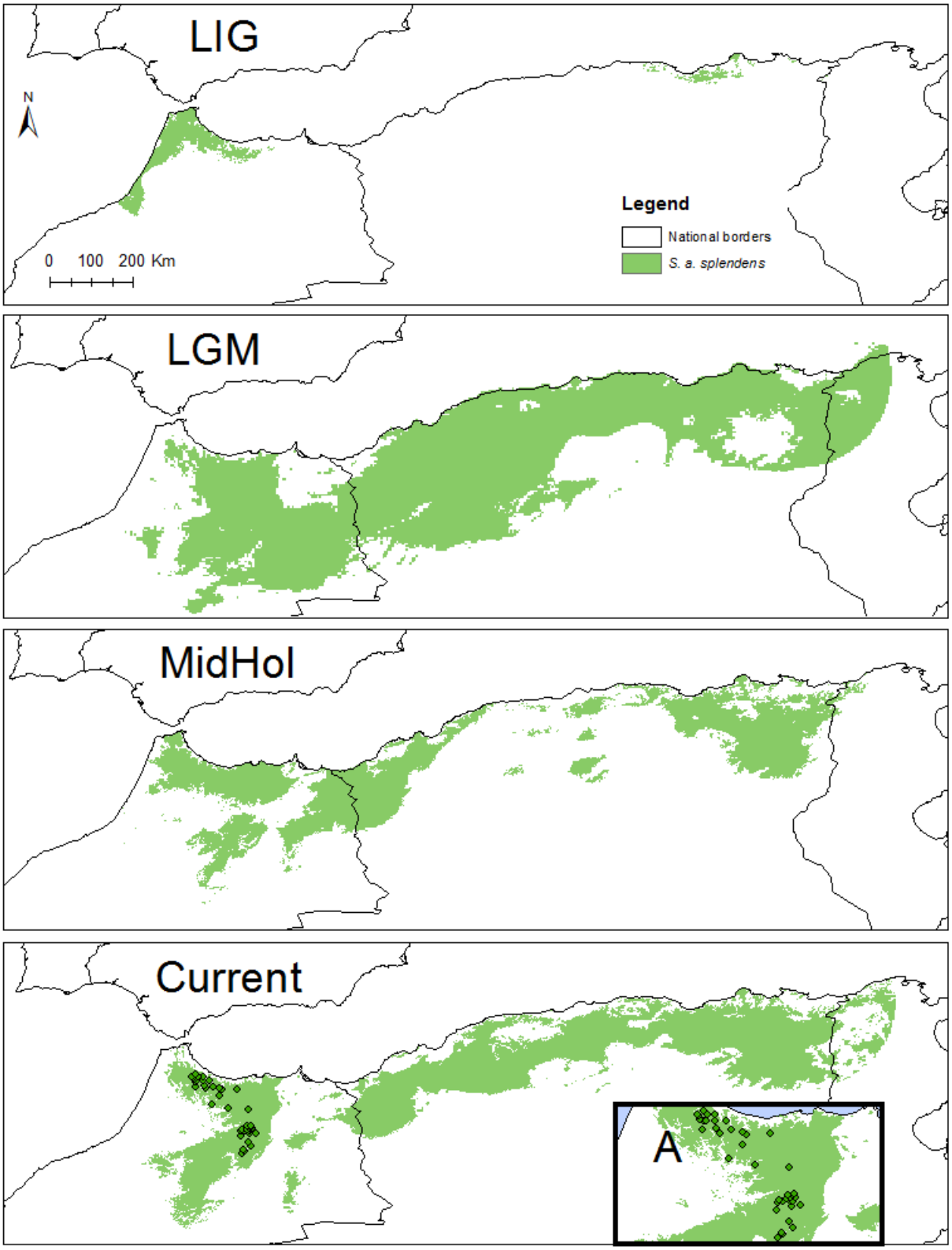

Figure 7.6 Binary climatic model and projections to the past for subspecies *S. a. splendens*. Ocurrence records are displayed over the model for current conditions. Inset A displays the occurrence records in detail

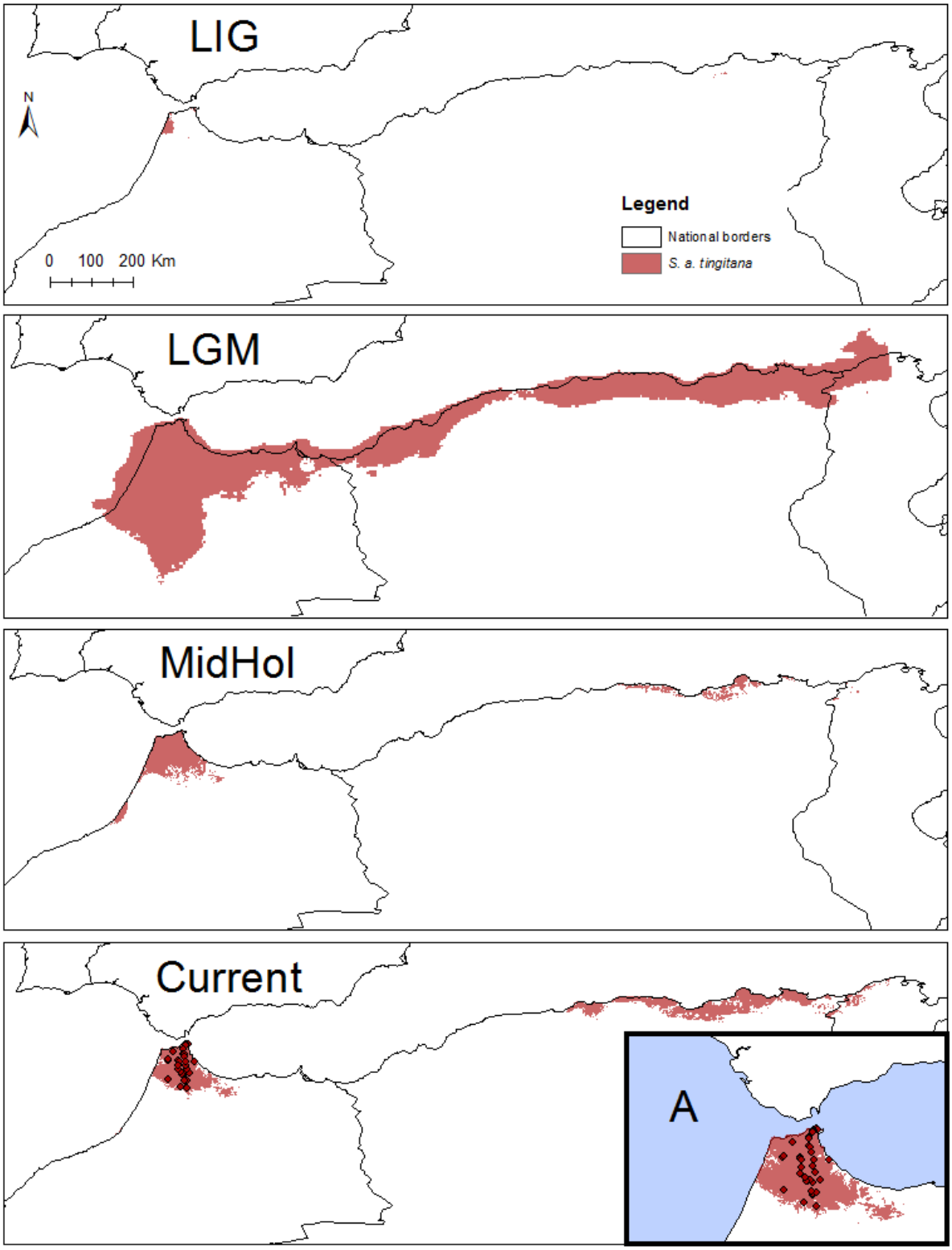

Figure 7.7 Binary climatic model and projections to the past for subspecies *S. a. tingitana*. Ocurrence records are displayed over the model for current conditions. Inset A displays the occurrence records in detail

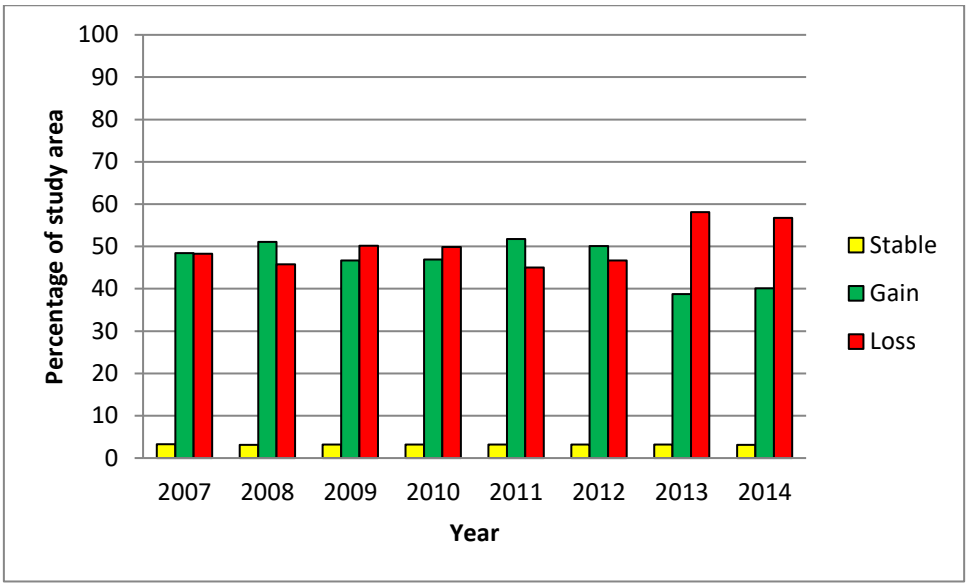

Figure 7.8: Temporal variation of maximum NDVI in North Africa between 2006 and 2014. Bars represent percentage of study area which remained stable (yellow), gained (green) or lost vegetation (red) between one year and the next.

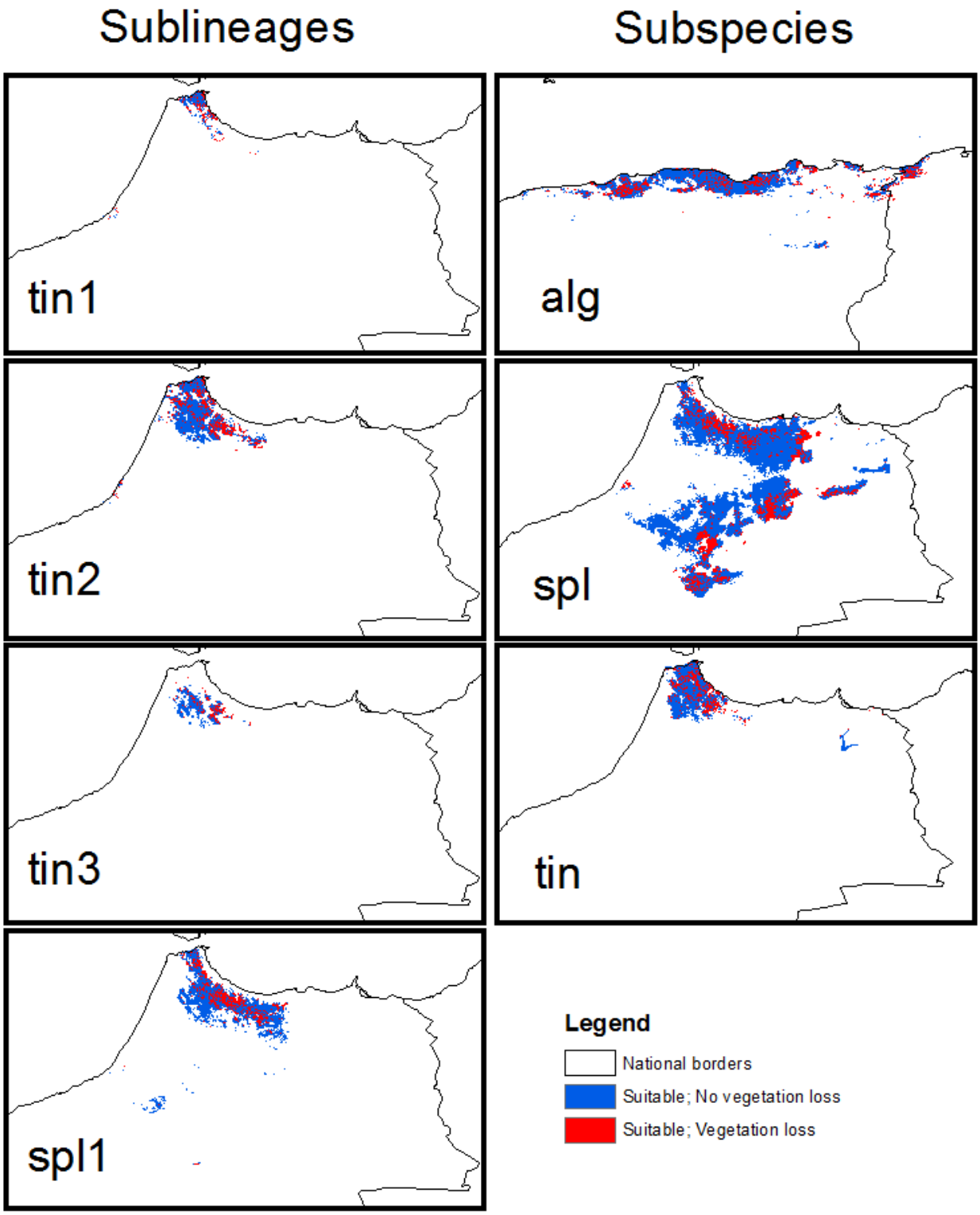

Figure 7.9 Overlap between vegetation loss and niche models for the sublineages (left) and subspecies (right) of *S. algira.* tin1: *S. a. tingitana* sublineage 1; tin2: *S. a. tingitana* sublineage 2; tin3: *S. a. tingitana* sublineage 3; spl1: *S. a. splendens* sublineage 1; alg: *S. a. algira;* spl: *S. a. splendens;* tin: *S. a. tingitana*

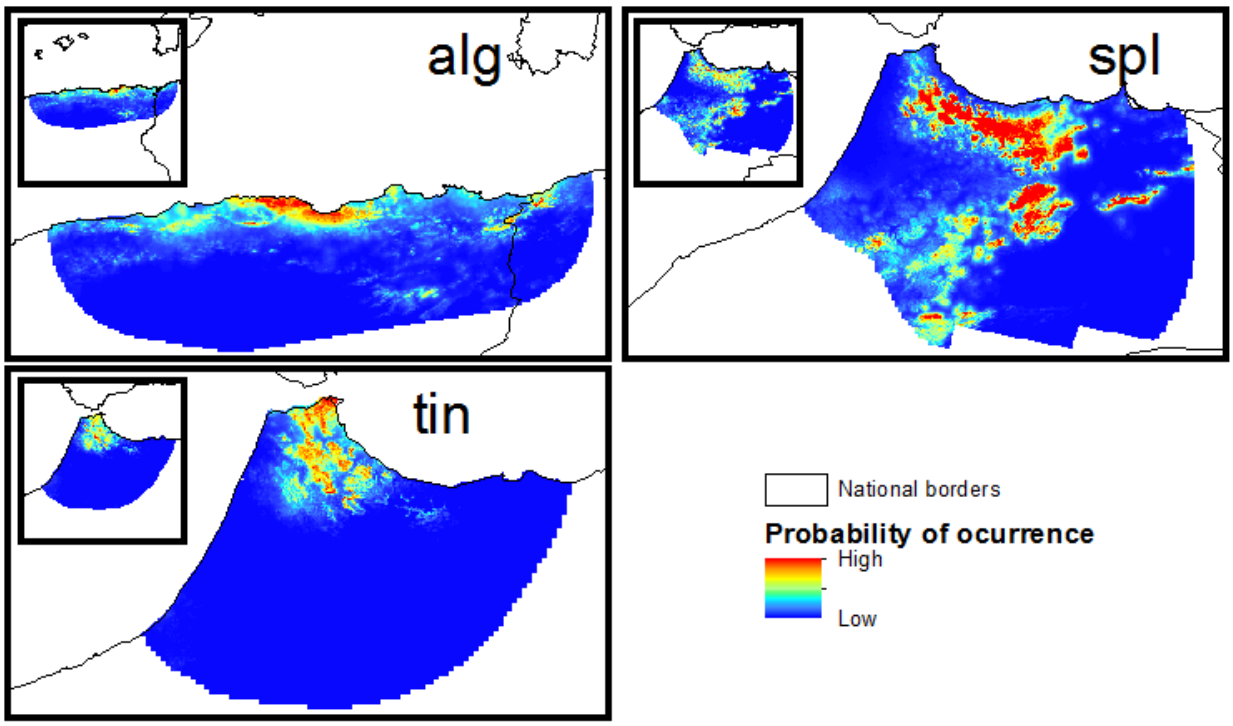

Figure 7.10 Average probabilistic combined models for the *S. algira* subspecies. Small insets represent standard deviation. alg: *S. a. algira*; spl: *S. a. splendens;* tin: *S. a. tingitana*

Table 7.6 Number of occurrence records, average (and SD) training/test AUC and variable percentage contribution for the combined models of *S. algira* subspecies. Most important variables are highlighted in bold. SAA: *S. a. algira*; SAS: *S. a. splendens*; SAT: *S. a. tingitana*

	subspecies		
	SAA	**SAS**	**SAT**
N	15	41	41
Training AUC	0.972 (0.011)	0.972 (0.006)	0.982 (0.003)
Test AUC	0.917 (0.079)	0.951 (0.016)	0.967 (0.010)
BIO4	6.3	**14.5**	10.7
BIO5	11.6	**19.7**	9.7
BIO16	**61.9**	**24.4**	**59.8**
BIO18	3.1	6.2	2.6
GCARB	9.4	3.7	4.3
GNCARB	2	7.5	5.6
LFOSH	0.7	13	6
LBNSH	4.9	11	1.3